



NTNU – Trondheim
Norwegian University of
Science and Technology

The Rate of HF Formation During Addition of Aluminas to Cryolite Melts

Dian Mughni Fellicia

Light Metals Production

Submission date: July 2012

Supervisor: Christian Rosenkilde, IMTE

Norwegian University of Science and Technology
Department of Materials Science and Engineering

ABSTRACT

One of the biggest contributors of gas emission in smelting process of aluminium is the fluoride. A major contributor to the fluoride emissions is the hydrogen fluoride (HF) gas. HF gas is formed when fluoro compounds from the cryolite react with water in the alumina. This study concerns on the rate of HF formation which is interesting due to its direct contribution to the material loss, the changing of chemical composition of the bath and also the loss of current efficiency. A tunable diode laser was used to measure the HF and H₂O concentration in the off gas during additions of alumina containing different types and amounts of water to a cryolite melt at 1000°C. The residence time of the alumina water was varied by varying inert nitrogen gas flows through the experimental cell. These types of experiments are referred to as “melt experiment”. The water content of the alumina samples was studied by loss on ignition (LOI). In addition to the melt experiments, the HF(g) behavior inside the experimental cell was studied by introducing argon gas with 1% HF to the cell at 1000°C when no melt was present. Finally, so called alumina water evolution experiments were conducted where the rate of alumina water released upon rapid heating was studied. Alumina was added to an empty quartz container holding 1000°C during which the off gas analyzed with respect to H₂O concentration. From the LOI result concluded that alumina B content more moisture, alumina B contains more under calcined matter compared alumina A and alumina B has higher HF formation potential than alumina A. The result of the alumina water evolution experiments and melt experiments shows that formation of HF is very rapid. HF formation is not dependent on the nitrogen flow rate and no HF adsorption occurs as a function of flow. The amount of HF generation is not necessarily flow dependent, but the profile (the curve shape) and the mixing flow are dependent. Since this experimental set-up furnace can be considered as a reactor, CSTR modeling was chosen to compare the experimental data and the model.

ACKNOWLEDGEMENT

It's a great pleasure for me to be a part of The KMB ROMA research project. In addition to provide funding for my research, the junior program of the research project also gave me so many great experiences, e.g. a participation at The Minerals, Metals and Materials Society (TMS) conference in Orlando, Florida and also a poster presentation at 7th Reactive Metal Workshops (RMW7) at MIT, Boston.

There were too many help that I have received during my project work and hereby I would like to express my highest gratitude to the following important persons,

First, my supervisor Professor II Christian Rosenkilde at Statoil who has a lot of brilliant ideas and gave details guidance for me. He provided me solution of all problems that were encountered just right on time.

My co-supervisor who also my mother of science Karen Sende Osen at SINTEF Materials and Chemistry for caring, support and helps during this work.

Henrik Gudbrandsen and Ole Kjos for their essentials help in the laboratory.

Aksel Alstad for creating a very nice drawing of nickel container.

Reidar Frog for fabricating a great nickel container for the experiments and also repaired it.

Astrid Johanne Meyer at Hydro Porsgrunn for providing me with alumina samples.

Suyuthi's family for a lot of their constructive comments on my thesis writing.

Mama & Papi for all prayer and encouragements, I guess I will not survive without their prayers for me.

Gatot Surahman for keeps my spirit up during thesis works. You are the best!

All families and friends (Mbak Derita & Sarah) for all prayers and joyful experience which certainly colored my life.

TABLE OF CONTENTS

| | |
|---|------------|
| ABSTRACT | I |
| ACKNOWLEDGEMENT | II |
| TABLE OF CONTENTS | III |
| LIST OF FIGURES | VI |
| LIST OF TABLES | IX |
| 1. INTRODUCTION | 1 |
| 2. LITERATURE STUDY | 3 |
| 2.1 ALUMINIUM CELL | 3 |
| 2.2 THE ELECTROLYTE | 4 |
| 2.3 ALUMINA..... | 5 |
| 2.4 ALUMINIUM WATER-LOI..... | 7 |
| 2.5 DISSOLUTION OF ALUMINA..... | 8 |
| 2.6 HF GENERATION IN THE ELECTROLYSIS CELL..... | 10 |
| 2.7 HF GENERATION IN THE EXPERIMENTAL SETUP IN AUTUMN PROJECT | 11 |
| 2.8 HYDROGEN MASS BALANCE..... | 13 |
| 3. EXPERIMENTAL METHODS | 15 |
| 3.1 ALUMINAS AND CRYOLITE | 15 |
| 3.2 MASS LOSS CHARACTERIZATION – LOI..... | 16 |
| 3.3 LOI IN FUNCTION IN TIME (160°C)..... | 16 |
| 3.4 NEO LASERGAS II SINGLE GAS MONITOR | 17 |
| 3.5 LASER TESTING AND VERIFICATION | 17 |
| 3.6 LABORATORY EXPERIMENTAL SETUP | 19 |
| 3.6.1 <i>NICKEL CONTAINER</i> | 19 |
| 3.6.2 <i>MELT EXPERIMENTS</i> | 21 |
| 3.6.3 <i>ARGON WITH 1% HF EXPERIMENT</i> | 22 |
| 3.6.4 <i>ALUMINA WATER EVOLUTION EXPERIMENTS</i> | 23 |

| | | |
|-----------|--|-----------|
| 3.7 | EXPERIMENTAL PROCEDURE | 24 |
| 3.7.1 | <i>MELT EXPERIMENTS PROCEDURE</i> | 24 |
| 3.7.2 | <i>ALUMINA WATER EVOLUTION EXPERIMENTS PROCEDURE</i> | 25 |
| 3.7.3 | <i>ARGON WITH 1% HF EXPERIMENT PROCEDURE</i> | 25 |
| 4. | CSTR MODELING | 26 |
| 4.1 | FLOWING REACTORS | 26 |
| 4.2 | CSTR ARGON WITH 1% HF EXPERIMENT | 27 |
| 4.3 | CSTR ALUMINA WATER EVOLUTION AND MELT EXPERIMENTS..... | 28 |
| 5 | RESULT | 33 |
| 1.1 | MATERIAL CHARACTERIZATION OF ALUMINA A AND ALUMINA B | 33 |
| 5.1.1 | <i>LOI OF SMELTER GRADE ALUMINA A AND ALUMINA B</i> | 33 |
| 5.1.2 | <i>LOI AS FUNCTION OF TIME AT 160°C BULK ALUMINA A AND ALUMINA B</i> | 33 |
| 5.2 | THREE TYPES OF EXPERIMENTAL EXPERIMENTS | 35 |
| 5.2.1 | <i>ARGON WITH 1% HF EXPERIMENT</i> | 35 |
| 5.2.2 | <i>ALUMINA WATER EVOLUTION EXPERIMENTS</i> | 37 |
| 5.2.3 | <i>MELT EXPERIMENTS</i> | 40 |
| 5.3. | CSTR MODELING | 43 |
| 5.3.1 | <i>TEMPERATURE</i> | 43 |
| 5.3.2 | <i>CSTR FIT FOR ARGON WITH 1% HF EXPERIMENT</i> | 44 |
| 5.3.3 | <i>CSTR FIT FOR ALUMINA WATER EVOLUTION EXPERIMENTS</i> | 46 |
| 5.3.4 | <i>CSTR FIT FOR MELT EXPERIMENTS</i> | 48 |
| 6. | ANALYSIS AND DISCUSSION | 51 |
| 6.1 | LOI PRIMARY BULK ALUMINA A AND B | 51 |
| 6.2 | LOI 160°C IN FUNCTION OF TIME | 52 |
| 6.3 | ARGON WITH 1% HF EXPERIMENT | 53 |
| 6.4 | CSTR FIT FOR ARGON WITH 1% HF EXPERIMENT | 54 |
| 6.5 | ALUMINA WATER EVOLUTION EXPERIMENTS..... | 54 |
| 6.6 | CSTR FIT FOR ALUMINA WATER EVOLUTION EXPERIMENTS | 55 |
| 6.7 | MELT EXPERIMENTS | 56 |
| 6.8 | CSTR FIT FOR MELT EXPERIMENTS | 56 |
| | CONCLUSIONS | 58 |

| | |
|--|-----------|
| FURTHER WORK..... | 59 |
| REFERENCES..... | 60 |
| APPENDIX A DRAWING OF NICKEL CONTAINER | A |
| APPENDIX B METHODS DEVELOPMENT..... | D |
| APPENDIX C CALCULATION OF NAF AND ALF₃ | I |
| APPENDIX D RIEMANN SUMS | J |
| APPENDIX E CALCULATION OF LOSS ON IGNITION | K |
| APPENDIX F CALCULATION OF LOSS ON IGNITION IN FUNCTION OF TIME (160°C)..... | L |
| APPENDIX G GRAPHS OF THE EXPERIMENTS..... | M |

LIST OF FIGURES

| | |
|---|----|
| Figure 1 Industrial aluminium electrolysis cell..... | 3 |
| Figure 2 The bayer process | 6 |
| Figure 3. Thermal decomposition pathways of gibbsite, adapted from Wefers et al..... | 7 |
| Figure 4. A principal drawing of the HF formation inside the electrolysis cell..... | 11 |
| Figure 5. Experimental set-up in the autumn project work..... | 12 |
| Figure 6. The result of HF formation with variation of nitrogen flow rate in autumn project..... | 13 |
| Figure 7. Illustration of HF formation inside the experimental cell..... | 14 |
| Figure 8. Schematic experimental setup of the laser to verifying HF and H ₂ O concentration | 18 |
| Figure 9. Laser testing and verification using nitrogen enriched with moisture..... | 18 |
| Figure 10. Drawing of the experimental set up inside the furnace by Aksel Alstad..... | 20 |
| Figure 11. Schematic laboratory setup of the laser when performing experiment to see HF formation by addition of alumina and variation of nitrogen flow | 22 |
| Figure 12. Schematic laboratory setup of the laser when performing experiment to see amount of HF from argon with 1% HF and variation of nitrogen flow rate | 23 |
| Figure 13. The types of reactor | 26 |
| Figure 14. CSTR assumption for the argon 1% HF experiment..... | 27 |
| Figure 15. Example of the CSTR plot 1..... | 30 |
| Figure 16. Example of CSTR Plot 2 | 31 |
| Figure 17. Alumina water evolution experiment 2 Add.13 (room temperature alumina B) with nitrogen flow 254ml/min..... | 32 |
| Figure 18. Weight loss of alumina A and B within 1774hours..... | 34 |
| Figure 19. LOI in Function of Time within 1774 hours | 35 |
| Figure 20. Eight addition of argon with 1% HF experiment with variation nitrogen flow rate..... | 37 |
| Figure 21. The first of alumina water evolution Experiment..... | 38 |
| Figure 22. 13 addition of argon with 1% HF in alumina water evolution experiment 2 | 39 |
| Figure 23. 1 addition of calcined alumina A and 8 additions of alumina B with variation of nitrogen flow rate in the melt experiment 2 | 41 |
| Figure 24. 2 addition of calcined alumina A and 10 additions of alumina B with variation of nitrogen flow rate in the melt experiment 3 | 42 |

| | |
|--|----|
| Figure 25. The temperature model for CSTR modeling | 44 |
| Figure 26. Experimental data and CSTR comparison with flow rate of nitrogen 97ml/min and 254ml/min | 45 |
| Figure 27. Experimental data and CSTR comparison with flow rate of nitrogen 700ml/min and 1033ml/min | 45 |
| Figure 28. CSTR fit for alumina water evolution experiments with nitrogen flow rate 27ml/min..... | 46 |
| Figure 29. CSTR fit for alumina water evolution experiments with nitrogen flow rate 97ml/min..... | 47 |
| Figure 30. CSTR fit for alumina water evolution experiments with nitrogen flow rate 97ml/min..... | 47 |
| Figure 31. CSTR fit for alumina water evolution experiments with nitrogen flow rate 254ml/min..... | 48 |
| Figure 32. addition 10 of melt experiment 3 with nitrogen flow rate 27ml/min and addition 12 of melt experiment 3 with nitrogen flow rate 97ml/min | 49 |
| Figure 33. addition 2 of melt experiment 2 with nitrogen flow rate 254ml/min and addition 7 of melt experiment 3 with nitrogen flow rate 700ml/min | 49 |
| Figure 34. addition 5 of melt experiment 3 with nitrogen flow rate 1033ml/min..... | 50 |
| Figure 35. The plot of melt experiment 1 | D |
| Figure 36. Testing of laser 27/4 before cleaning. Transmission 68%..... | E |
| Figure 37. Testing laser after opening and cleaning. Transmission 99% | F |
| Figure 38. The structure of the powder inside the furnace after dismantled was performed..... | G |
| Figure 39. Method development of argon with 1% HF using syringe..... | H |
| Figure 40. Argon with 1% HF experiment with nitrogen flow rate 97ml/min and 254ml/min | M |
| Figure 41. Argon with 1% HF experiment with nitrogen flow rate 700ml/min and 1033ml/min | M |
| Figure 42. Alumina water evolution experiments dried Al ₂ O ₃ B with nitrogen flow rate 27ml/min | N |
| Figure 43. Alumina water evolution experiments room temperature Al ₂ O ₃ A and B with nitrogen flow rate 97ml/min..... | N |
| Figure 44. Alumina water evolution experiments room temperature Al ₂ O ₃ B with nitrogen flow rate 97ml/min..... | O |
| Figure 45. Alumina water evolution experiments dried Al ₂ O ₃ A with nitrogen flow rate 97ml/min | O |
| Figure 46. Alumina water evolution experiment dried Al ₂ O ₃ B with nitrogen flow rate 97ml/min..... | P |
| Figure 47. Alumina water evolution dried Al ₂ O ₃ B experiment with nitrogen flow rate 97ml/min..... | P |
| Figure 48. Alumina water evolution dried and room temperature Al ₂ O ₃ B with nitrogen flow rate 254ml/min..... | Q |
| Figure 49. Melt experiment dried Al ₂ O ₃ B with nitrogen flow rate 97ml/min | R |

Figure 50. Melt experiment dried Al_2O_3 B with nitrogen flow rate 254ml/min R
Figure 51. Melt experiments dried Al_2O_3 B with nitrogen flow rate 254ml/min..... S
Figure 52. Melt experiments dried Al_2O_3 B with nitrogen flow rate 700ml/min..... S
Figure 53. Melt experiment dried Al_2O_3 B with nitrogen flow rate 700ml/min T
Figure 54. Melt experiment dried Al_2O_3 B with nitrogen flow rate 1033ml/min T

LIST OF TABLES

| | |
|--|----|
| Table 1. Influence of cell conditions on alumina dissolution times, from Welch (2)..... | 9 |
| Table 2. Factors affecting alumina dissolution ⁽¹¹⁾ | 10 |
| Table 3. Conditions of supplied reagent | 15 |
| Table 4. Gas flow variation..... | 25 |
| Table 5. Value of t max and a which is used in CSTR modeling | 32 |
| Table 6. Data description of Figure 17 | 32 |
| Table 7. Average undried basis and dried basis LOI measurement of alumina A and B in 160°C, 350°C and 1000°C..... | 33 |
| Table 8. Weight of alumina (Al ₂ O ₃) A and B as function in hours at 160°C..... | 34 |
| Table 9. Loss on ignition of alumina (Al ₂ O ₃) A and B as function of time at 160°C | 35 |
| Table 10. The result of Argon (Ar) with 1% HF experiment which is flushed into the furnace for one minute with varied of nitrogen (N ₂) flow | 36 |
| Table 11. Eight addition of alumina water evolution experiment 1 for room temperature alumina (Al ₂ O ₃) A, B and dried alumina (Al ₂ O ₃) A, B..... | 38 |
| Table 12. The Result from 13 addition of alumina A and B in alumina water evolution experiment 2 | 39 |
| Table 13. The result of eight addition of dried alumina B in the melt experiment 2 with varied of nitrogen flow | 41 |
| Table 14. The result of twelve addition of dried alumina B in the melt experiment 3 | 42 |
| Table 15. Parameters used when calculating the temperature model for CSTR..... | 44 |
| Table 16. temperature approximation in function of flow rate (Nml/min) | 44 |
| Table 17. The result of experimental data of melt experiment 1 | D |
| Table 18. Activity of nickel and its compound..... | E |
| Table 19. Parameters used when calculating the riemann sum of the HF formation..... | J |

1. INTRODUCTION

Fluoride emission during aluminium production is one of the main hazards to the environment. The term fluoride emission means the escape of some amount of fluoride directly from the top, side walls and bottom of the aluminium electrolysis cell to the environment.⁽¹⁾ Even though after 1965 the fluoride emissions has been minimized by the installation of the dry scrubbers, the fluoride emissions still occurs through the emission of hydrogen fluoride (HF) gas. HF gas is formed when fluoro compounds originated from the cryolite react with absorbed water in the alumina surface. Water reacts with alumina, via physisorption and chemisorption and structural hydroxyl in the crystal lattice.⁽²⁾ Aluminas containing different types and amount of absorbed water will form different amount of HF. The rate of HF formation affects directly to the material loss and changing of chemical composition of the bath and also the loss of current efficiency. The main source of proton (H) could be from water, hydroxide associated with the alumina, hydrogen content in the anode and moisture in the air. Osen et al⁽³⁾, suggest that the hydrogen containing species with long residence times can exist in the system.

It has been argued that in an industrial cell, it is the structural hydroxyl in the alumina that contribute more to the HF formation and that the more loosely bonded water flashed off before it meets the hot fluoride. Sommerseth⁽¹⁾ conducted experimental works about HF formation comparison from several type of smelter grade alumina varied with different water content. She added small amount of alumina to a relatively closed cell containing crucible with the standard composition industrial bath. The cell was purged with nitrogen inert gas. Downstream of the cell, the gas was analyzed online for HF. Sommerseth⁽¹⁾ reported that all type of adsorbed water in the alumina (structural hydroxyl, physisorbed and chemisorbed water) give contribution to HF formation, the reason is because the set-up which was used (as compared to an industrial cell), all the different waters probably had enough time to react with the hot fluoride.

The present thesis work is a continuation from the autumn project work where the objective was to study the rate of HF formation. The purpose of that work was mainly to check if the laboratory set-up used by Sommerseth ⁽⁴⁾ showed any variations in the amounts of HF formed when the inert gas flow rate during alumina addition was changed, thereby varying the residence time of the alumina water in the hot zone. This is expected to be case if the reaction between moisture and fluorides takes place on the same timescale as the gas residence time. The results of the project work indicated that the HF formation decreased with the gas flow rate (decreasing alumina water residence time). However the trend was not very strong due only one experiment was conducted. In the current work, some modifications of the experimental set-up will be done to get better result. In this experiment, measurement of HF formation was conducted by hydrolysis of alumina without any electrolysis activity.

To measure the moisture content of alumina characterization by loss on ignition and loss on ignition at function at time at 160°C were performed. Continuous stirred tank reactor (CSTR) was used to show the trend of HF evacuation from crucible.

Three types of experiments were conducted i.e. melt experiments as a laboratory scale of electrolysis cell, alumina water evolution experiment to look at the rate of water evolution upon rapid heating and the last experiment is addition of argon with 1% HF to empty nickel container at various nitrogen flow rates to see the HF behavior inside the furnace, to find whether nickel apparatus will absorbed a lot of HF and also to check the nitrogen flow dependency towards HF amount.

2. LITERATURE STUDY

The following chapter is mainly taken from Chapter 2 of the autumn project work ⁽⁵⁾ with the same title. In this chapter, the concept on aluminium production and its correlation with the rate of HF formation are presented.

2.1 ALUMINIUM CELL

Aluminium is always found in the combined form of oxides and silicates due to high affinity to bind with oxygen and silicates. It took some time for scientists to know how to produce this metal on an industrial scale. In 1886 Hall and Héroult independently developed and patented an electrolysis process by electrochemical reduction. During the process, the alumina (Al_2O_3) as raw material is dissolved in cryolite bath material (Na_3AlF_6) at approximately 960°C .

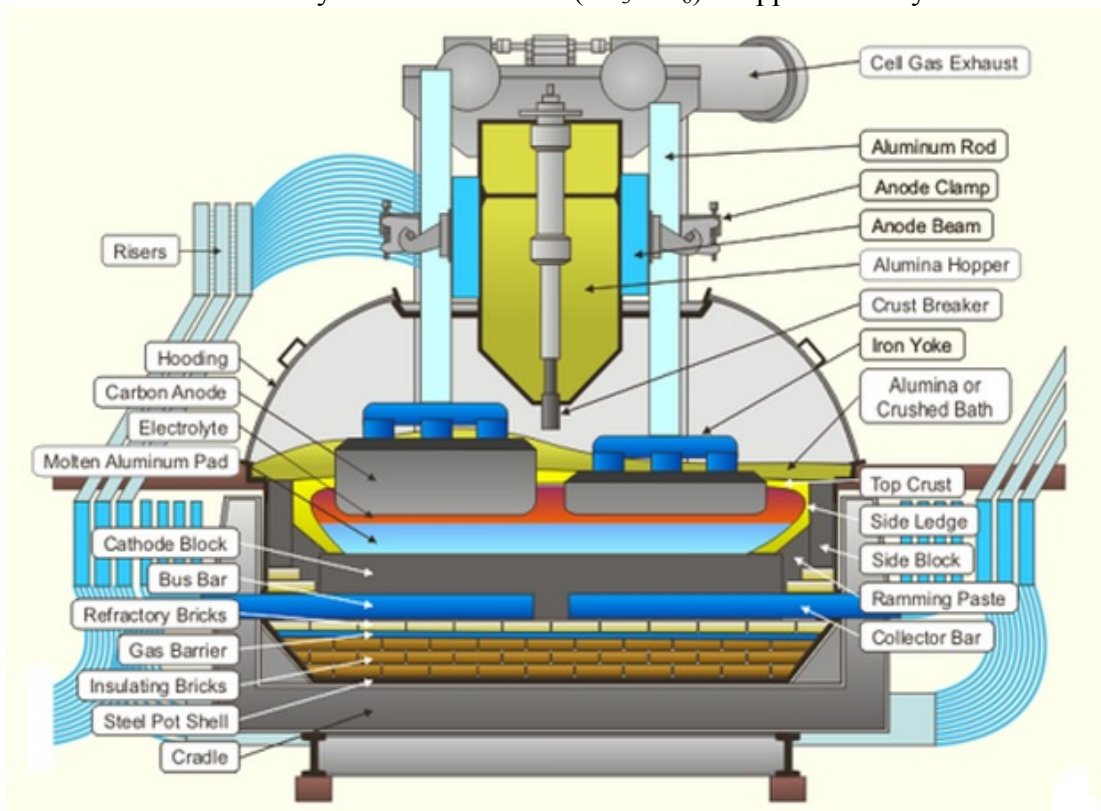


Figure 1 Industrial aluminium electrolysis cell ⁽²¹⁾

Typically bauxite is being treated chemically by bayer process to produce alumina. With continuous improvement for more than a century this process is being used commercially since 1886. Industrial technical electrolysis cell which adopt hall- hérout process is illustrated in Figure 1.

The carbon anode and aluminium cathode are react electrochemically can be described in the following equation,

Reaction on anode



Reaction on cathode



Total reaction



By passing current, alumina is electrolyzed and form O^{2-} and Al^{3+} . Cathodes as electrode negative attract Al^{3+} which accept electron to form pure aluminium. O^{2-} ions migrate to anode where they form oxygen atoms by depositing extra electrons which released at the anode and then reacts with the carbon to form carbon dioxide.

2.2 THE ELECTROLYTE

Four main functions of electrolyte are passing electricity from anode (positive electrode) to cathode (negative electrode), being a solvent for alumina to enable its electrolytic decomposition to form aluminium, providing a physical separation between the cathodically produced liquid aluminium metal and the anodically evolved carbon dioxide gas and acting as a heat generating resistor that enables the cell to be self-heating. ⁽⁶⁾

The main component of electrolyte in aluminium electrolysis cell is cryolite (Na_3AlF_6) with typical addition of 6-13mass % AlF_3 , 4-6 mass % CaF_2 and 2-4 mass % Al_2O_3 . ⁽⁷⁾ Cryolite is being chosen due to its high solubility of alumina. Some other additives can be added to improve

the physicochemical properties of electrolyte. According to the phase diagram of the system NaF-AlF₃, cryolite congruently melts at 1010°C.

In the electrolyte, the relative amount of sodium fluoride and aluminium fluoride on molar basis may be expressed as the cryolite ratio (CR), bath ratio (BR) or excess AlF₃. The cryolite ratio is the molar ratio between NaF and AlF₃. Lowering the cryolite ratio can increase current efficiency of metal production, increase the volatility of the electrolyte and also decrease the electrical conductivity, the alumina solubility and the melting point of the bath. In today's industrial cells, a CR around 2.2 is common. Bath ratio is the mass ratio between NaF and AlF₃. The value of cryolite ratio is usually double the value of the bath ratio. Excess AlF₃ is the mass % AlF₃ in excess of the Na₃AlF₆ composition.⁽⁷⁾ Current efficiency also increases with increasing AlF₃ content. It is considered as neutral bath when compound cryolite containing 3 moles NaF and 1 mole of AlF₃. The acidic bath is the result of cryolite ratio lower than 3 caused by excess AlF₃ and basic bath is the result of cryolite ratio higher than 3 caused by excess NaF.⁽⁸⁾

2.3 ALUMINA

Alumina is produced from bauxite by Bayer process, which was invented in 1888 by Karl Joseph Bayer (see Figure 2). Bauxite contains boehmite, gibbsite and diasporite in varying proportions, and are found as rock or clay-like material, consisting 30-60% Al₂O₃. Figure 3 summarizes the possible reaction for gibbsite dehydroxylation under different reaction conditions. The reactions are influenced by several parameters (such as temperature, heating rate, residence time, particle size and morphology, crystallinity, impurities and atmospheric conditions). Some of which are directly related to Bayer operations.

Three functions of alumina are the raw material for production of aluminium, thermal insulation material on top of the self-formed crust and on the prebaked anodes and material for gas cleaning and fluoride adsorption by the dry scrubbing method.⁽⁹⁾

The grade of the alumina (particle size, α - and γ - Al_2O_3 content) can be influenced by precipitation and calcining condition. Flourey alumina is highly calcined and contains mostly α - Al_2O_3 , and sandy alumina which is calcined in the lower temperature mainly consists of γ - Al_2O_3 in the hydrated form. It is called sandy due to free flowing properties and it also has high surface area of alumina which is preferable for aluminium production. Flourey alumina has surface area below $5\text{m}^2\text{g}^{-1}$. This low surface area makes this type of alumina dissolves slowly and also makes it to be a bad adsorbent for fluorides in the scrubber.

In aluminium production, it is common to call alumina (as the raw material) as smelter grade alumina (SGA). SGA properties and impurities will give big effect to the metal product quality and also to the scrubber efficiency. In general SGA has below 30% of α - Al_2O_3 content.

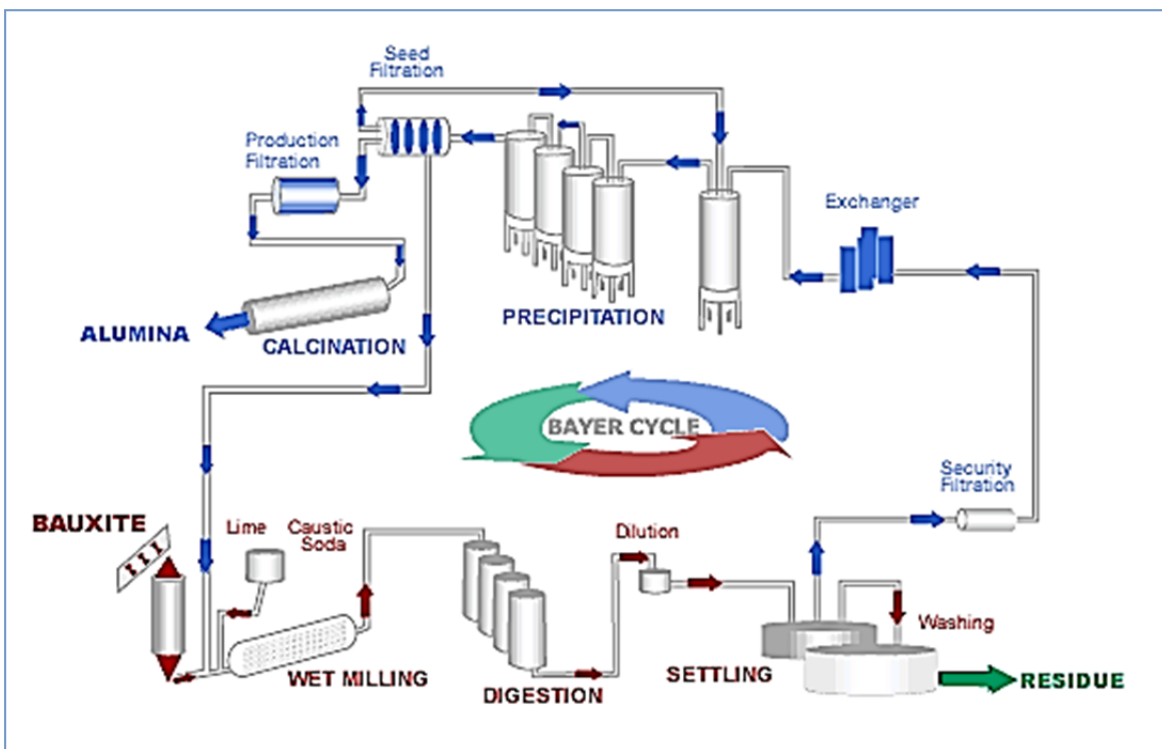


Figure 2 The bayer process ⁽²²⁾

The main step in the bayer process is grinding of bauxite, digestion, settling, precipitation and calcination.

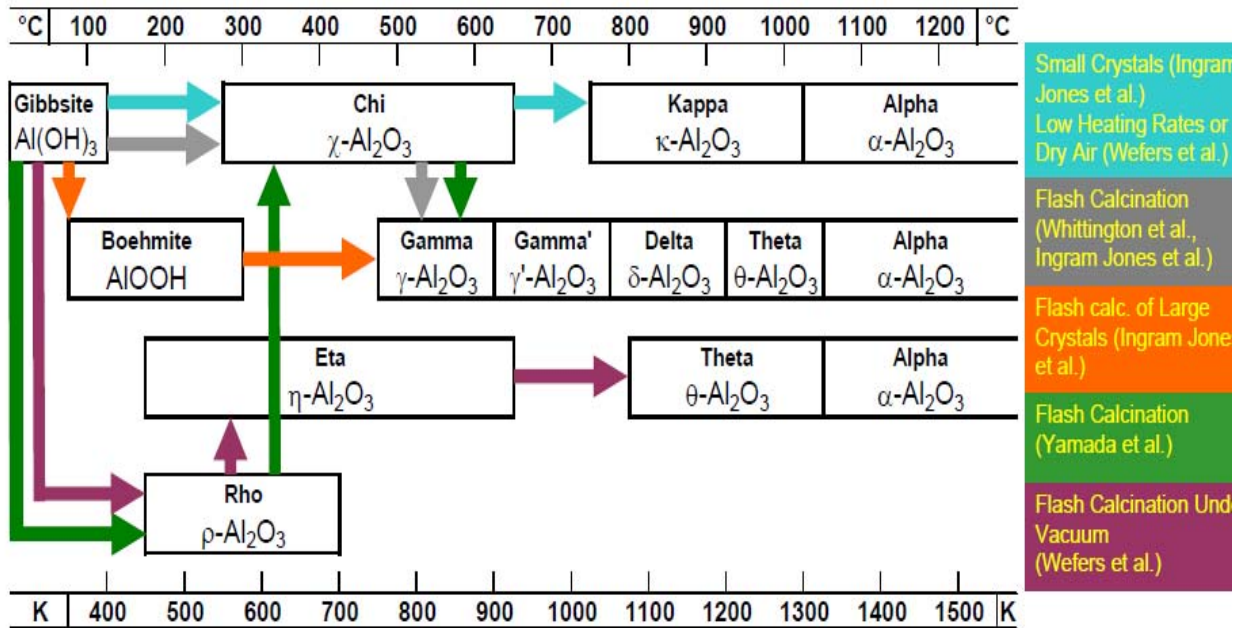


Figure 3. Thermal decomposition pathways of gibbsite, adapted from Wefers et al. ⁽⁹⁾

2.4 ALUMINIUM WATER-LOI

The polar surface of alumina gives strong affinity for water. Adsorbed water in alumina surface may lead to hydrolysis reactions in the fluoride melt and may also be partly reduced to hydrogen.

According to Hyland et al ⁽²⁾ there are three types of water in alumina,

1. Physisorbed water
2. Chemisorbed water
3. Structural hydroxyl in the crystal lattice

The physisorbed water is loosely bound water. The water adsorption into alumina surface is initiated by electrostatic (Van der Waals forces) interactions between the induced dipoles. The chemisorbed water is strongly bound water. This adsorption is driven by strong chemical interaction where water and the alumina surfaces, which then create covalent bonds. According

to R. Desai ⁽¹⁰⁾ the chemisorbed water is typical of surface hydroxyl and the properties are determined by their coordination number and net electrical charge. The structural hydroxyl is OH⁻ group which is bonded with aluminium atom in the crystal lattice. Considering all of these adsorption mechanisms, water on alumina can be rapidly lost or gained depending on the relative humidity of the surrounding environment. ⁽¹¹⁾ Depending on the moisture content, some parts of water will be evaporated immediately after alumina is added into the cell but some other parts of water has stronger bound and will follow into the melts. ⁽¹²⁾ Based on the tentative explanation of Grjotheim et al ⁽¹³⁾, reaction between hydroxide and fluoride ions happens because of close resemblance of the size, charge and polarizability and can substituted for each other in many compounds.

Due to alumina water rapidly lost and gained depending on the relative humidity, loss on ignition to measure the the mass loss (humidity and moisture) of the alumina when heated in a certain range of temperature in an inert atmosphere need to perform. Heating to 0-110°C will remove physisorbed water and some chemisorbed water. It reported by Hyland et al ⁽¹⁴⁾ that heating to temperatures 110-300°C removes more chemisorbed and structural hydroxyl associated with gibbsite. Heating to the temperature 300-1000°C will remove the strongly chemisorbed water and structural hydroxyl incorporated in the transition alumina phase. Another reference ⁽¹¹⁾ use term MOI (moisture in ignition) instead LOI to calculate the loss of mass at 300°C. Typically, smelter grade alumina has LOI value of 0.5-0.9%. ⁽⁷⁾

2.5 DISSOLUTION OF ALUMINA

Grjotheim et al ⁽⁷⁾ stated that heat transfer and mass transfer can be rate determining step (the slowest step that determines all reactions) for the dissolution of alumina. Chemical reactions and physical processes such as dispersion and lump formation mainly influence the process. The rate of dissolution of alumina also affects the solubility of alumina in the electrolyte.

The step of dissolution of alumina in the electrolyte are listed below, ⁽⁹⁾

1. Heating up the cold alumina to the electrolyte temperature.
-

2. Transformation of the added gamma alumina to alpha alumina.
3. Dissolution of alpha alumina and chemical reaction with Al-F species to form Al-O-F complex anions ($\text{Al}_2\text{O}_2\text{F}_4^{2-}$ and $\text{Al}_2\text{OF}_6^{2-}$).
4. Uniform mixing and dispersion in the electrolyte.

When alumina reacts with electrolyte in the bath, the following may happen,

1. It rapidly disperses as a single grain and dissolves easily.
2. It can agglomerate as a lump mass and freeze bath around it, which either may float on the bath surface or sink as dense crust to the surface of $\text{Al}_{(l)}$ or to the graphite cathode surface.
3. It can sink without dispersing (this is typical behavior of alpha alumina)

The variables that affect the rate of dissolution can be divided into two categories,

1. Cell operating variables
2. Alumina properties

In industrial practice, cell operating variables can be assumed to be constant. Table 1 shows the influence of the cell conditions on alumina dissolution times. The dissolution rate of alumina is mostly affected by particle size distribution, density, surface area, alumina phase distribution, water content and chemical composition (see Table 2).

Table 1. Influence of cell conditions on alumina dissolution times, from Welch (2)

| Property | Typical Value | Range | Change in dissolution time (%) |
|---------------------------------------|---------------|-----------|--------------------------------|
| Bath velocity (cm.s^{-1}) | 15 | 4 – 25 | -100 to +500 |
| Bath acidity (mass % AlF_3) | 9 | 13 - 7 | -20 to +80 |
| Superheat ($^{\circ}\text{C}$) | 10 | 5 - 15 | -20 to +300 |
| Alumina content (mass %) | 2 | 1.6 - 4.6 | <20 |
| Dissolution time (s) | 26 | 13 - <500 | -50 to +3000 |

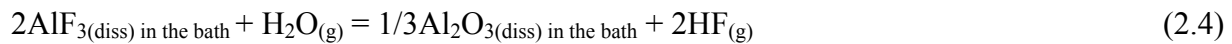
Table 2. Factors affecting alumina dissolution ⁽¹¹⁾

| Parameter | Effect on dissolution time in alumina properties |
|-----------------------------|--|
| Particle Size | None observed for size fractions |
| Adsorbed Water | Strong effect – high MOI gives shorter dissolution times |
| Adsorbed HF | Small decrease in dissolution time |
| Adsorbed NaAlF ₄ | None with laboratory prepared sample |

2.6 HF GENERATION IN THE ELECTROLYSIS CELL

Three main sources of HF are the water and hydroxyls associated with the fed alumina, hydrogen content in the anode and moisture in the air. The HF formation inside the electrolysis cell is shown in Figure 4. Hyland ⁽¹⁴⁾ also reported that hydroxyl can dissolve in molten cryolite electrolytes and generate HF electrochemically. The electrochemically generated HF could be distinguished from HF which was generated by thermal hydrolysis. Patterson et al ⁽¹²⁾ concluded that the HF generation increases proportionally with the amount of structural water. They claimed that adsorbed water is lost before entering the bath due to high temperature gradient between surrounding and inside the cell. Overall only fractional amount of the total alumina water react (4-8 wt%) and forms HF. Still according to Patterson et al ⁽¹²⁾ the dissolved water contributes to approximately 8kg/tonne Al of the HF evolution. It also proposed that dissolved water species in the bath is in a hydroxide ion form.

Formation of HF is occurring by hydrolysis of bath and hydrolysis of electrolysis cell vapor shows as reaction follows, ⁽¹⁵⁾



The equilibrium constant is favorable for both reactions at the cell temperatures. According to Haupin and Kvande ⁽¹⁵⁾ the kinetics limits of HF formation is about 25% of the equilibrium value.

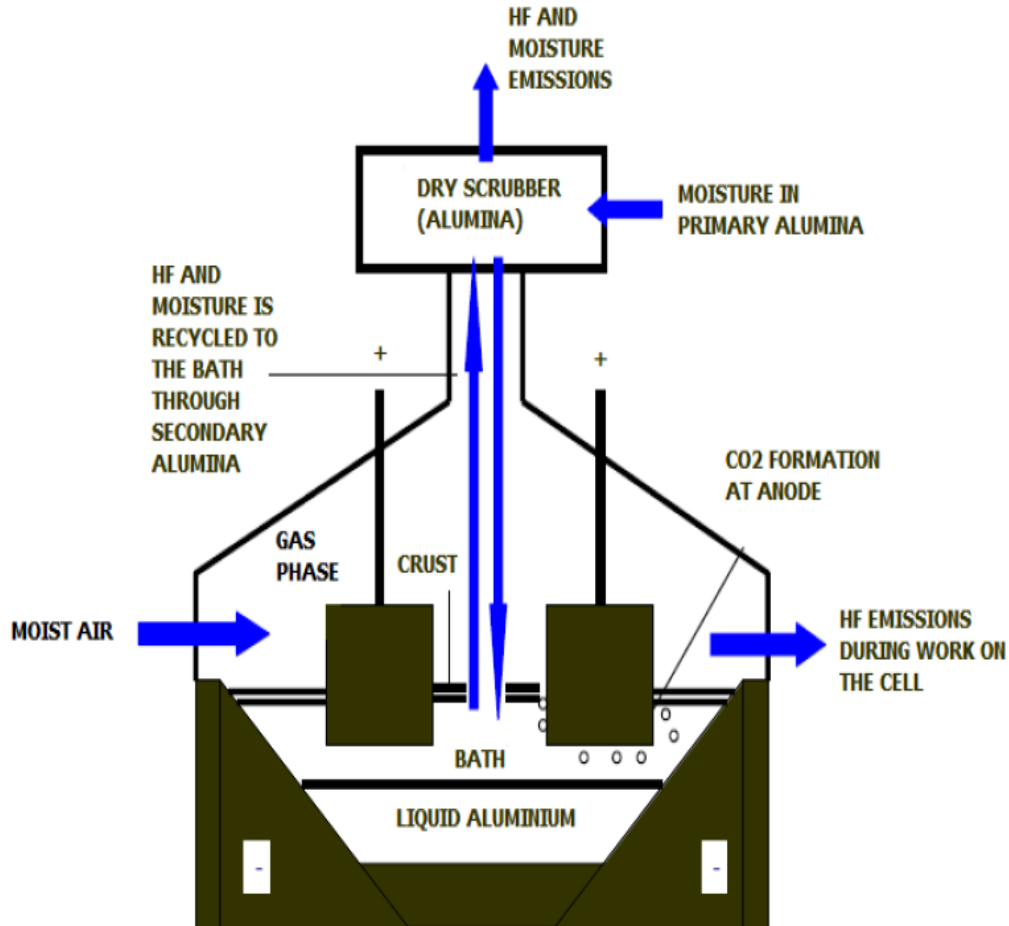


Figure 4. A principal drawing of the HF formation inside the electrolysis cell ⁽¹⁵⁾

2.7 HF GENERATION IN THE EXPERIMENTAL SETUP IN AUTUMN PROJECT

The main purpose of this work was mainly to check if the experimental set-up used by Sommerseth ⁽⁴⁾ allows studying the variation of the HF formation when the alumina water

residence time was varied by changing the inert nitrogen gas flow during alumina addition. This was expected to be the case if the reaction between moisture and fluorides takes place on the same timescale as the gas residence time. Oxide material pythagoras tube which made from alsint was being used during the experiments as presented in Figure 5,

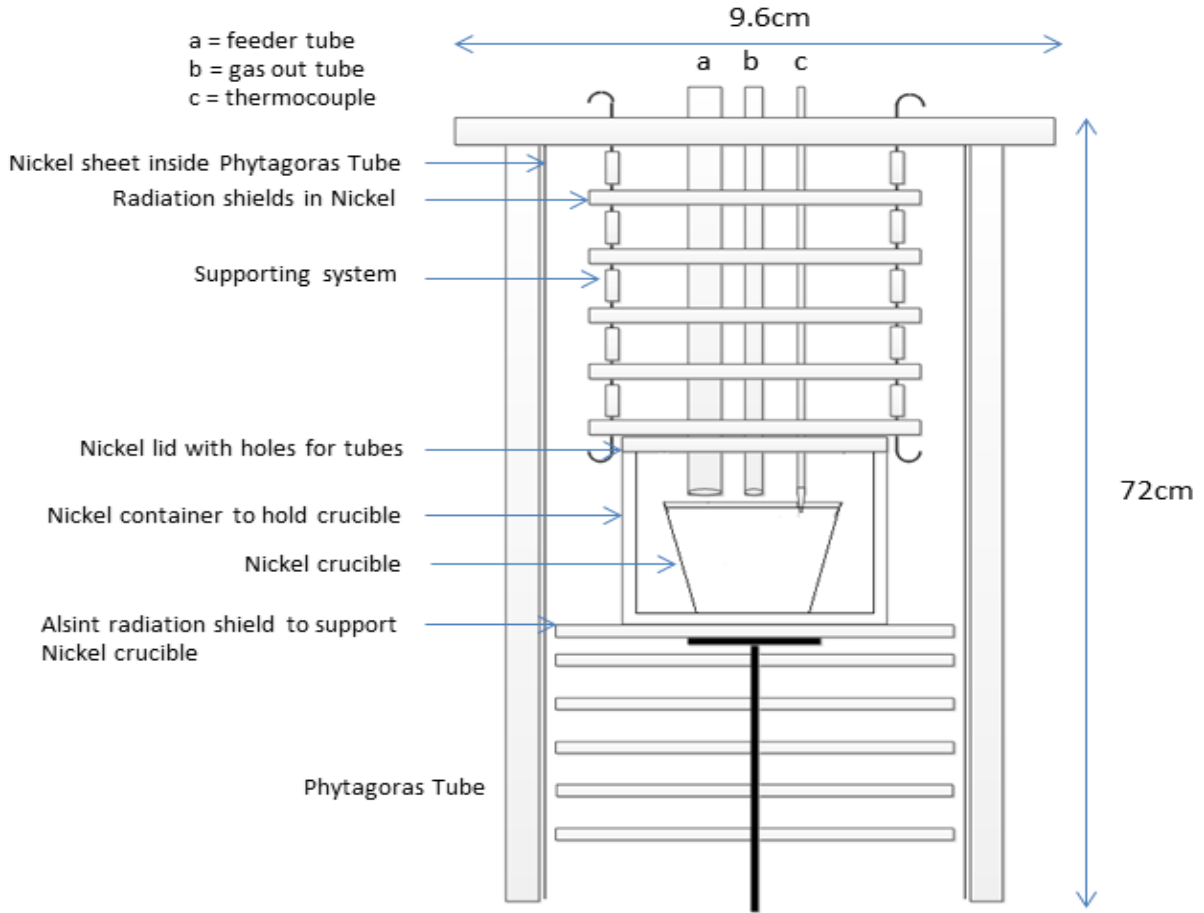


Figure 5. Experimental set-up in the autumn project work

In that set-up, nickel sheet was used as a liner inside the pythagoras tube to avoid adsorbed water from alumina to enter the furnace and to avoid HF adsorbed on the pythagoras tube surface. These two factors might cause an unwanted higher baseline and measurement errors during the HF measurements. Due to the corresponding set up did not reach maximum result, the modifications in the current thesis work were employed.

The preliminary result from the autumn project in Figure 6 indicates that the HF formation increase with increases of increasing alumina water residence time (decreasing nitrogen flow rate). The trend was not very strong due only one experiment was conducted.

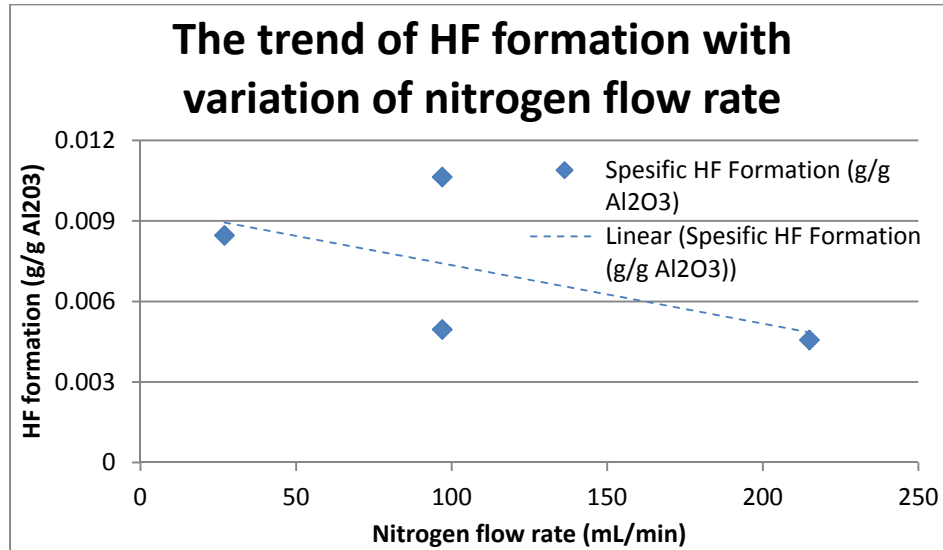


Figure 6. The result of HF formation with variation of nitrogen flow rate in autumn project

2.8 HYDROGEN MASS BALANCE

HF gas is formed when fluoro compounds from the AlF_3 or bath vapor NaAlF_4 reacts with H from absorbed water from alumina. The rate of HF formation may be connected to the rate of alumina dissolution. As mentioned in the previous sub chapter about the effect of hydrogen on the HF formation, alumina dissolves fast in the beginning and this may also lead to a fast release of water/ hydroxide. When the alumina agglomerates and the dissolution rate go down, the alumina might protect the hydroxides inside and they will be released more slowly. Accordingly, the rate of the alumina water available for reaction with fluorides goes down. Osen et al ⁽³⁾, suggested that hydrogen containing species with long residence times can exist.

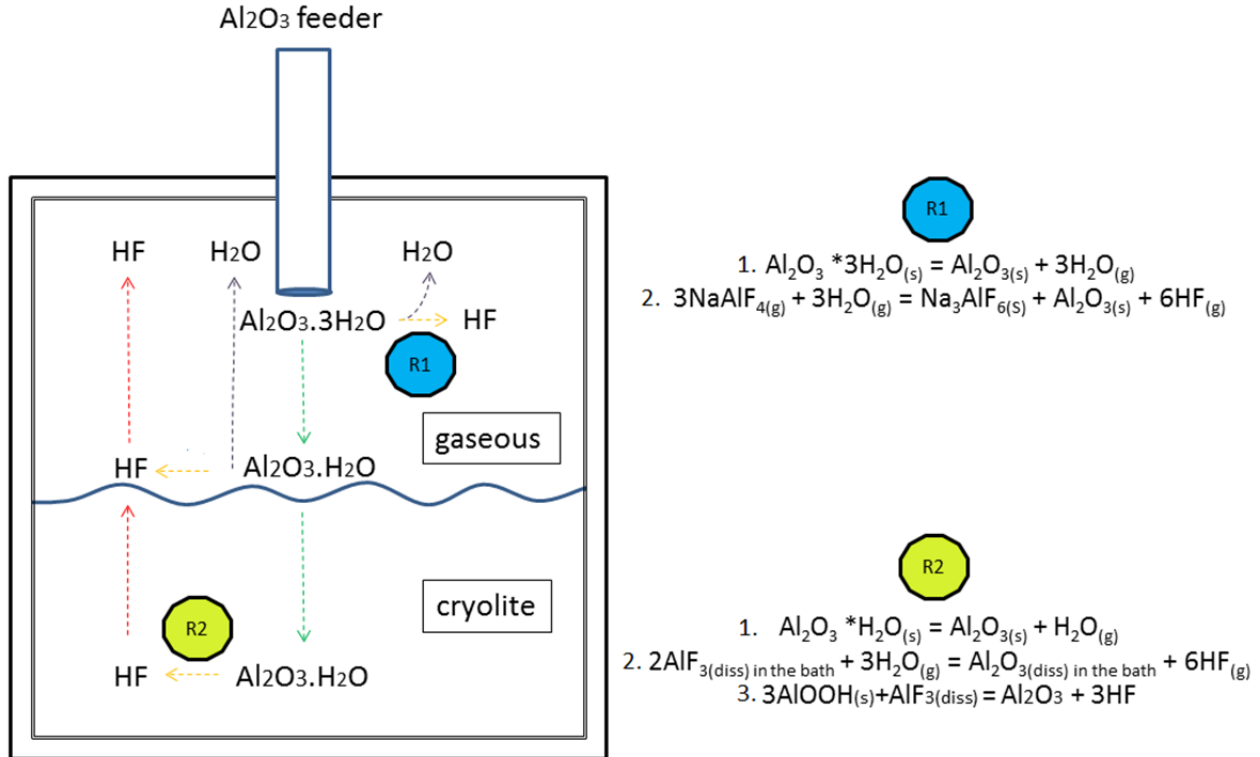


Figure 7. Illustration of HF formation inside the experimental cell

Figure 7 shows when SGA which contain different types of alumina water (physisorbed, gibbsite, etc) goes down into the laboratory furnace, while some water evaporated as water (R.1.1). And consequently, some water vapor reacts with NaAlF_4 (R1.2). When the alumina is immersed in the bath, there is bath hydrolysis from dissolution of SGA and water released from γ to α phase in dissolved SGA. Some water evaporates as water (R2.1) or reacts with fluorides in the vapor or reacts with HF at the bath surface (R2.2). Some water is released in longer time when the alumina is dissolved in the bath. Some of this water may react with the bath to HF (R2.3). According to Dando et al ⁽¹⁶⁾ the last reaction (R2.3) represent hydrolysis of boehmite from flash dehydration of gibbsite and gamma phase. Furthermore some of hydrogen goes into melted pure aluminium, some of them dissolved in the metal and some other escape the cell.

3. EXPERIMENTAL METHODS

The following chapter is mainly taken from chapter 3 of autumn project work ⁽⁵⁾ with the same title. In this chapter, the methods of the experiments will be presented.

3.1 ALUMINAS AND CRYOLITE

There were two types of smelter grade alumina i.e. type A and B, which were used during the experiment. According to previous autumn work alumina B releases more HF than alumina A. Due to secondary alumina has complex additives and contains adsorbed HF in the surface and this experiment concerns to the kinetic of HF formation inside the furnace, then only primary alumina (alumina before entered the dry scrubber and adsorbed HF in the surface) was used.

Cryolite consisting NaF and AlF₃ was applied in this experimental work. AlF₃ was sublimated at 1090°C under vacuum condition for almost 24 hours to remove oxides. NaF was heated up to 160°C in the heater before used. AlF₃ was crushed in the crusher before it is mixed with the fine powder of NaF. The same cryolite ratio of 2.2 and the same amount of AlF₃, NaF₃ and Al₂O₃ were used. This is also very close to the standard industrial bath composition. The detail for the calculation of NaF and AlF₃ is shown in Appendix C.

Table 3. Conditions of supplied reagent

| Bath Component | Producer | Pre-treatment | Amount (g) |
|---|------------------|------------------|------------|
| AlF ₃ | Noralf/Norzink | Sublimated | 71.42 |
| NAF | Fluka Analytical | No pre-treatment | 78.59 |
| Al ₂ O ₃ A | Confidential | Calcined 1200°C | 0.15 |
| Al ₂ O ₃ B | Confidential | No pre-treatment | 0.15 |
| Sum (excl. add of Al ₂ O ₃) | | | 150 |

3.2 MASS LOSS CHARACTERIZATION – LOI

LOI measurement was performed in three ranges of temperature, i.e. room temperature up to 160°C, 160°C up to 350°C and 350°C up to 1000°C. This temperature ranges were chosen to differentiate which type of adsorbed water (physisorbed, chemisorbed and structural hydroxyl) was evaporating and causes the mass loss.

The measurement of each type of alumina was performed on two parallel samples. The samples were heated for two hours in each temperature range. Each sample with weight 5g was put in platinum crucible, In order to ensure the moisture to evaporate without any barrier, heating was done without the lid at the top of the crucible. After heated for two hours, samples were put out from the furnace and covered with the lid to avoid influence of moisture from environment. All the samples were cooled down on a refractory plate and as soon as possible were brought to the analytical balances. Consequently the weight of the mass loss was measured.

3.3 LOI IN FUNCTION IN TIME (160°C)

Same as LOI in the previous sub chapter, the measurement of each type of alumina was performed on two parallel samples. Five grams of sample was put in the platinum crucible and then heated up to temperature 160°C. To ensure the moisture was evaporated without any barrier, heating was done without the lid at the top of the crucible. Before the samples were brought to analytical balances to weigh the mass loss, the samples were took out from the furnace and placed on a refractory plate. The crucibles were then covered with the lid to avoid the influence of moisture from environment.

The first five measurements were performed for each two hours and the next measurements conducted in random time. After conducting five measurements within one day, the samples were kept in the heater and measurement of the LOI of alumina A and B in function of time (160°C) keep continued for three months long.

3.4 NEO LASERGAS II SINGLE GAS MONITOR

The measurement of the reaction rate of HF formation and its concentration in ppm and also the measurement of the percentage of H₂O in these experiments were performed by using a Neo Laser Gas II Single Gas Monitor. This diode laser was connected with the furnace and it measured the concentrations of HF and water in the nitrogen flow, which was exiting the furnace.

“The Laser Gas Monitor utilizes a transmitter/receiver configuration (mounted diametrically opposite each other) to measure the average gas concentration along the line-of-sight path. The measuring principle is infrared single-line absorption spectroscopy, which is based on the fact that each gas has distinct absorption lines at specific wavelengths”.⁽¹⁷⁾

3.5 LASER TESTING AND VERIFICATION

Before experiments were performed, the testing and verification of the laser had been carried out to ensure that the laser can work well. The moisture concentration testing was performed by purging nitrogen through three glass bubble flask containing water that held a temperature around 10°C. Eventually nitrogen enriched with moisture (approximated 1%) was introduced into the laser. Mass flow controller A and B had previously been calibrated for nitrogen and were used to control the gas flow. The flow diagram is showed in Figure 8 and the result of the calibration is presented in figure 8.

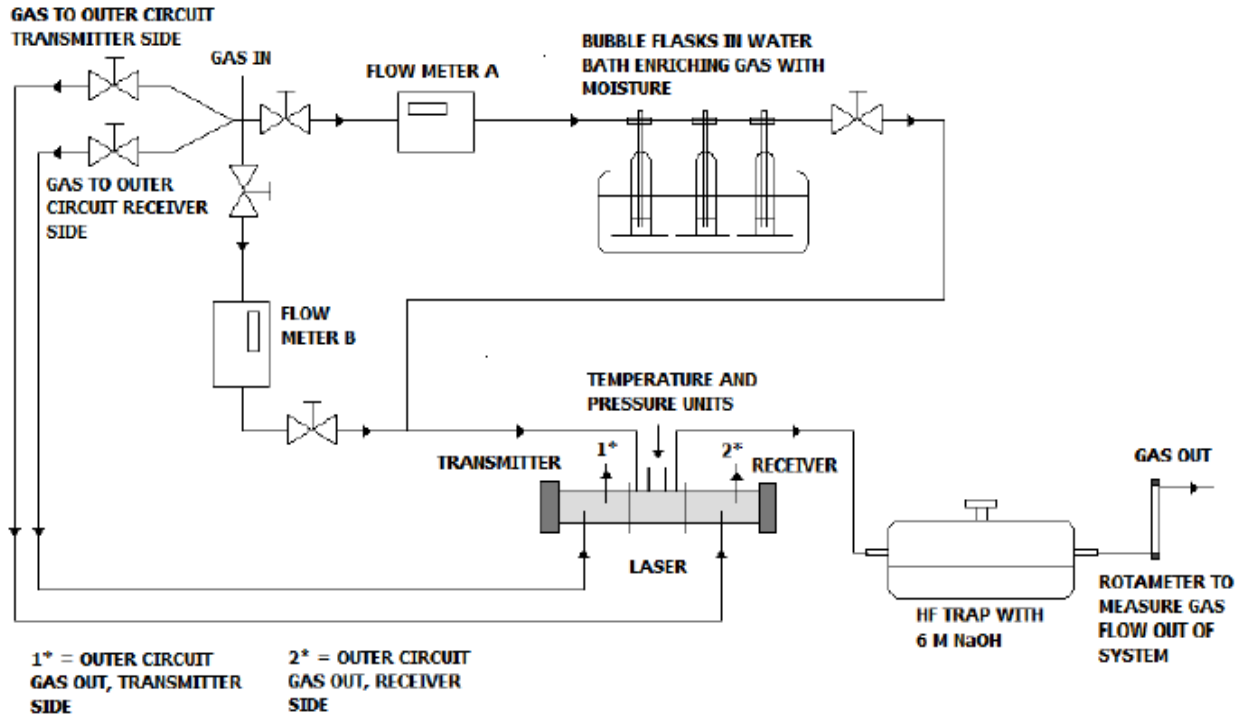


Figure 8. Schematic experimental setup of the laser to verifying HF and H₂O concentration ⁽²⁰⁾

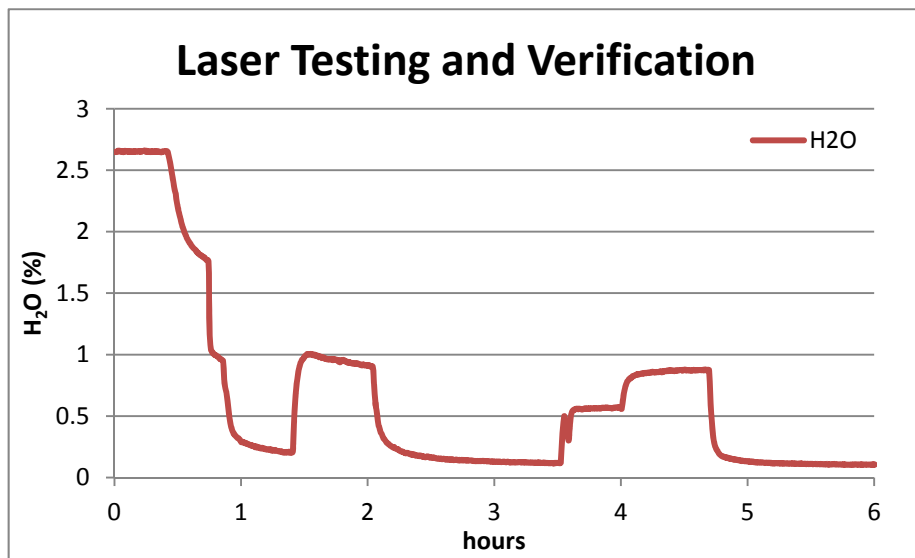


Figure 9. Laser testing and verification using nitrogen enriched with moisture

Figure 9 shows laser testing using nitrogen enriched moisture. It is clear that moisture reaches the approximate theoretical value of H₂O, i.e. around 1% when nitrogen was purged into the furnace.

3.6 LABORATORY EXPERIMENTAL SETUP

3.6.1 NICKEL CONTAINER

Before start the experiments, inconel and nickel became an option to use for the container. Inconel is a nickel chromium alloy, which is much stronger but less pure than nickel. In this work, the nickel container is being chosen to use because it less reacted to HF as compared to inconel.

The new design of the container was made in order to avoid leakage as good as possible and seal the volume much better than the previous work. The size of the nickel container should be fit with the experiment because when the container is too large, most of the water will stay inside the container. While when the container is too small all the water will go out without any chance to react with fluoro compounds. Nickel was preferred as the material inside the furnace both to avoid adsorbed water from oxide material in the set up to enter the furnace and to avoid HF adsorbing on the container in the furnace. Both these two factors could lead to an unwanted higher baseline during the HF measurements.

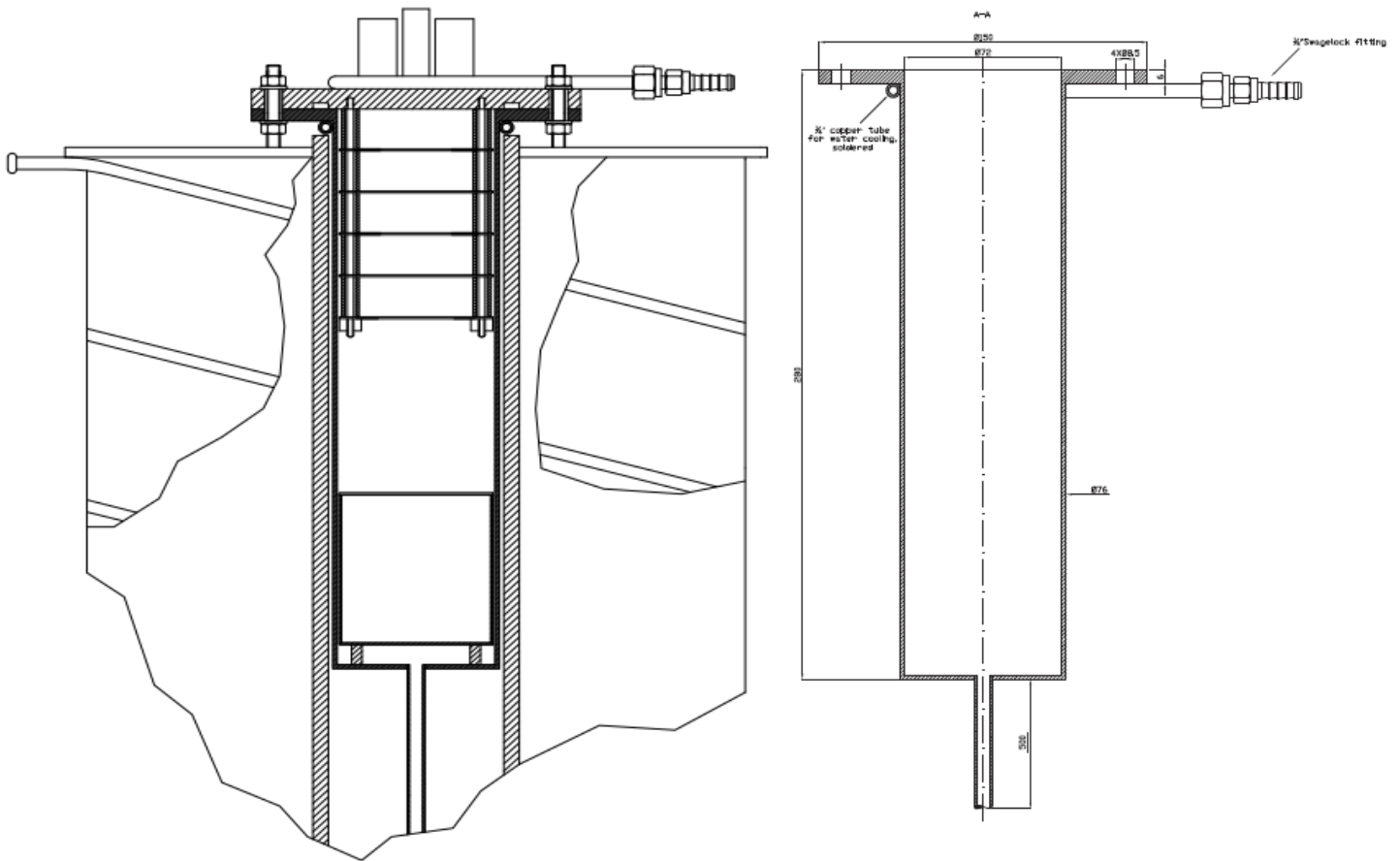


Figure 10. Drawing of the experimental set up inside the furnace by Aksel Alstad

Figure 10 shows the experimental setup inside the furnace. The Pythagoras is being used as a support system. In this figure there are three holes on the top of the lid. The bigger holes are used for feeder tube and gas outlet tube. The smaller hole in the middle is used for thermocouple. The feeder tube has the size of $od=10\text{mm}$, $id=8\text{mm}$, $h=40\text{mm}$ and the outlet gas tube has the size of $od=10\text{mm}$, $id=8\text{mm}$, $h=50\text{mm}$. The materials for those tubes were made from nickel. The material tube for thermocouple ($\phi=4\text{mm}$, $h=40\text{mm}$) was made from alsint. Thermocouples of type S were used in this process. It was constructed using 90% Platinum and 10% Rhodium for the positive wire and of 100% platinum for the negative wire). This thermocouple survives up to temperature of $1600\text{ }^{\circ}\text{C}$. During the experiment, nickel crucible ($h=5.9\text{cm}$, $\phi_{\text{top}}=6.5\text{cm}$, $\phi_{\text{bottom}}=5.9\text{cm}$) without lid was used as electrolyte container. As shown in Figure 10, nickel container volume of 1140ml was used. The detail part sizes of the container are attached in the Appendix A.

In this thesis work, three experimental works were conducted to check the methodology and reproducibility of HF and H₂O measurement with the new set up.

3.6.2 MELT EXPERIMENTS

Similar to the experimental setup for the laser verification of HF and H₂O concentration, 1/8” PFA tubes were used to transport nitrogen gas which was used during the experiment. Prior to the experiment, dry nitrogen was purged through the outer circuits of the laser to remove moisture from the transmitter and receiver compartments. Flow meter A and flow meter C were used to control nitrogen gas flow through the bottom of the furnace. These are the main flow of the gas into the furnace. The flow meter C provides higher flow rate of nitrogen gas comparing with flow meter A. When high flow rate is needed flow meter A will be closed and the nitrogen will be flowed through flow meter C.

As shown in Figure 11, flow meter B was used to control nitrogen gas flow from the alumina feeder tube from the lid of the furnace (this flow rate is always the same in all alumina additions of experiments). The function of this gas flow is to help the alumina goes down to the crucible and also to avoid plugged of alumina inside the feeder tube. In this thesis works, lid of the melt crucible was not used any longer.

In these experiments, total nitrogen gas flow was purged through the furnace with five variation of the flow (see Table 4). Inert nitrogen carried HF gas from the furnace through the laser for analysis. After leaving the laser, nitrogen leads HF to the HF trap containing 6M NaOH in order to neutralize HF into sodium fluoride. A rotameter was placed after the HF trap to measure the out flow gas and to check whether there was a leakage or not in the system. The remaining gas left the system through the ventilation system in the laboratory.

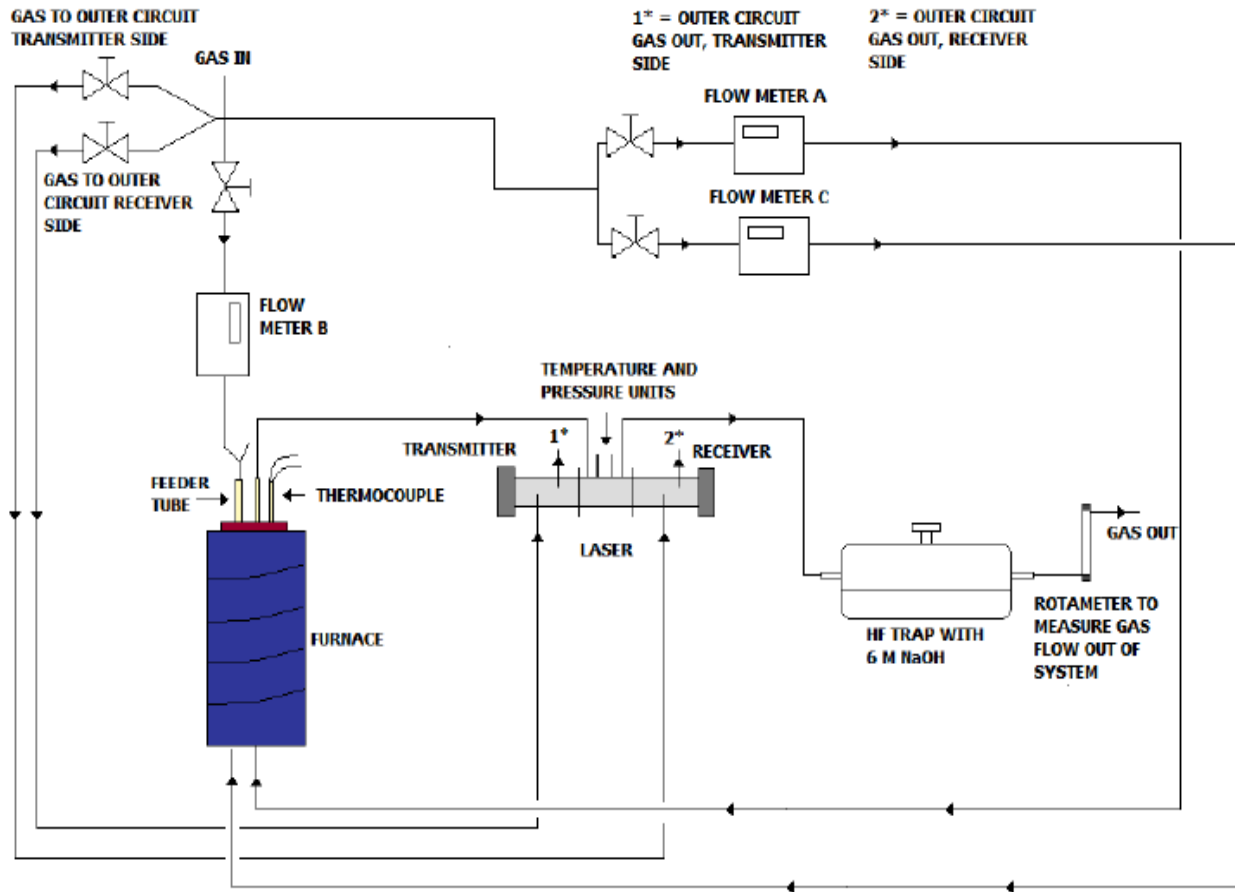


Figure 11. Schematic laboratory setup of the laser when performing experiment to see HF formation by addition of alumina and variation of nitrogen flow ⁽¹⁾

3.6.3 ARGON WITH 1% HF EXPERIMENT

Since there wasn't any gas controller in the argon 1% HF gas cylinder, rotameter after gas cleaning system was used to measure and control the gas quantity. In all addition of this experiment, 238 ml/min argon with 1% HF was purged directly to the furnace for one minute.

Due to the density difference between argon with 1% HF and nitrogen, nitrogen purged first in the one of the flow rate in Table 4 until it stable and then it was flowed out from the system for a while when argon with 1% HF was purged to the system. When argon with 1% HF was stable,

nitrogen gas was flowed in again to the system and the mixed flow rate gas was measured. This sequent was developed in order to control and in order to get the same quantity of argon with 1% HF gas for each addition. Three ways valve was used to control the duration of the mixed gas argon with 1% HF and nitrogen goes in to the furnace. Figure 12 shows the set-up of the argon with 1% HF experiment.

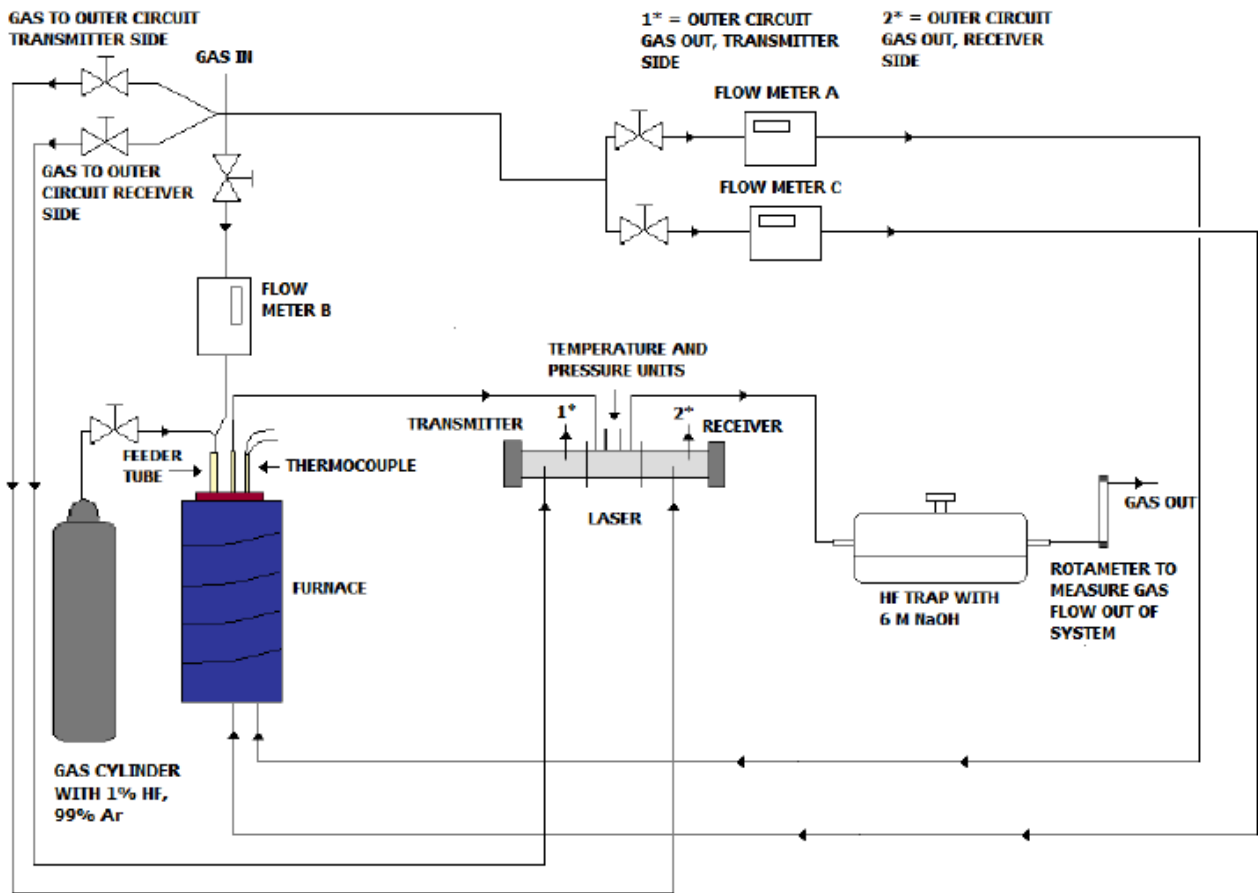


Figure 12. Schematic laboratory setup of the laser when performing experiment to see amount of HF from argon with 1% HF and variation of nitrogen flow rate

3.6.4 ALUMINA WATER EVOLUTION EXPERIMENTS

Instead of using nickel container as applied in the argon with 1%HF and melt experiments, these experiments were performed using quartz as a container with thickness, inner diameter and

height were 2mm, 58mm, and 95mm, respectively. The total volume of this container was 830ml. In the alumina water evolution experiments, nitrogen gases were flow in and out through the top of the container. It is noted that position of the outlet gas tube was higher than the inlet gas tube. Except of the inlet and outlet gas configurations and also the volume of the quartz container, the schematic of the laboratory set up was the same as the melt experiments.

There was not any electrolyte being used in these experiments. Dried alumina and room temperature alumina A and B were dropped from the feeder tube into the empty container. The water released (% H₂O) from the alumina is carried out from the furnace to the laser by nitrogen.

3.7 EXPERIMENTAL PROCEDURE

3.7.1 MELT EXPERIMENTS PROCEDURE

NaF and AlF₃ were weighed out on an analytical balance and mixed thoroughly in the nickel crucible. The Ni-crucible was placed in the furnace. In order to ensure that there was no leakage, rubber ring under the lid was smeared with grease prior the lid of the furnace was closed and screwed. The furnace was closed with little bit loosening the screw because when the temperature is rising, the furnace will become tighter. The furnace was preheated (by means of automatic programming) over night at 200°C to remove any surface moisture in the NaF-AlF₃ mixture. In the following day furnace temperature was increased to 700°C and several hour before experiment was performed, temperature of the furnace was increased up to 1000°C.

When the NaF-AlF₃ mixture had melted and a stable HF concentration baseline had been reached, 0.15 g alumina powder which was put inside the glass feeder tube was weighed out and added to the melt through the feeder system and the feeder tube. Between each addition of the alumina into the bath, the silicon tube and the glass feeder tube had to be changed. A clamp squeezed the silicon tube, and this clamp was unscrewed to release the alumina into the bath. The HF and H₂O concentrations measured by the laser were logged by a computer. New additions of alumina were made when a new stable baseline of HF had been reached.

As part of the procedure for melt, quart and Ar1% HF experiments, the 1/8" PFA gas tube leading the gas out of the system was cleaned every time the feeder container had to be cleaned (in between every feeding of the cell). The gas outlet tube was changed to prevent it from getting blocked by condensation from the bath. The gas flows through mass flow controller A, B and C are summarized in Table 4 below,

Table 4. Gas flow variation

| Flow Meter Gas Flow | Rotameter A (main flow from the bottom of the cell) | Rotameter B (flow through alumina addition tube) | Rotameter C (main flow from the bottom of the cell) |
|------------------------|---|--|---|
| Lowest flow | 7 ml/min | 20 ml/min | - |
| Low flow | 77 ml/min | 20 ml/min | - |
| Normal flow | - | 20 ml/min | 234ml/min |
| High flow | - | 20ml/min | 680ml/min |
| Highest flow | - | 20ml/min | 1013ml/min |

3.7.2 ALUMINA WATER EVOLUTION EXPERIMENTS PROCEDURE

After the furnace reached 1000°C and stable water concentration baseline in the laser had been reached, 0.15 g alumina powder inside the glass feeder tube was added into the furnace through the feeder system. Between each addition of alumina into the bath, the silicon tube and the glass feeder tube had to be changed. A clamp squeezed the silicon tube, and this clamp was unscrewed to release the alumina into the bath. The H₂O concentrations were logged by a computer. New additions of alumina were made when a new stable baseline of H₂O had been reached.

3.7.3 ARGON WITH 1% HF EXPERIMENT PROCEDURE

When the set-up was ready and the laser detected stable HF concentration baseline, 10000ppm HF from argon with 1% HF gas was purged into the empty nickel container through the feeder system for one minute. The HF concentrations were logged by a computer. New additions of argon 1% HF were made when a new stable baseline of HF had been reached.

4. CSTR MODELING

Continuous Stirred Tank Reactor (CSTR) is an idealized model used to describe well mixed systems. CSTR modeling can be used to estimate the residence times of the gas inside the experimental set-up furnace and the expected exit concentrations. Since this experimental set-up furnace can be considered as a reactor, explanation about the theories and models used in the work will be described in this chapter.

4.1 FLOWING REACTORS

Two types of flowing reactors which common to be used are the CSTR and the PFR.

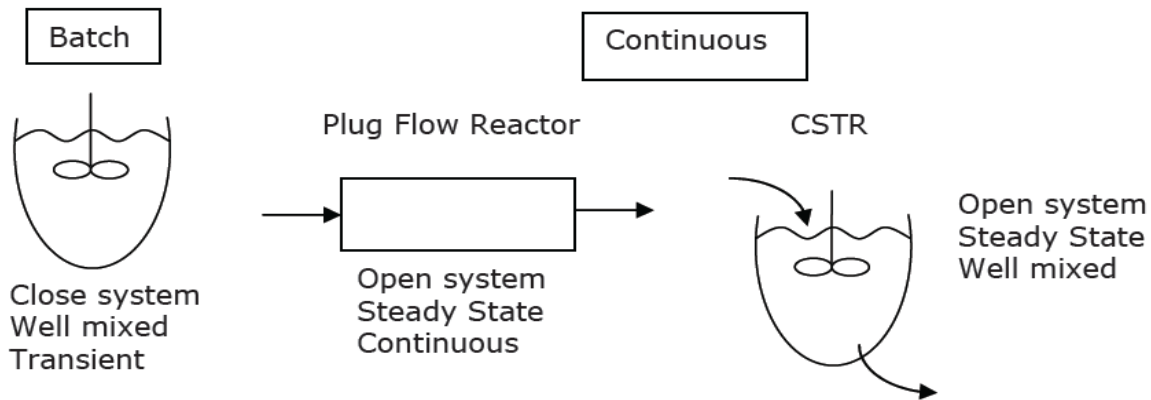


Figure 13. The types of reactor ⁽¹⁷⁾

The continuous stirred tank reactor (CSTR) is configured like a batch reactor except reactants and products continuously flow as input and output of the reactor. A plug flow reactor (PFR) can be configured as a pipe into which reactants are injected into one end and products flow out the other. ⁽¹⁸⁾

There are some basic assumptions made in analyzing CSTR reactors which listed below,

- a. The reactor runs at steady state i.e. all of the time derivatives go to zero.

- b. None of the variables (i.e. temperature, concentration, reaction rate) are functions of position, i.e. all of the spatial derivatives go to zero.
- c. The conditions that exist at the exit are the same as those everywhere in the reactor.

4.2 CSTR ARGON WITH 1% HF EXPERIMENT

Argon with 1% HF experiment was made to know whether the experimental set-up behaved very close with CSTR or not. Figure 14 shows the CSTR assumption for the argon with 1% HF experiment. By using assumption below, the CSTR model for this experiment can be calculated.

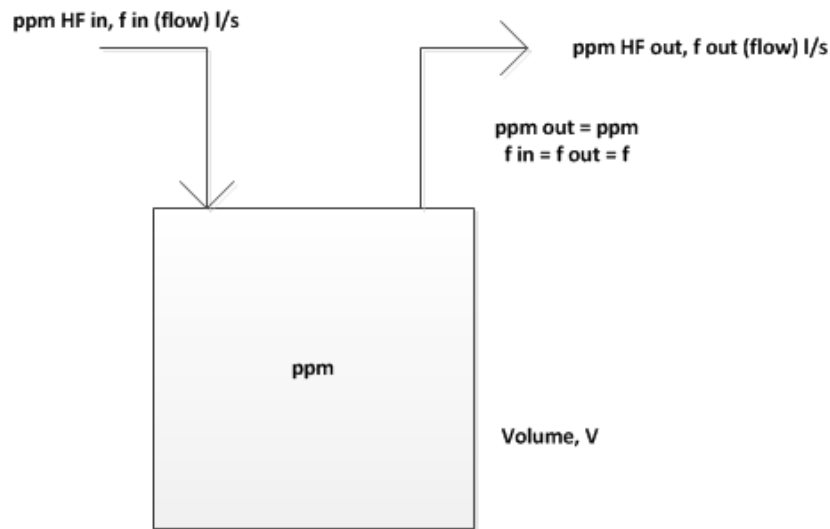


Figure 14. CSTR assumption for the argon 1% HF experiment

Mass Balance,

Molar flow water in = Molar flow water out + accumulate

$$\frac{dn_{in}}{dt} = \frac{dn_{out}}{dt} + \frac{dn}{dt} \quad (4.1)$$

$$ppm_{in} \cdot f = ppm_{out} \cdot f + \frac{dppm}{dt} V \quad (4.2)$$

$$\frac{f}{V}(ppm_{in} - ppm) = \frac{dppm}{dt} \quad (4.3)$$

$$\int_0^t \frac{f}{V} dt = \int_{ppm_0}^{ppm} \frac{dppm}{(ppm_{in} - ppm)} \quad (4.4)$$

Final equation

$$ppm f = ppm (in) + (ppm_0 - ppm in) \exp\left(-\frac{f}{V} \cdot t\right) \quad (4.5)$$

f = ppm HF in l/s

V= volume

t = time

There were two regimes being used in this experiment, first when adding argon with 1% HF together with the nitrogen flow for one minute and the second when argon with 1% HF flow was stopped and only the nitrogen flow maintained. In this time ppm was in equal with 10000ppm and second assumption when switching to nitrogen normal dilution was start and ppm in equal with 0. In the formula above, ppm 0 is the initial HF concentration at time equal with 0.

4.3 CSTR ALUMINA WATER EVOLUTION AND MELT EXPERIMENTS

An option to describe water release among many others is CSTR. CSTR were calculated using final equation 4.12. Water evolution rate from the alumina was calculated using equation 4.13.

CSTR

In reality F_{in} is not constant but in CSTR model it can be assumed F_{in} constant in certain time.

$$F_{in} = c \cdot f + \frac{dc}{dt} V \quad (4.6)$$

$$\frac{dt}{V} = \frac{dc}{F_{in} - c \cdot f} \quad (4.7)$$

$$\int_0^t \frac{dt}{V} = \int_{c_0}^c \frac{1}{F_{in} - c \cdot f} dc \quad (4.8)$$

$$\frac{t}{V} = \frac{-1}{f} \ln \left(\frac{F_{in}-c.f}{F_{in}-c0.f} \right) \quad (4.9)$$

$$\exp \left(\frac{-f}{V} \cdot t \right) = \frac{F_{in}-c.f}{F_{in}-c0.f} \quad (4.10)$$

$$c = \frac{F_{in}}{f} \left(1 - \exp \left(\frac{-f}{V} \cdot t \right) \right) + c0. \exp \left(\frac{-f}{V} \cdot t \right) \quad (4.11)$$

Final equation for water concentration

$$c(\Delta t) = \frac{F_{in}(t)}{f} \left(1 - \exp \left(\frac{-f}{V} \cdot \Delta t \right) \right) + c0. \exp \left(\frac{-f}{V} \cdot \Delta t \right) \quad (4.12)$$

The water concentration curve can be calculated for each time step Δt . Every CSTR step where water release from alumina is suggested constant in period Δt . In the calculation of CSTR modeling, initial concentration taken into account in the first point of calculation due to the different baseline or water background in the experimental never reached 0. The water concentration found after a time step is used as the initial concentration in the next time step.

Rate equation for water evolution

$$F_{in}(t) = \frac{n0}{\sqrt{a.\pi}} \exp \left[\frac{-(t-tmax)^2}{a} \right] \quad (4.13)$$

$F_{in}(t)$ = water released from alumina as a function of time (mol/s)

c = concentration in reactor and outgoing flow (mol/l)

V = volume of container (l)

f = flow in and out of container (l/min)

t = time (s)

$n0$ = water released from alumina (mol)

a = the wide of the curve and it indicate how quickly the water release is happen (s^2)

t_{max} = parameter of time when temperature reach the peak in water evolution curve (s)

The value of $F(t)$ is used as the average water release rate.

From the equation above, all the variables are taken from the experimental data except n_0 , t_{max} and a . To understand the influence of those three variables, two examples below are given.

When all the variables are the same and $t_{max} = 50$ and $a = 1500$, the curve will look like in the Figure 15, blue curve is f function. Water evolution doesn't start from 0.

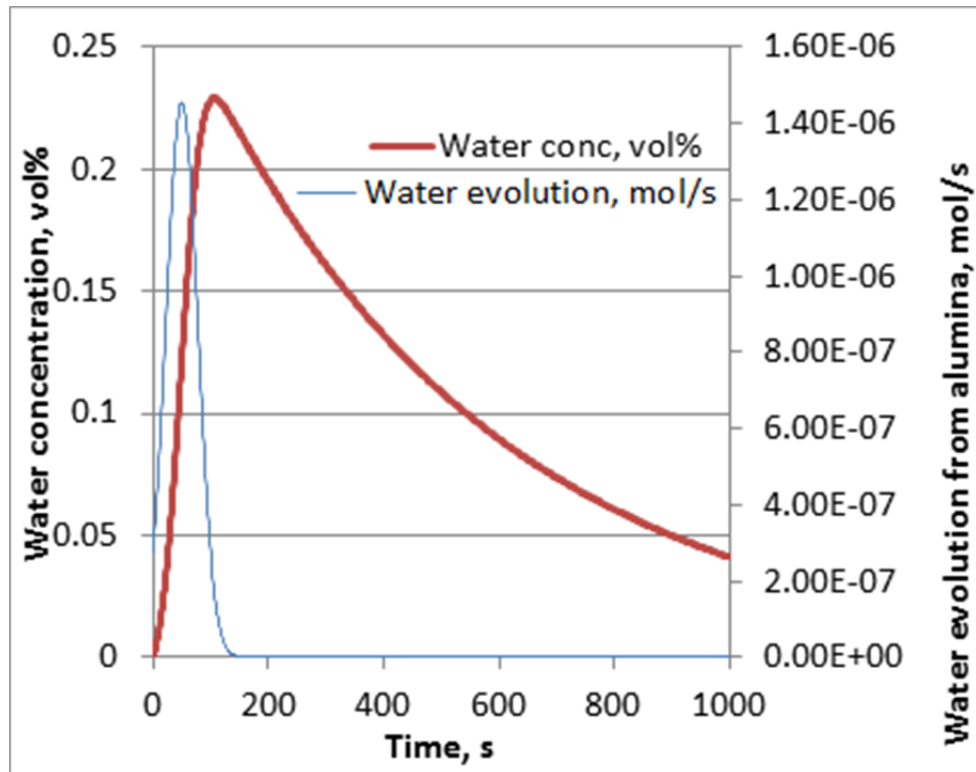


Figure 15. Example of the CSTR plot 1

And when we changed the $t_{max} = 100$ and $a = 10000$ the curve will change as below,

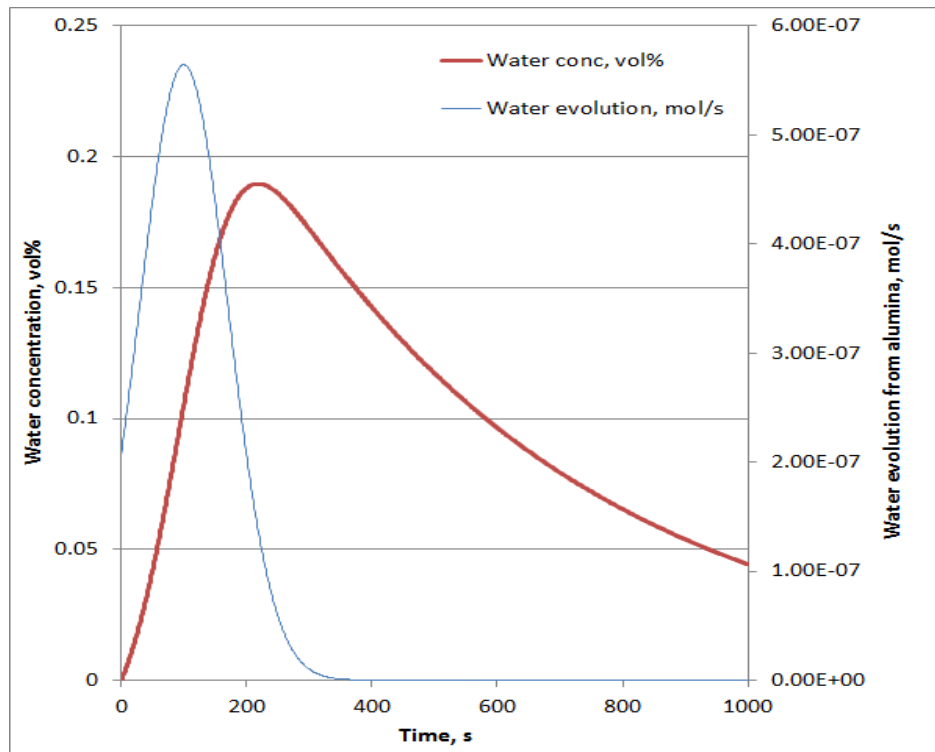


Figure 16. Example of CSTR Plot 2

From the two examples in Figure 15 and Figure 16 above, it can be seen the position of the blue curve peak changed when t_{max} changed from 50 to 100s. In this model, t_{max} is the time at which water evolution is at its maximum in water evolution and a value indicate how fast water released happen. The red curve width will change when the value of a is changed. Blue curve shows how water released from alumina, hardly bound shows long t_{max} and large a while loose bound shows shorter t_{max} low and lower a . t_{max} and a value is different for every type of alumina. Table 5 in the next page shows value of t_{max} and a which being used in the CSTR modeling. Since a and t_{max} are related to the water release kinetics from the alumina, the value should not change with the flow rate. The a and t_{max} values listed were simply found by visual curve fitting the model to the experimental data.

Table 5. Value of t_{max} and a which is used in CSTR modeling

| Alumina type | t_{max} (s) | a (s ²) |
|----------------------------|---------------|-----------------------|
| Room Temperature alumina B | 75 | 1500 |
| Dried alumina B | 50 | 800 |
| Room Temperature alumina A | 70 | 2000 |
| Dried alumina A | 50 | 1500 |

Example of CSTR model from alumina water evolution is taken to show the detail of the application of the formula.

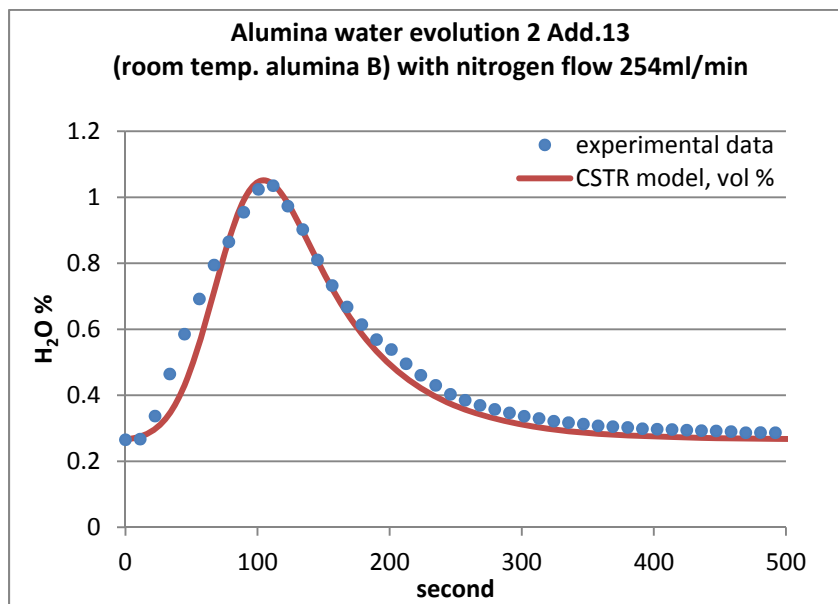


Figure 17. Alumina water evolution experiment 2 Add.13 (room temperature alumina B) with nitrogen flow 254ml/min

Table 6. Data description of Figure 17

| data description of Figure 17 | value |
|-------------------------------|-------------|
| nitrogen flow rate (ml/min) | 254 |
| volume of the quartz cell (l) | 0.83 |
| t_{max} (s) | 75 |
| a (s ²) | 1500 |
| n_0 (mol) | 1.81913 E-4 |
| flow rate (l/s) | 0.01337 |
| temperature (K) | 862.4291 |

5 RESULT

5.1 MATERIAL CHARACTERIZATION OF ALUMINA A AND ALUMINA B

In order to characterize the sample of smelter grade alumina A and B, LOI and LOI as function of time (160°C) have been done.

5.1.1 LOI OF SMELTER GRADE ALUMINA A AND ALUMINA B

In this thesis work, the average LOI values from two parallel samples were measured with standard. LOI in temperatures range 160°C, 350°C and 1000°C are presented. In LOI 1000°C, undried basis was calculated with room temperature alumina as denominator while dried basis was calculated with dried alumina (350°C) as denominator.

Appendix E will show how to calculate the moisture loss in three range temperatures. The average and standard deviation of undried and dried basis LOI are presented in Table 7. In this table, mass loss of alumina B is higher than alumina A in all temperature ranges. The total mass loss of alumina B is also 0.5 fold bigger than alumina A.

Table 7. Average undried basis and dried basis LOI measurement of alumina A and B in 160°C, 350°C and 1000°C

| Type of Al ₂ O ₃ | UNDRIED BASIS | | | | | DRIED BASIS | | |
|--|------------------------------|------------------------------|-------------------------------|----------------------|----------------------|-----------------------------|----------------------|----------------------|
| | LOI 160°C Avg±stdv (%) | LOI 350°C Avg±stdv (%) | LOI 1000°C Avg±stdv (%) | Total LOI 160-1000°C | Total LOI 350-1000°C | LOI 1000 Avg±stdv (%) | Total LOI 160-1000°C | Total LOI 350-1000°C |
| Al ₂ O ₃ A | 1.12+0.0032 | 0.51+0.003 | 0.79+0.022 | 2.42 | 1.3 | 0.8+0.022 | 2.43 | 1.31 |
| Al ₂ O ₃ B | 1.74+0.007 | 0.86+0.018 | 0.95+0.01 | 3.55 | 1.81 | 0.97+0.01 | 3.57 | 1.83 |

5.1.2 LOI AS FUNCTION OF TIME AT 160°C BULK ALUMINA A AND ALUMINA B

LOI as function of time at 160 °C also measured. The measurement of LOI in function of time is performed to observe the limiting time of the physisorbed water stays in the alumina surface.

Before calculating LOI as function of time for about 1774 hours at 160°C, weight loss as function of time was calculated. The result of the weight loss as function of time is given in Table 8. To see the trend, the data is plotted in the Figure 18. From 10 times weight loss measurement in the Figure 18, the biggest mass loss happen in the first two hours while afterwards there is also mass loss but only in the small amount and sometime it's very easily changed due to moisture contamination from the air when the crucible is carried from the heater to the balance. Whilst data of LOI (160°C) as function of time is presented in Table 9 and Figure 19. It is noted that sample alumina B2 tumbled and some of the powder spilled out before it was weighted for the last time.

Table 8. Weight of alumina (Al₂O₃) A and B as function in hours at 160°C

| Hours | Weight sample Al ₂ O ₃ A1 (g) | Weight sample Al ₂ O ₃ A2 (g) | Weight sample Al ₂ O ₃ B1 (g) | Weight sample Al ₂ O ₃ B2 (g) |
|-------|---|---|---|---|
| 0 | 5.0018 | 5.008 | 5.0054 | 5.0005 |
| 2 | 4.9363 | 4.9446 | 4.8958 | 4.9153 |
| 4 | 4.9355 | 4.9434 | 4.8933 | 4.9138 |
| 6 | 4.9347 | 4.9421 | 4.8918 | 4.9122 |
| 8 | 4.9346 | 4.9429 | 4.8927 | 4.9126 |
| 28 | 4.9319 | 4.9409 | 4.8884 | 4.9088 |
| 72 | 4.931 | 4.9389 | 4.8842 | 4.9067 |
| 142 | 4.9293 | 4.9392 | 4.8851 | 4.9066 |
| 862 | 4.9325 | 4.94 | 4.8856 | 4.9019 |
| 1294 | 4.9319 | 4.9387 | 4.8842 | 4.9028 |
| 1774 | 4.9322 | 4.9397 | 4.884 | X |

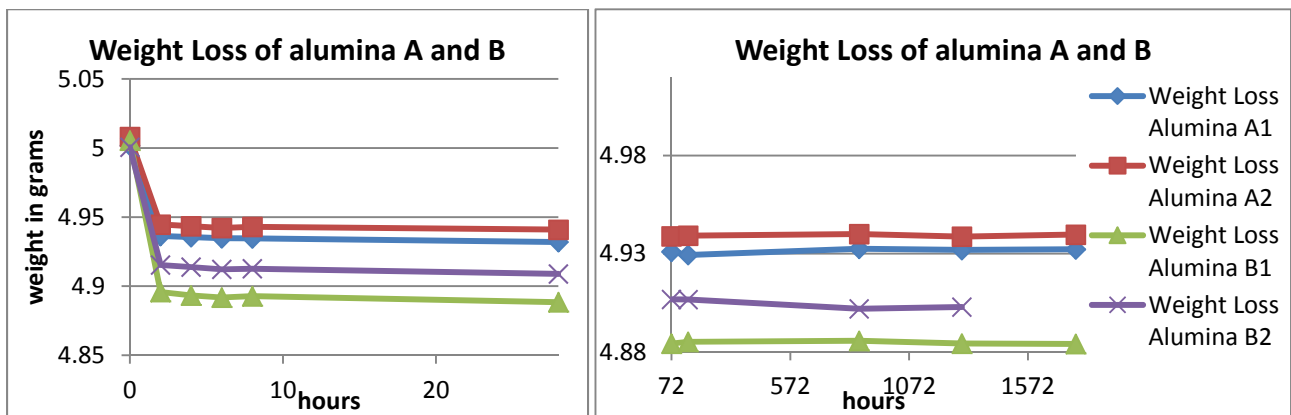


Figure 18. Weight loss of alumina A and B within 1774hours

Table 9. Loss on ignition of alumina (Al₂O₃) A and B as function of time at 160°C

| hours | LOI Al ₂ O ₃ A1 (%) | LOI Al ₂ O ₃ A2 (%) | LOI Al ₂ O ₃ B1 (%) | LOI Al ₂ O ₃ B2 (%) |
|---------|---|---|---|---|
| 2 | 1.3095 | 1.2660 | 2.1896 | 1.7038 |
| 4 | 1.3255 | 1.2899 | 2.2396 | 1.7338 |
| 6 | 1.3415 | 1.3159 | 2.2695 | 1.7658 |
| 8 | 1.3435 | 1.2999 | 2.2516 | 1.7578 |
| 28 | 1.3975 | 1.3399 | 2.3375 | 1.8338 |
| 72 | 1.4155 | 1.3798 | 2.4214 | 1.8758 |
| 142 | 1.4495 | 1.3738 | 2.4034 | 1.8778 |
| 862 | 1.3855 | 1.3578 | 2.3934 | 1.9718 |
| 1294 | 1.3975 | 1.3838 | 2.4214 | 1.9538 |
| 1774 | 1.3915 | 1.3638 | 2.4254 | X |
| Average | 1.3757 | 1.3371 | 2.3353 | 1.8305 |

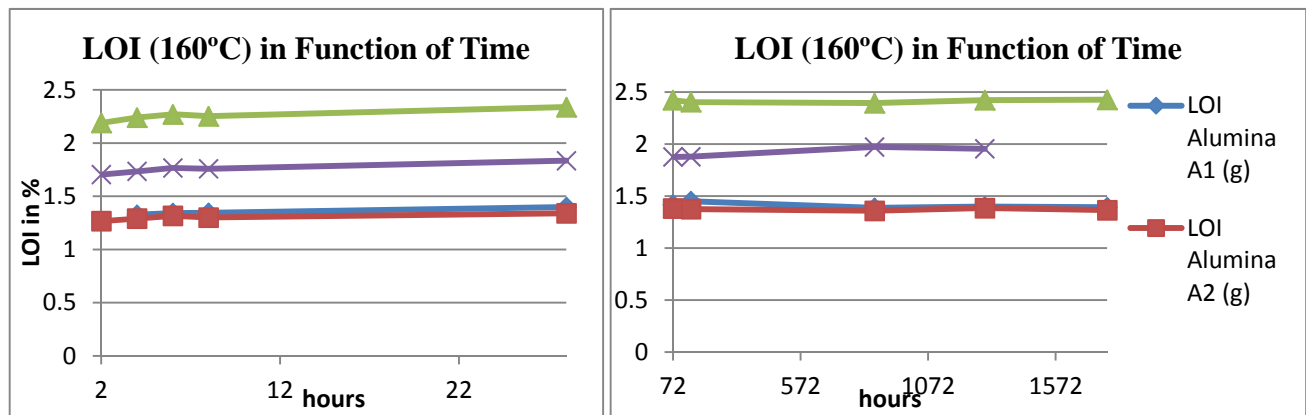


Figure 19. LOI in Function of Time within 1774 hours

5.2 THREE TYPES OF EXPERIMENTAL EXPERIMENTS

5.2.1 ARGON WITH 1% HF EXPERIMENT

Table 10 shows the addition of the Argon with 1% HF using four variations of nitrogen flow rate and constant argon flow. Theoretical amount of 1% HF (l/min) and mol HF also showed.

$$\text{Maximum theoretical HF} = 10000 \cdot \text{argon flow} / (\text{argon flow} + \text{nitrogen flow}) \quad (5.1)$$

The HF is flushed for one minute. The experiment of argon with 1% HF was conducted one time due to the result was reproducible and representative the main purpose of this experiment.

Table 10. The result of Argon (Ar) with 1% HF experiment which is flushed into the furnace for one minute with varied of nitrogen (N2) flow

| Add. no. | N2 flow (ml/min) | Ar flow (ml/min) | theoretical 1% HF (l/min) | theoretical mol HF | real HF (mol) | real HF (g) | Baseline (ppm) |
|-----------------|-------------------------|-------------------------|----------------------------------|---------------------------|----------------------|--------------------|-----------------------|
| Add. 1 | 254 | 237.8 | 0.00238 | 1.0616 E-4 | 2.1E-4 | 4.24E-3 | 4.0393 |
| Add. 2 | 254 | 237.8 | 0.00238 | 1.0616E-4 | 3.2E-4 | 6.51E-3 | 27.3146 |
| Add. 3 | 699 | 237.8 | 0.00238 | 1.0616E-4 | 4.0E-4 | 8.08E-3 | 7.2105 |
| Add. 4 | 699 | 237.8 | 0.00238 | 1.0616E-4 | 4.3E-4 | 8.72E-3 | 6.7526 |
| Add. 5 | 1033 | 237.8 | 0.00238 | 1.0616E-4 | 4.64E-4 | 9.28E-3 | 2.3752 |
| Add. 6 | 1033 | 237.8 | 0.00238 | 1.0616E-4 | 5.32E-4 | 10.63E-3 | 2.4160 |
| Add. 7 | 97 | 237.8 | 0.00238 | 1.0616E-4 | 2.68E-4 | 5.37E-3 | 9.2222 |
| Add. 8 | 97 | 237.8 | 0.00238 | 1.0616E-4 | 2.54E-4 | 5.09E-3 | 39.0807 |

From the laser, baseline for each addition in ppm and amount of HF in ppm is obtained for each 11.18 second. The amount of the real HF in mol and HF in grams was found by integral by Riemann sums to calculate the total area under the curve in each addition as shown in Figure 19. Baseline of the HF also shown in the Table 10, it's used in order to know the initial concentration (ppm₀) when adding Argon with 1% HF into the furnace. The baseline value has been subtracted from the total amount of HF for each point of measurement. The formula for Riemann sums given in Appendix D.

In the Figure 20, eight additions were performed. The nitrogen flow was 254ml/min, 700ml/min, 1033ml/min, and 97ml/min during the first and second additions, third and fourth additions, fifth and sixth additions, and seventh and eight additions, respectively. In this experiment, the slowest flow of nitrogen in addition 7 and 8 accumulated the highest peak of HF although the biggest amount of HF was reached in fastest flow addition 5 and addition 6 (see Table 10).

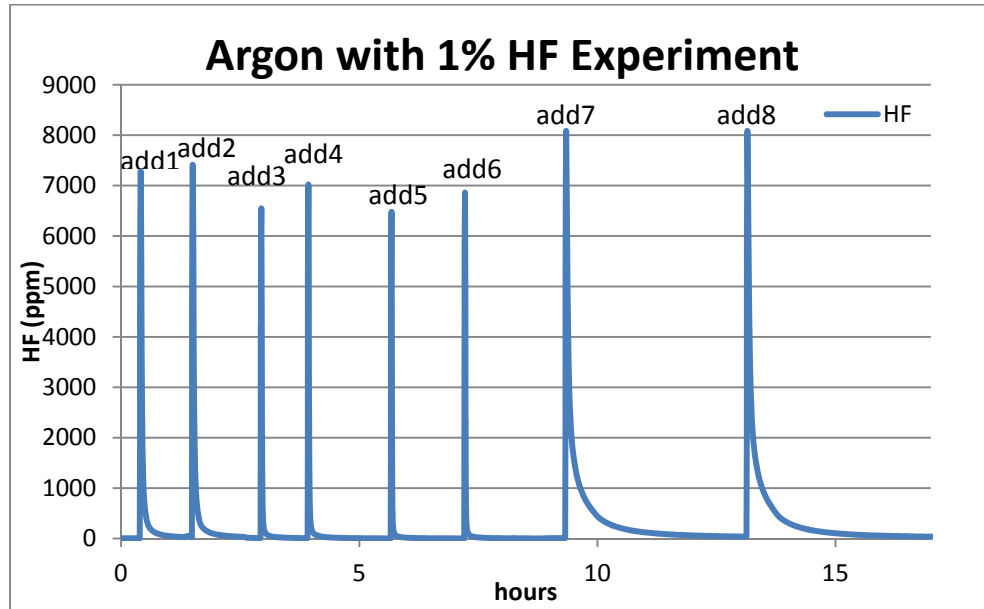


Figure 20. Eight addition of argon with 1% HF experiment with variation nitrogen flow rate

5.2.2 ALUMINA WATER EVOLUTION EXPERIMENTS

In this experiment dried alumina was added into an empty cell and the water which released from alumina was measured from the laser. From the laser reading, the baseline as initial concentration of H₂O in percentage for each addition and the amount of H₂O for each 11.18 second in ppm was obtained. The amount of the real H₂O in gram/gram Al₂O₃ was found by integral of Riemann sums. In order to calculate the total H₂O in g/gAl₂O₃, % H₂O divided by gram alumina which was dropped into the furnace. The amount of the alumina which was dropped should be less than 0.15g.

Two experimental series were conducted. In the first experiment series, eight additions had been done. In the first series, the flow rate of the nitrogen was made fixed (97ml/min). The room temperature alumina A, B and also dried alumina A and B were used. In the second series, 11 additions of dried alumina B and 1 addition of calcined alumina A had been done. In this experiment, nitrogen flow rate of 27ml/min, 97ml/min, 254ml/min were used. Ratio between %H₂O analysed on laser and total LOI (for temperature 350°C and 1000°C) were also calculated

(ideally this should be 100%). In Table 11 and 12 some parameter for CSTR i.e. t_{max} and a also presented.

Alumina Water Evolution Experiment 1

Table 11. Eight addition of alumina water evolution experiment 1 for room temperature alumina (Al_2O_3) A, B and dried alumina (Al_2O_3) A, B

| Add. no. | Al_2O_3 type | N2 flow rate ml/min | Baseline (ppm) | H_2O (g/g Al_2O_3) | Al_2O_3 (g) | ratio | nO H_2O (mol) | t_{max} (s) | a^2 |
|----------|-------------------|---------------------|----------------|-------------------------|---------------|--------|-----------------|---------------|-------|
| Add. 1 | RT Al_2O_3 A | 97 | 0.1115 | 0.0114 | 0.1264 | 0.5129 | 7.99E-05 | 70 | 2000 |
| Add. 2 | RT Al_2O_3 A | 97 | 0.1075 | 0.0144 | 0.1163 | 0.7166 | 9.3E-05 | 70 | 2000 |
| Add. 3 | RT Al_2O_3 B | 97 | 0.1169 | 0.0189 | 0.1343 | 0.6030 | 14.1E-05 | 75 | 1500 |
| Add. 4 | RT Al_2O_3 B | 97 | 0.1192 | 0.0186 | 0.1149 | 0.5619 | 11.9E-05 | 75 | 1500 |
| Add. 5 | dried Al_2O_3 A | 97 | 0.1112 | 0.0074 | 0.0815 | 0.5951 | 3.36E-05 | 50 | 1500 |
| Add. 6 | dried Al_2O_3 A | 97 | 0.1136 | 0.0065 | 0.1186 | 0.5001 | 4.25E-05 | 50 | 1500 |
| Add. 7 | dried Al_2O_3 B | 97 | 0.1122 | 0.0093 | 0.1278 | 0.5175 | 6.59E-05 | 50 | 800 |
| Add. 8 | dried Al_2O_3 B | 97 | 0.1068 | 0.0094 | 0.1188 | 0.5377 | 6.24E-05 | 50 | 800 |

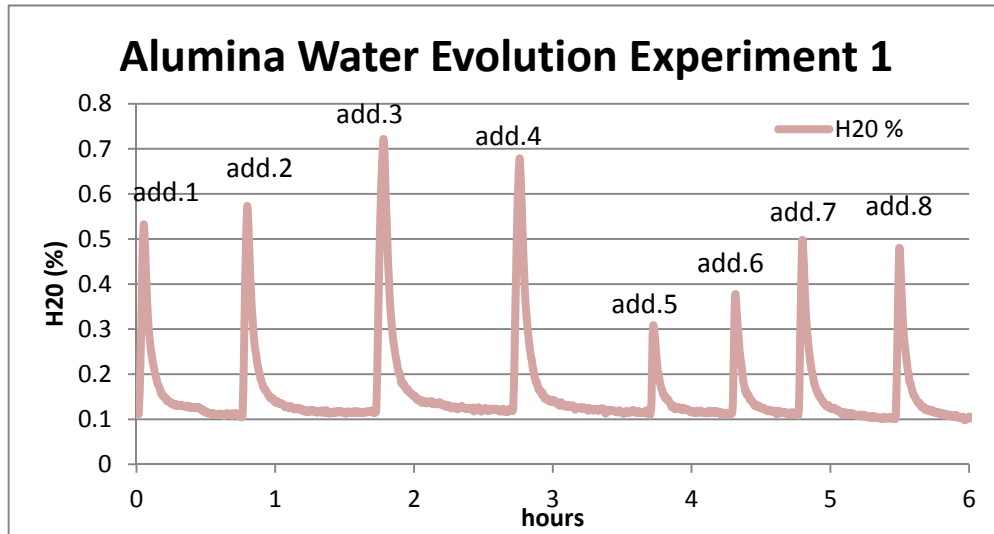


Figure 21. The first of alumina water evolution Experiment

Alumina Water Evolution Experiment 2

Table 12. The Result from 13 addition of alumina A and B in alumina water evolution experiment 2

| Add. No. | Al ₂ O ₃ type | N ₂ flow rate ml/min | Baseline (ppm) | H ₂ O (g/g Al ₂ O ₃) | Al ₂ O ₃ (g) | ratio | nO (mol) | t max (s) | a (s ²) |
|----------|--|---------------------------------|----------------|--|------------------------------------|--------|----------|-----------|---------------------|
| Add. 6 | dried Al ₂ O ₃ B | 27 | 0.2723 | 0.0049 | 0.1369 | 0.2700 | 3.69E-05 | 50 | 800 |
| Add. 7 | dried Al ₂ O ₃ B | 27 | 0.2814 | 0.0053 | 0.1227 | 0.2972 | 3.64E-05 | 50 | 800 |
| Add. 2 | dried Al ₂ O ₃ B | 97 | 0.2484 | 0.0092 | 0.1143 | 0.5145 | 5.87E-05 | 50 | 800 |
| Add. 4 | dried Al ₂ O ₃ B | 97 | 0.2514 | 0.0097 | 0.1409 | 0.5382 | 7.58E-05 | 50 | 800 |
| Add. 10 | dried Al ₂ O ₃ B | 254 | 0.2696 | 0.0104 | 0.1171 | 0.5761 | 6.74E-05 | 50 | 800 |
| Add. 12 | dried Al ₂ O ₃ B | 254 | 0.2721 | 0.0088 | 0.1338 | 0.4882 | 6.52E-05 | 50 | 800 |
| Add. 8 | RT Al ₂ O ₃ B | 27 | 0.2593 | 0.0107 | 0.132 | 0.3034 | 7.85E-05 | 75 | 1500 |
| Add. 9 | RT Al ₂ O ₃ B | 27 | 0.2712 | 0.01 | 0.132 | 0.2832 | 7.33E-05 | 75 | 1500 |
| Add. 3 | RT Al ₂ O ₃ B | 97 | 0.2497 | 0.0196 | 0.1351 | 0.5559 | 0.000147 | 75 | 1500 |
| Add. 5 | RT Al ₂ O ₃ B | 97 | 0.2624 | 0.0198 | 0.1259 | 0.5626 | 0.000139 | 75 | 1500 |
| Add. 11 | RT Al ₂ O ₃ B | 254 | 0.2842 | 0.0253 | 0.116 | 0.7167 | 0.000163 | 75 | 1500 |
| Add. 13 | RT Al ₂ O ₃ B | 254 | 0.2656 | 0.0253 | 0.1295 | 0.7167 | 0.000182 | 75 | 1500 |

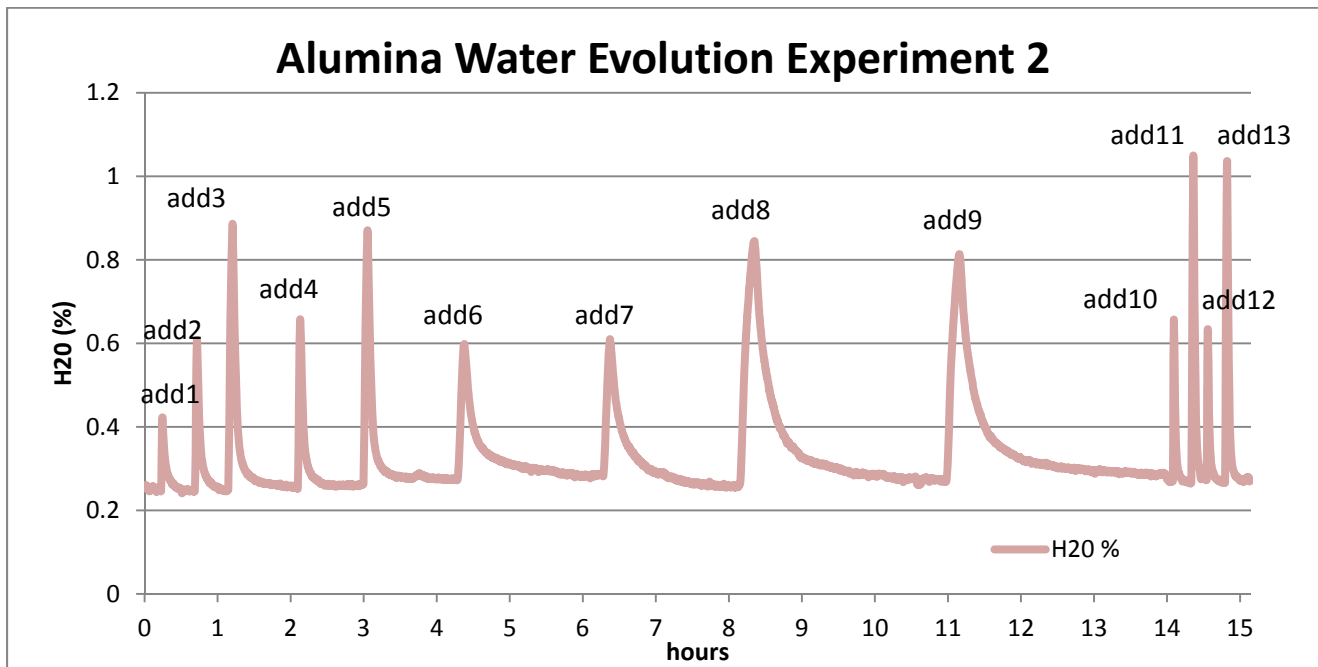


Figure 22. 13 addition of argon with 1% HF in alumina water evolution experiment 2

5.2.3 MELT EXPERIMENTS

In this experiment dried alumina was added into the nickel container containing bath inside the hot furnace. Dried alumina dropped in the electrolyte which is put in the small crucible inside nickel container (see Figure 10). The reaction between H (originated from water which was released from alumina) and F (originated from the cryolite) which formed HF was measured in the laser. From the laser, baseline as initial concentration of HF (ppm) for each addition and amount of HF for each 11.18 second in ppm was obtained. The amount of the real HF in gram/gram Al_2O_3 was found by integral of riemann sums. The amount of the alumina which was dropped should be less than 0.15g.

In Table 13, nine additions had been done. In this experiment, the flow rates of the nitrogen were 97ml/min, 254ml/min, 700ml/min and 1033ml/min. Calcined alumina A and dried alumina B were used. In Table 14, 10 additions of dried alumina B and 2 addition of calcined alumina A had been done. In this experiment, nitrogen flow rates of 27ml/min, 97ml/min, 254ml/min, 700ml/min and 1033ml/min were applied. Ratio between HF in mol and total LOI in mol (for temperature 350°C and 1000°C) were also calculated. In Table 13 and 14, some parameters for CSTR, i.e. t_{\max} and a are also presented.

MELT EXPERIMENT 2

Table 13. The result of eight addition of dried alumina B in the melt experiment 2 with varied of nitrogen flow

| Add. no. | Al ₂ O ₃ type | flow rate ml/min | Baseline (ppm) | Al ₂ O ₃ (g) | HF (g/g Al ₂ O ₃) | ratio | nO (mol) | t max (s) | a ² |
|----------|--|------------------|----------------|------------------------------------|--|--------|----------|-----------|----------------|
| Add. 2 | dried Al ₂ O ₃ B | 254 | 86.6155 | 0.1181 | 0.02241 | 1.1207 | 0.0001 | 50 | 800 |
| Add. 3 | dried Al ₂ O ₃ B | 254 | 111.389 | 0.1035 | 0.02776 | 1.3880 | 0.0001 | 50 | 800 |
| Add. 4 | dried Al ₂ O ₃ B | 97 | 189.091 | 0.1012 | 0.0198 | 0.9899 | 0.0001 | 50 | 800 |
| Add. 5 | dried Al ₂ O ₃ B | 700 | 131.28 | 0.1182 | 0.03324 | 1.6621 | 0.0002 | 50 | 800 |
| Add. 6 | dried Al ₂ O ₃ B | 700 | 82.6735 | 0.2524 | 0.01452 | 0.7258 | 0.0002 | 50 | 800 |
| Add. 7 | dried Al ₂ O ₃ B | 1033 | 28.2038 | 0.113 | 0.03989 | 1.9944 | 0.0002 | 50 | 800 |
| Add. 8 | dried Al ₂ O ₃ B | 1033 | 30.2924 | 0.1011 | 0.03185 | 1.5923 | 0.0002 | 50 | 800 |
| Add. 9 | dried Al ₂ O ₃ B | 97 | 213.92 | 0.0929 | 0.01619 | 0.8095 | 8E-05 | 50 | 800 |

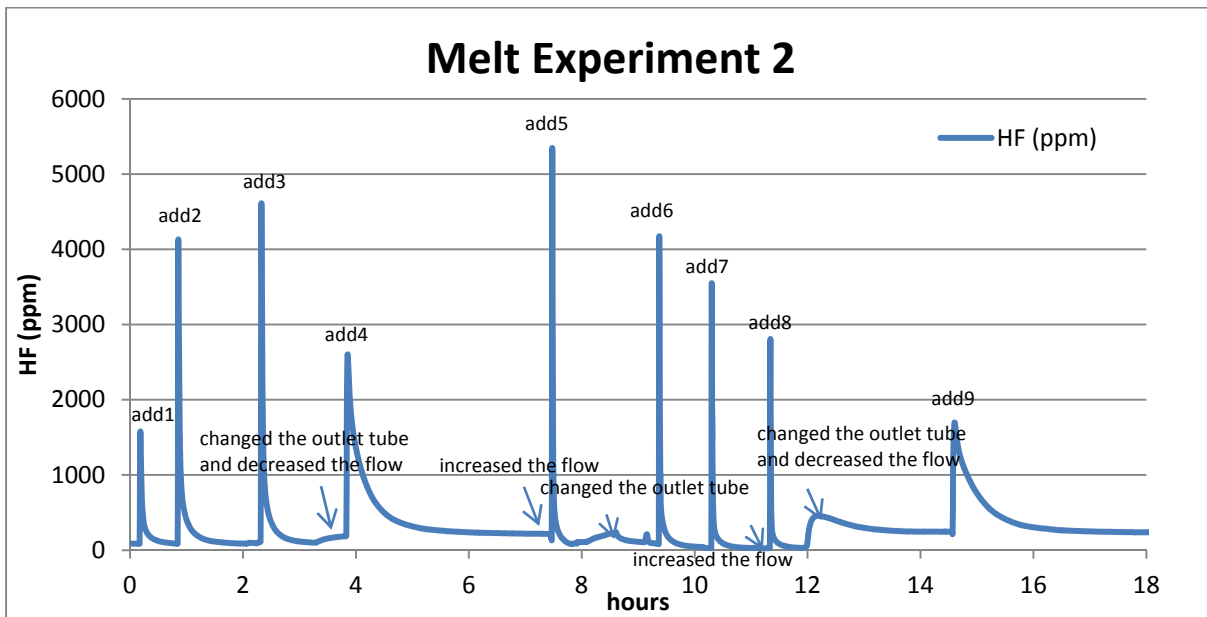


Figure 23. 1 addition of calcined alumina A and 8 additions of alumina B with variation of nitrogen flow rate in the melt experiment 2

MELT EXPERIMENT 3

Table 14. The result of twelve addition of dried alumina B in the melt experiment 3

| Add. no. | Al ₂ O ₃ type | N ₂ flow rate ml/min | Baseline (ppm) | HF (g/g Al ₂ O ₃) | Al ₂ O ₃ (g) | ratio | nO H ₂ O (mol) | t max (s) | a ² |
|----------|--|---------------------------------|----------------|--|------------------------------------|--------|---------------------------|-----------|----------------|
| Add. 3 | dried Al ₂ O ₃ B | 254 | 312.4990 | 0.0257 | 0.0856 | 1.2915 | 0.00011 | 50 | 800 |
| Add. 4 | dried Al ₂ O ₃ B | 254 | 200.9790 | 0.0236 | 0.1108 | 1.1798 | 0.000131 | 50 | 800 |
| Add. 5 | dried Al ₂ O ₃ B | 1033 | 64.5484 | 0.0314 | 0.1148 | 1.5683 | 0.00018 | 50 | 800 |
| Add. 6 | dried Al ₂ O ₃ B | 1033 | 60.9265 | 0.0294 | 0.1126 | 1.4675 | 0.000165 | 50 | 800 |
| Add. 7 | dried Al ₂ O ₃ B | 700 | 112.5760 | 0.0333 | 0.12 | 1.6671 | 0.0002 | 50 | 800 |
| Add. 8 | dried Al ₂ O ₃ B | 700 | 123.3380 | 0.0347 | 0.1214 | 1.7333 | 0.00021 | 50 | 800 |
| Add. 9 | dried Al ₂ O ₃ B | 97 | 301.1740 | 0.0208 | 0.1347 | 1.0381 | 0.00014 | 50 | 800 |
| Add. 10 | dried Al ₂ O ₃ B | 27 | 916.7190 | 0.0400 | 0.1188 | 2.0140 | 2.39E-05 | 50 | 800 |
| Add. 11 | dried Al ₂ O ₃ B | 254 | 201.9210 | 0.0452 | 0.1175 | 2.2589 | 0.000265 | 50 | 800 |
| Add. 12 | dried Al ₂ O ₃ B | 97 | 485.4410 | 0.0248 | 0.1104 | 1.2406 | 0.000137 | 50 | 800 |

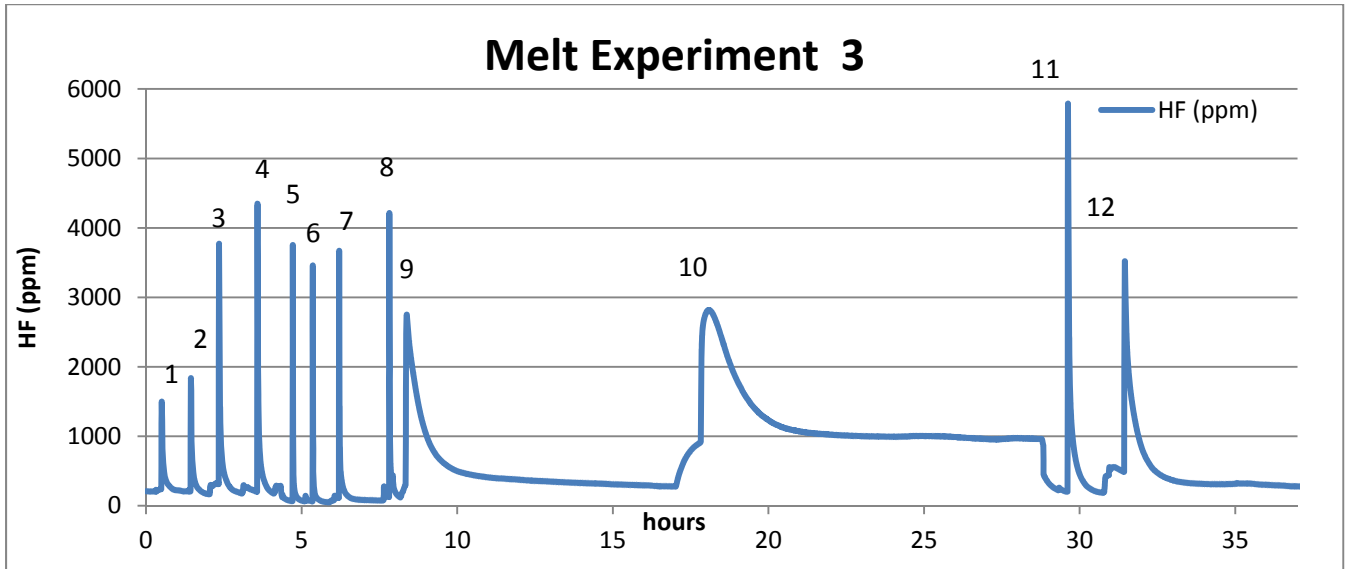


Figure 24. 2 addition of calcined alumina A and 10 additions of alumina B with variation of nitrogen flow rate in the melt experiment 3

5.3. CSTR MODELING

5.3.1 TEMPERATURE

The temperature-flow profiles for CSTR modeling should be the same for all experiments. It is assumed that higher flow of room temperature nitrogen leads to lower temperatures in the cell. The temperature is a quite important parameter in the CSTR model since it directly influences the molar volume of the gas and thus flow rates and residence times. To relate flow and temperature, the following temperature model approximation was used for all the experiments.

$$Q = cp. (T - T_{gas}). flow = k. (T_{furnace} - T) \quad 5.1$$

$$T = \frac{(k.T_{furnace}.cp.flow.T_{gas})}{(flow.cp+k)} \quad 5.2$$

$$T = \frac{(T_{furnace} + \frac{cp}{k}.flow.T_{gas})}{(\frac{cp}{k}.flow+1)} \quad 5.3$$

Final equation,

$$T = \frac{(T_{furnace} + const.flow.T_{gas})}{(const.flow+1)} \quad 5.4$$

Q = heat flow in the bath (W)

cp = heat capacity in the gas (J/K mol)

T = temperature gas in the reactor (K)

T gas = inlet gas 300K

flow = gas flow (mol/s)

k = heat transfer coefficient from the wall to the gas (W/K)

T furnace = temperature in the furnace (K)

Constant can be chosen to optimize the fit to the experimental data.

Table 15. Parameters used when calculating the temperature model for CSTR

| Parameter | Value | Unit |
|-----------|--------|--------|
| T furnace | 1273 | kelvin |
| Constanta | 0.0005 | -s/mol |
| T gas | 300 | kelvin |

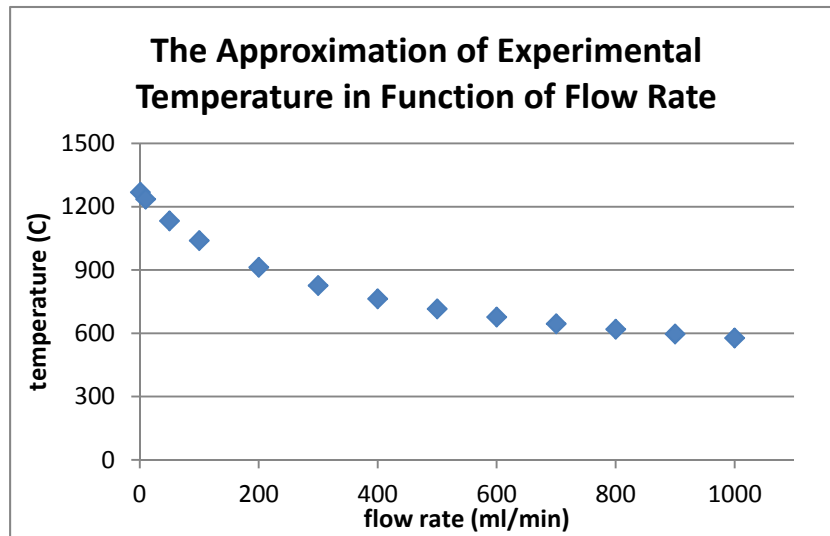


Figure 25. The temperature model for CSTR modeling

By using final equation 5.4, temperature approximation can be generated as per Table 16 below,

Table 16. temperature approximation in function of flow rate (Nml/min)

| flow Nml/min | 1 | 10 | 50 | 100 | 200 | 300 | 400 | 500 | 600 | 700 | 800 | 900 | 1000 | 10000 |
|-----------------|--------|--------|--------|--------|-------|-------|-------|-------|-------|-------|-----|-------|-------|-------|
| T (K) | 1268.2 | 1235.8 | 1132.3 | 1039.7 | 912.4 | 826.5 | 763.7 | 715.3 | 676.8 | 645.3 | 619 | 596.7 | 577.5 | 346.5 |

Temperature slow flow is higher than high flow the temperature due to high flow wouldn't have a time to heat it much so temperature goes down.

5.3.2 CSTR FIT FOR ARGON WITH 1% HF EXPERIMENT

Based on the experimental result presented in Table 10, CSTR modeling was calculated using mass balance approximation. Detail for the formulation is given in Chapter 4.

In Figure 26 and 27, the comparisons between the experimental data and CSTR model for each nitrogen flow rates of 97ml/min, 254ml/min, 700ml/min and 1033ml/min are plotted during period of 500 second. The time period five hundred second was selected due to HF dilution finished before 500 second when high flow rate (1033ml/min) of nitrogen flushed into the furnace.

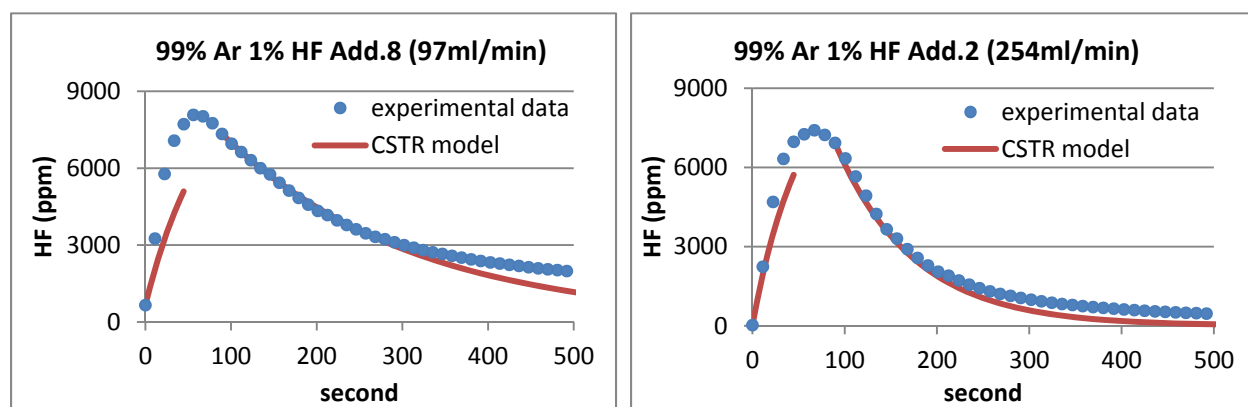


Figure 26. Experimental data and CSTR comparison with flow rate of nitrogen 97ml/min and 254ml/min

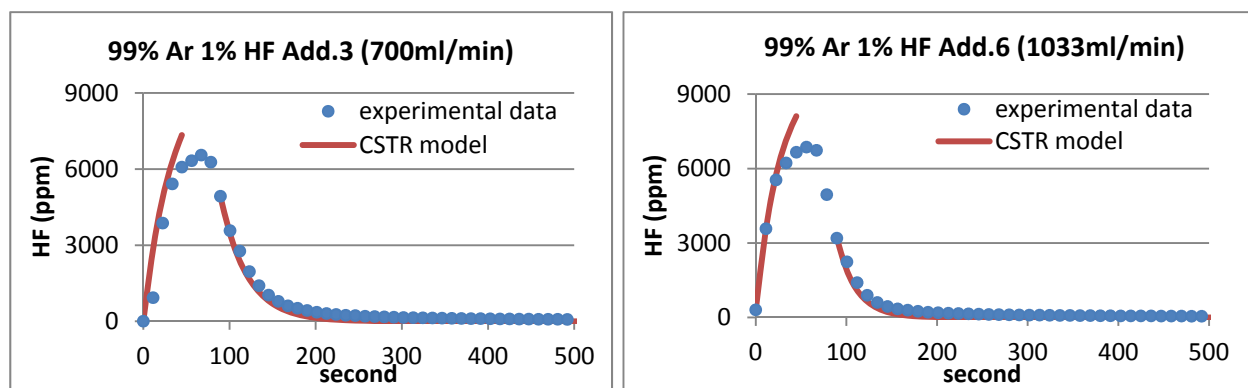


Figure 27. Experimental data and CSTR comparison with flow rate of nitrogen 700ml/min and 1033ml/min

The red curve in Figure 26 and 27 represent the CSTR models while blue curve represent the experimental data. According to the Figures 26 and 27, when nitrogen flow rate 97ml/min CSTR model reaches peak of the HF concentration far down lower than the experimental data. When

nitrogen flow rate 254ml/min the model curve slightly fit with the experimental data. Figure 27 shows that CSTR model peak getting higher when nitrogen flow rate is also getting high.

5.3.3 CSTR FIT FOR ALUMINA WATER EVOLUTION EXPERIMENTS

Basically, the CSTR model for this type of experiment and the melt experiment are the same model as argon with 1% HF experiment but in this experiment water evolution was counted for every 11.18 second. Based on the experimental result in Table 11 and 12 CSTR modeling was calculated using mass balance water evolution. The detail for the formula is given in Chapter 4.

In Figure 28, 29, 30 and 31, the comparison between experimental data and CSTR model for each nitrogen flow rate of 27ml/min, 97ml/min and 254ml/min are plotted. In additions using 27ml/min nitrogen flow rate the curves plotted in 3000 second, for 97ml/min nitrogen flow rate the curves plot in 1000 second and for 254ml/min nitrogen the curves plot in 500second. Observing the curves, it can be seen that the peak of the curves are varied with the LOI. The peak of alumina A is always lower than alumina B. Peak of dried alumina always lower than room temperature alumina. Clearly seen from the plot, every addition using room temperature alumina always has shoulder before it reached the peak.

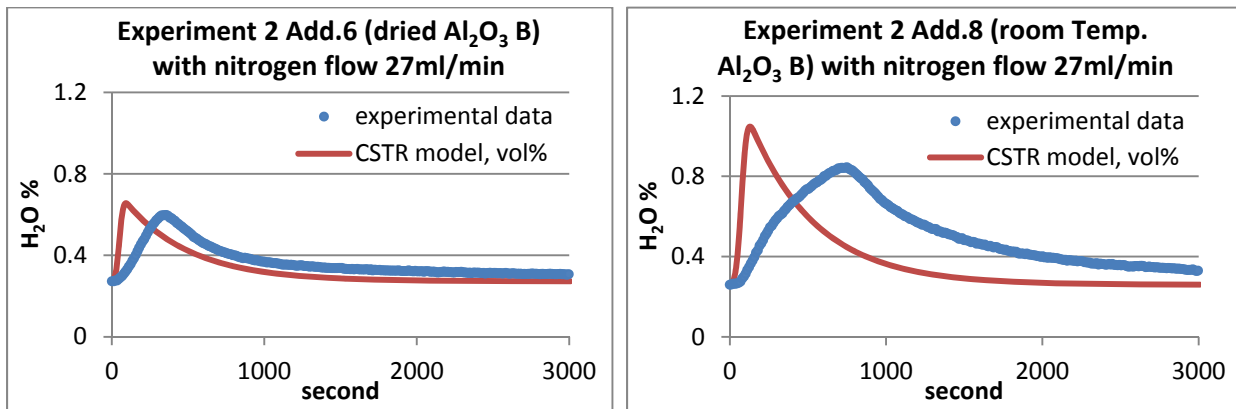


Figure 28. CSTR fit for alumina water evolution experiments with nitrogen flow rate 27ml/min

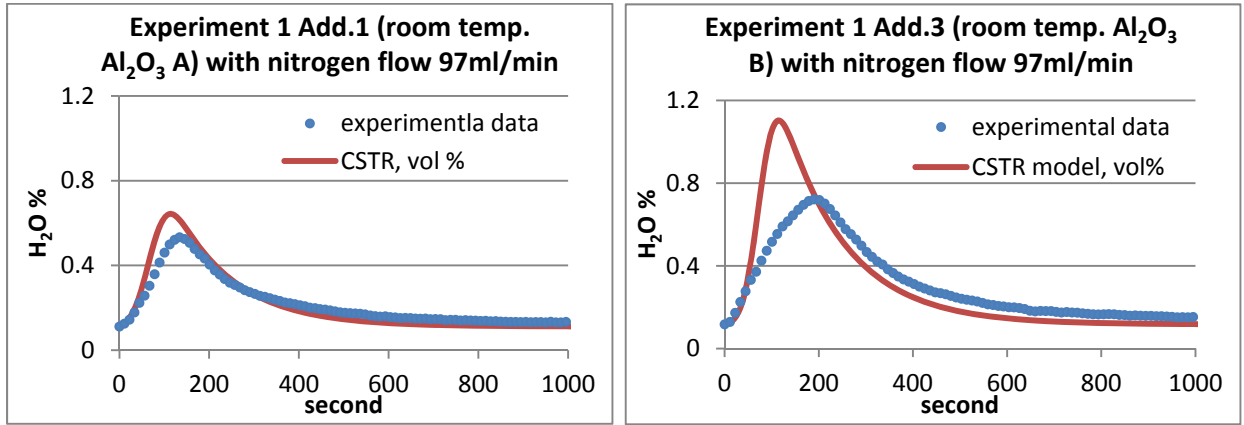


Figure 29. CSTR fit for alumina water evolution experiments with nitrogen flow rate 97ml/min

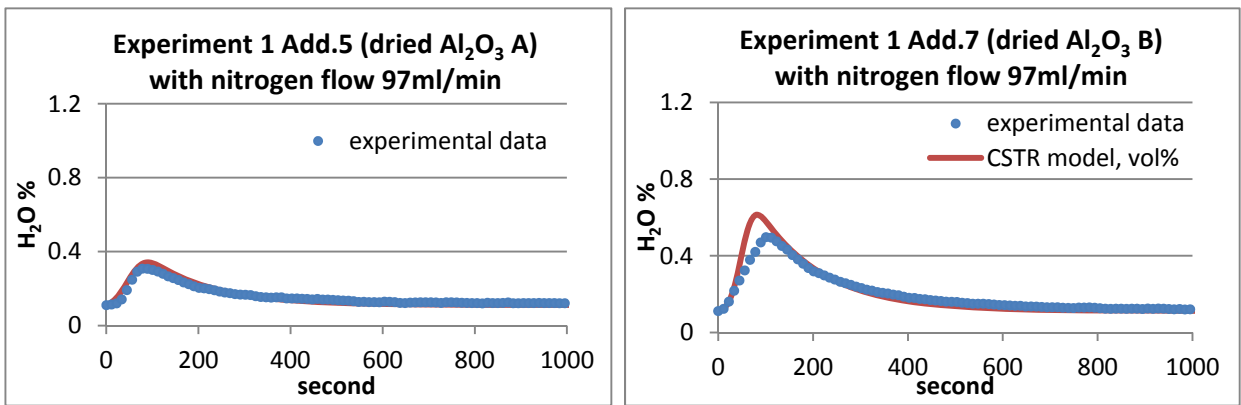


Figure 30. CSTR fit for alumina water evolution experiments with nitrogen flow rate 97ml/min

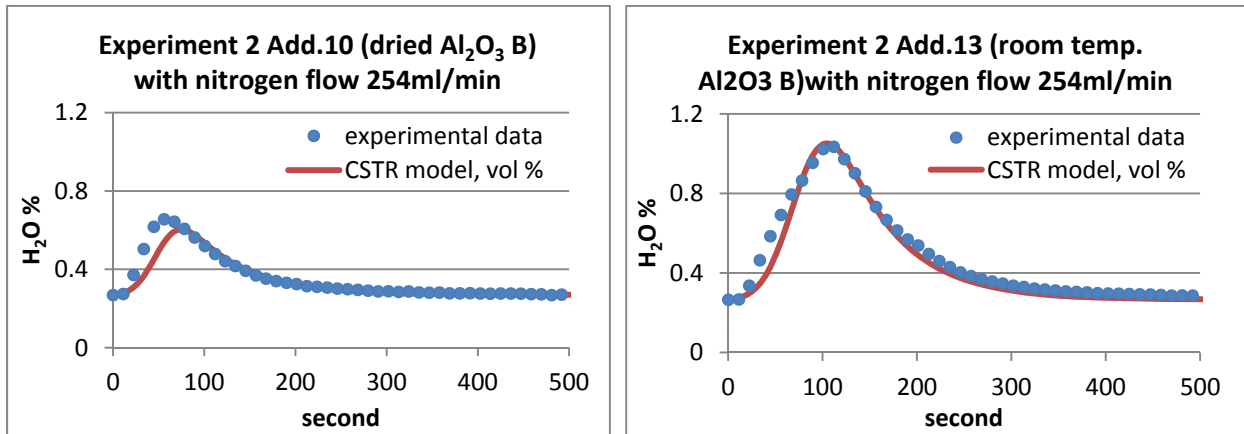


Figure 31. CSTR fit for alumina water evolution experiments with nitrogen flow rate 254ml/min

5.3.4 CSTR FIT FOR MELT EXPERIMENTS

In melt experiments, HF formation was counted for every 11.18 second. Based on the experimental result presented in Table 13 and 14, CSTR modeling was calculated using mass balance water evolution. The detail for the formula is given in chapter 4.

Figure 32, 33, 34 and 35 show the comparisons between experimental data and CSTR model for each nitrogen flow rate 27ml/min, 97ml/min, 254ml/min, 700ml/min and 1033ml/min. In additions which applied 27ml/min nitrogen flow rate the curves are plotted in 4000 second, for 97ml/min nitrogen flow rate, the curves are plotted in 1000 second and for other nitrogen flows rate the curves are plotted in 500 second. According to the CSTR model, the slowest flow reaches the highest peak and the fastest flow reaches lowest peak.

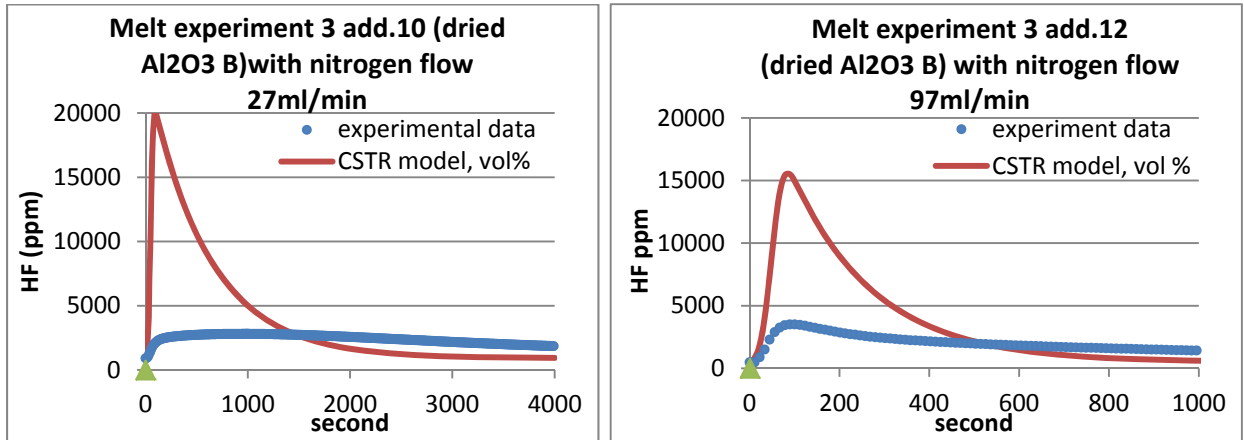


Figure 32. addition 10 of melt experiment 3 with nitrogen flow rate 27ml/min and addition 12 of melt experiment 3 with nitrogen flow rate 97ml/min

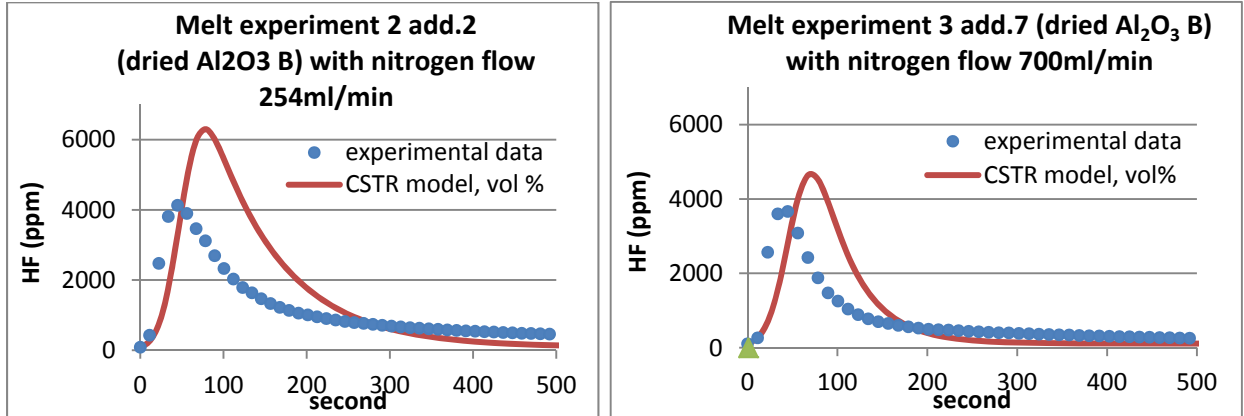


Figure 33. addition 2 of melt experiment 2 with nitrogen flow rate 254ml/min and addition 7 of melt experiment 3 with nitrogen flow rate 700ml/min

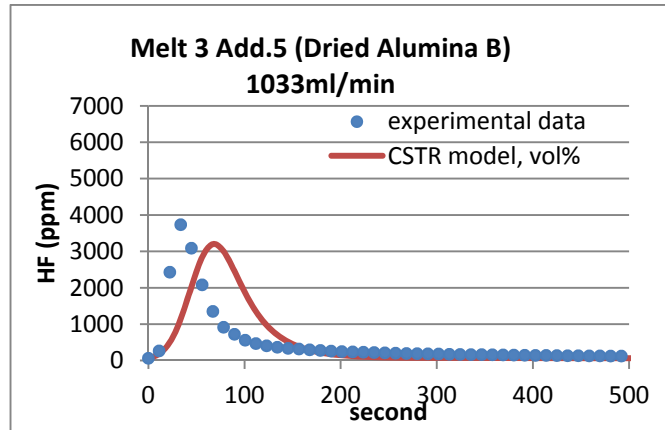


Figure 34. addition 5 of melt experiment 3 with nitrogen flow rate 1033ml/min

6. ANALYSIS AND DISCUSSION

6.1 LOI PRIMARY BULK ALUMINA A AND B

The result of the loss on ignition of smelter grade alumina A and B is presented in Table 7. The LOI (RT-160 °C) value for alumina A is 1.12% and a quite low standard deviation of 0.0032. This LOI value of alumina A is larger than the previous autumn work (i.e.0.89%) and it is somehow at the similar level of the Sommerseth's ⁽⁴⁾ work, i.e. 1.14%. The LOI (RT-160 °C) value for alumina B is 1.74%and a standard deviation of 0.007. This value is smaller than the previous autumn work (i.e.2.8%) and it is somehow slightly larger than Sommerseth's ⁽⁴⁾ work, i.e. 1.51%. As a comparison, the values of LOI (RT-160 °C) in this thesis work are more and less the same as the result of Sommerseth's. Both of the LOI in this work and Sommerseth's ⁽⁴⁾ were performed in February-March during the period of dry weather while LOI of autumn project was performed in November. LOI in this range temperature really easy to change according to the ambient moisture content as the samples are not kept in completely closed container. It is proved that LOI in this range temperature reaches the highest value as compared to others. In this temperature range, physisorbed and some chemisorbed water are evaporated.

The LOI (160-350°C) value for alumina A is 0.51% and standard deviation of 0.003. The corresponding value of the previous autumn work was 0.36% and Sommerseth's work was 0.44%. The LOI (160-350°C) value for alumina B is 0.86% and standard deviation 0.018. The corresponding value from the previous autumn work was 0.82% and Sommerseth's work was 0.68%. In this temperature ranges (160-350°C), the ambient moisture does not give any effect but the transportation from the furnace to the balance during the weighing process may gave small effect to the value deviation. In this temperature ranges, the LOI was higher as compared to the previous work and Sommerseth's. The heating temperature ranges removed more chemisorbed and gibbsite.

The LOI (350-1000°C) value for alumina A is 0.8% and standard deviation of 0.022. The value from the previous autumn work was 0.78% and Sommerseth's⁽⁴⁾ was 0.64%. The result was more and less at the same range as the previous work's result. The LOI (350-1000 °C) value for alumina B is 0.97 and standard deviation of 0.01. The value from the previous autumn work was 0.95% and Sommerseth's⁽⁴⁾ was 1.08%. The result was more and less at the same level as compared to the previous work and Sommerseth's⁽⁴⁾ work. It can be concluded that the accuracy of the data can be trusted.

Eventually, alumina B contains more moisture than alumina A at all the temperature ranges. The reason is probably that alumina B contains more under calcined matter as compared to alumina A. Since the total LOI of alumina B is higher than alumina A, alumina B has higher HF formation potential than alumina A.

6.2 LOI 160°C IN FUNCTION OF TIME

In Table 9 loss on ignition is presented and can be concluded that the LOI is getting bigger as function of time. Most of the LOI happens during the first two hours. In the first two hours LOI alumina A1 is 1.3095%, LOI alumina A2 is 1.2659%, LOI alumina B1 is 2.1896% and LOI alumina B2 is 1.7038%. Alumina A1, A2 and B1 were heated for 1774 hours and alumina B2 was heated for 1294 hours. At the last measurement, LOI for alumina A1 was 1.3757%, A2 was 1.3370%, B1 was 2.3353% and B2 was 1.8305%.. In the first two hours all loosely bound physisorbed water and small of chemisorbed water were evaporated, as can be observed observed from the significant amount of water loss. After two hours some other small amount of chemisorbed water was released. Since alumina water is really easy to lost or gained depending on the relative humidity, sometimes the weight of the alumina gained due to some moisture attached in the alumina. LOI give some different amount when heated more than two hours. A consistency on heating rate of the sample exactly for two hours before the experiment is needed in order to obtain good result. Consistent with the result of LOI, alumina B contains more moisture than alumina A.

6.3 ARGON WITH 1% HF EXPERIMENT

The objectives of this experiment are to observe the HF behavior inside the furnace, to find whether nickel apparatus will absorb a lot of HF or not and also to check the nitrogen flow dependency towards HF amount. According to the result in Table 10, it's clearly seen that the HF amount measured by the laser is not depending on the flow rate. Thus, there is no HF adsorption in the container as a function of flow. Table 10 shows that the result of the real HF in mol is higher than theoretical HF. The real HF amount should be lower than theoretical HF but there is some difficulty to control the rate of the flow. This difficulty is because none of flow controller can stand with HF. Some modification had been done to control the argon with 1% HF flow as illustrated in the appendix A. Even though the flow controller was put after gas cleaning system, white powder was found stick in the ball inside the flow controller immediately after argon with 1% HF purged into the system. Cleaning routine had been done before each addition but the HF attacked the ball inside the flow controller very fast. HF is very sticky and corrosive gas and none of the flow controller can stand with it.

This difficulty may give some uncertainty to the exact argon 1% HF flow to the system. The argon with 1% HF flow is typically higher than expected. Mixing of the gas and also pressure drop in the argon with 1% HF reduction valve also play role. Even though there some uncertainties, it still can be concluded that the real HF (mol) in Table 10 are reproducible for each addition. Figure 20 also showed that all additions in each nitrogen flow rate also reproducible. It is concluded that this experiment can be used as a parameter that the system is a reactor with mixed system inside. With all these finding, it shows CSTR behavior and CSTR modeling can be used as one of the model approximation. It's assumed that argon experiment can be used as the CSTR model event though there is imperfect mixing. From this comparison we can also know the condition between the real experimental work and the model.

6.4 CSTR FIT FOR ARGON WITH 1% HF EXPERIMENT

The objectives from this experiment are answered by CSTR modeled. The flow rate of the model was varied. The experimental value is higher when nitrogen 97ml/min and 254ml/min was purged but when nitrogen flow rate is increased up to 700ml/min and 1033m/min the experimental value become lower than CSTR model. In nitrogen flow rate 97ml/min and 254ml/min the CSTR curve below the experimental curve, this result should be reversed. The deviations for these flow rates due to the positioning of the inlet and outlet tubes. The position of the inlet tube really closed with the outlet tube and the concentration will be higher than average concentration inside the cell and also the reaction is not really CSTR particularly for low flow rate.

The high spike was happen due to the high nitrogen flow rate. The height of the spike was depending on the flow rate. The spike is higher in the high nitrogen flow rate due to dilution or CSTR similarity. In the low flow imperfect mixing and some plug flow is assumed to be happened due to HF gas and nitrogen mixed in the radial direction but not in the axial direction (forward and backward) of the nickel container. Gas residence time is a function of its position in the nickel container.

6.5 ALUMINA WATER EVOLUTION EXPERIMENTS

In this experiment, alumina was added to the empty hot clean crucible to measure the water released from the pure alumina as a function of time. From the ratio between % water and LOI water (see Table 11 and 12), half of the water goes to the laser and the rest not stay any longer with alumina.

Two type of alumina used, i.e. dried alumina and alumina at the room temperature. The room temperature alumina curves in this type of experiment have two peaks. After first peak water evolution goes down and it's overlapping with the second one and generates “shoulder” before

the curve reached the second peak. It is believed that the first peak is due to the loosely bound physisorbed water, while the second peak is due to more strongly bound water.

This experiment gives some information about water evolution kinetics. It's indicated that the most important factor affected the kinetic of the amount of alumina added might be water released. Since alumina is an insulator, it takes time to get heat from outside. The heat transfer is the rate determining step of the water released. Water evolution during the alumina additions to the quartz cell is slower than CSTR model for nitrogen flow rate 27ml/min, this condition applied for both dried alumina B and room temperature alumina B shows in Figure 29. This condition also happens for room temperature alumina A and B shows in Figure 30. The reason could be the same as experiment using argon with 1% HF. In those experiment, at low flow there is incomplete mixing in the reactor. Water released from the alumina is therefore takes more time to reach the outlet tube.

Different curve shape shows in Figure 30. In this figure the experimental data fit the CSTR plot. Moreover Figure 31 shows water released from alumina faster than the CSTR model. Water measurement the different of amount of water related to the flow rate. Alumina releases water quite rapidly, as demonstrated by the water release curves in the CSTR model (blue curves). Nearly all water is released in the first couple of minutes.

6.6 CSTR FIT FOR ALUMINA WATER EVOLUTION EXPERIMENTS

The deviation caused by addition of nitrogen flow rate 27ml/min is due to not completely good mixing and it's not CSTR. The position of the gas in and out can be assumed that the mixing was not complete. The released of water is not a fast released. It slowly released to the reactor and gets delayed in the real signal. It's not alumina behaved differently but toward incomplete mixing. At nitrogen flow rate 97ml/min the CSTR plot get better fit. The CSTR model for alumina B is higher than alumina A. This is due to alumina B contain much water. The dried curve follows CSTR very well.

6.7 MELT EXPERIMENTS

In this experiment, the way of alumina spread in the surface give not significant different to the water released rate. This is because the amount of alumina is very small. The water released in small addition in the hot furnace is quit rapid. Heat transfers are much higher in the melt so the water evolution also faster in this type of experiment. It's reach peak before the model. Due to the position of the outlet gas tube, while alumina was added into the container the concentration of the water released in the bottom is slightly higher than CSTR model. It's need little time to resemble the concentration in the top of the container.

The ratio between $\text{gHF/gAl}_2\text{O}_3$ and the total LOI quite constant and it's independent to the temperature. In the higher flow rate, the experimental data is higher than the model. It's happened due to very rapid HF formation. The water release not in the same rate but faster than the model. This is because of independent dissolution and better thermal exchanges of different type of water.

According to the ratio, almost all the water in this type of experiment was found back compared with alumina water evolution experiment. It could be due to better set-up. In the old set-up, it's difficult to get the total amount of HF due to some water will go out and go back again and react. It's also believed that laser works better for HF then H_2O .

6.8 CSTR FIT FOR MELT EXPERIMENTS

The deviation between the model and the experimental data happen due to CSTR hypothetical volume could be lower. This could be because the outlet tube not in the bottom when we put it in the top maybe will give better fit. Water is released in the longer tail in all addition in melts experiment except for the nitrogen low flow rate. The heating of the gas expand a lot and has shorter residence time. (The gas will expand inside). After 1 minute the deviation becomes larger. It could be some adsorption of HF.

Water evolution when adding alumina to the bath is faster than water released in the alumina water evolution experiment. This is a strong indication that water is mainly released during alumina dissolution. If so the reaction between water flashing off from the alumina and the vapor above the bath are not so important. In addition, in the rate of water evolution, the reaction from water to HF is happened very fast because bigger heat transfers, dissolution and larger spread area of alumina. The rate determining step of HF formation is water released.

The deviation between model and experimental data for slow flow due to incomplete mixing is common for alumina water evolution experiment and melt experiments. The error from the model happens in nitrogen flow with rate 27ml/min. It could be happened because at this flow, the rate of the system does not act as CSTR.

CONCLUSIONS

The following is a summary of the finding during this master work,

- Alumina B contains more uncalcined matter compared alumina A and since the total LOI of alumina B is higher than alumina A, alumina B has higher HF formation potential than alumina A.
- The set-up is working very good. It behaves quite close to a CSTR reactor except at low flow rates, where incomplete mixing occurs. There is still some room for improvements. Not all HF and water evolved is detected by the analyzer. The reason for this has not been found.
- Formation of HF is very rapid. In the experimental data, there is no water peak when HF formation happens because all the water is reacting. This is supported by comparison of measurements of water evolution rate from alumina added to an empty cell and HF formation rate measurements of alumina added to bath. HF formation rate was not slower than the water evolution rate.
- HF formation is not dependent on the nitrogen flow rate and no HF adsorption occurs as a function of flow. From the result there is not dependency of HF because it reacts very fast. The amount HF generation is not necessarily flow dependent but the profile (the curve shape) and the mixing flow is dependent.

FURTHER WORK

Some further work below is suggested on the basis of the present work,

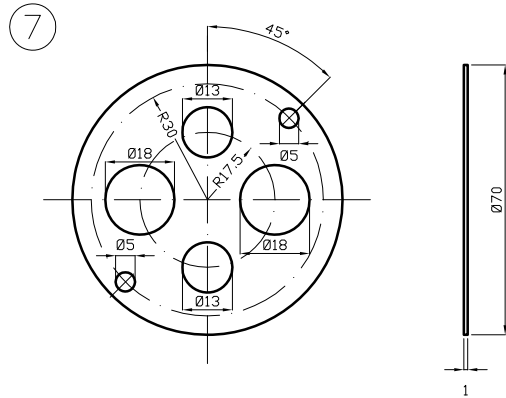
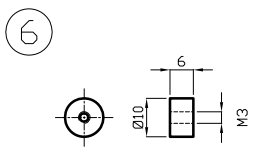
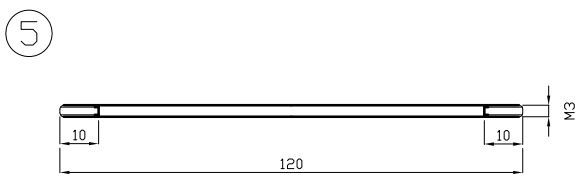
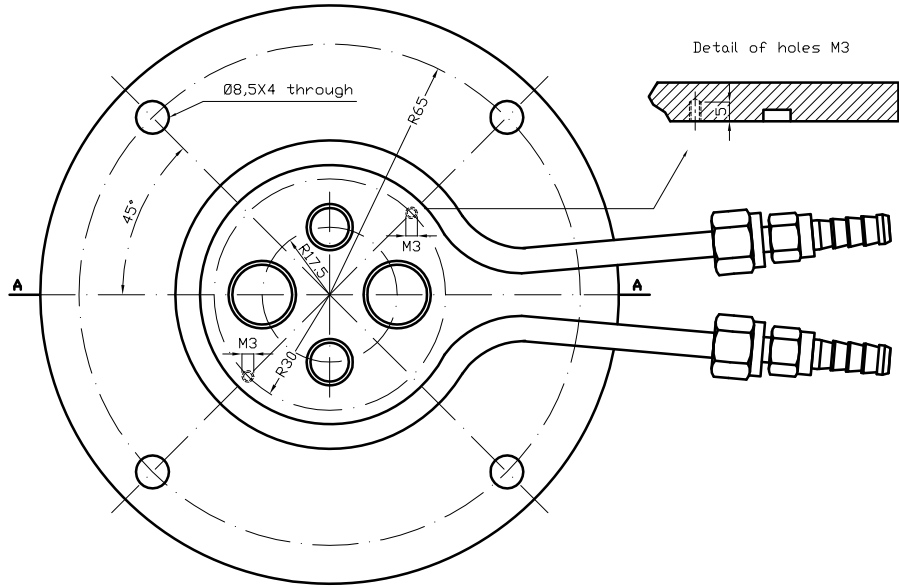
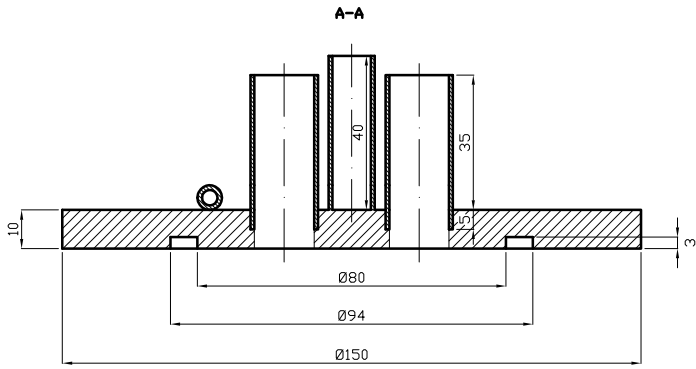
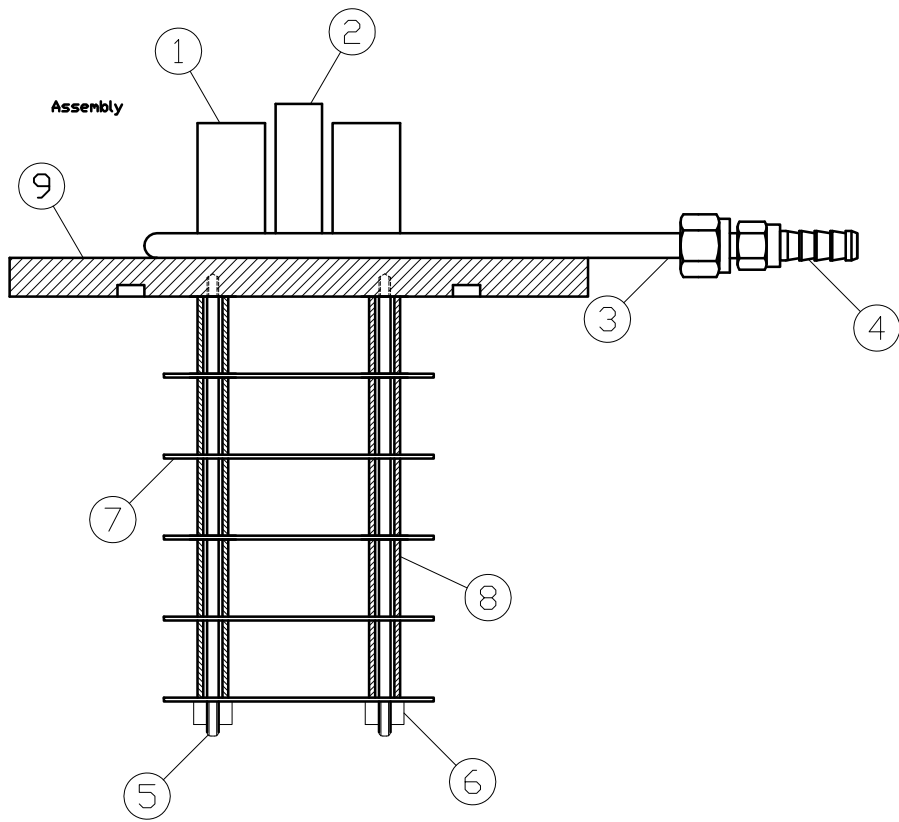
1. Perform LOI at function of time at 350°C and also 1000°C.
2. Improve the CSTR model using precise parameter for each type of experiment.
3. Improve the set-up by move the outlet gas tube further up so the cell may better resemble a perfect continuous stirrer tank reactor.
4. Study the effect of alumina water residence time on HF formation for surface adsorbed alumina water.

REFERENCES

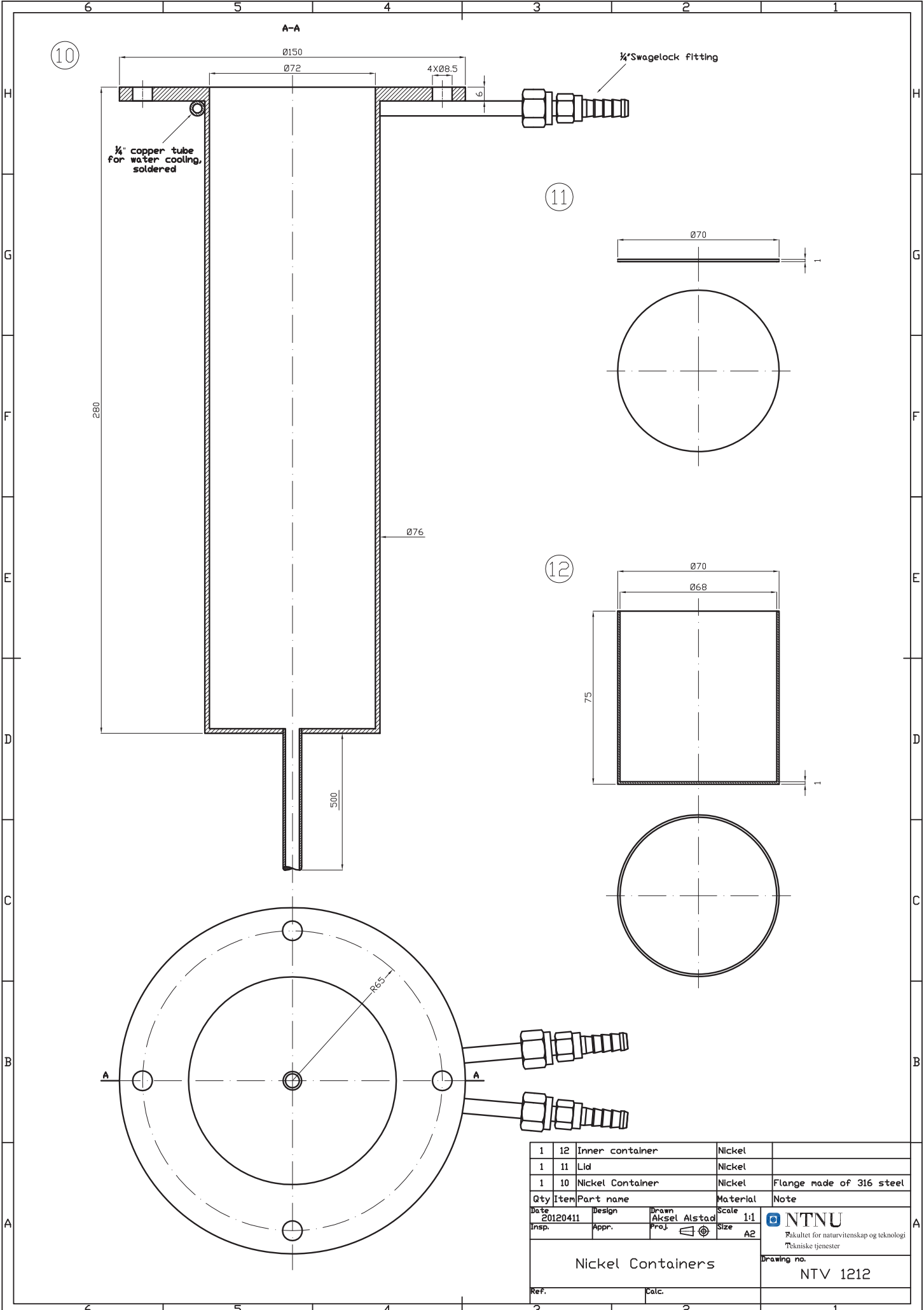
1. **Jomar Thonstad, Pavel Fellner, Geir Matin Haarberg, Jan Hives, Halvor Kvande, Åsmund tertén.** *Aluminium Electrolysis "Fundamentals of the Hall-Heroult Process"*. 3. Dusseldorf : Aluminium-Verlag, 2001. pp. 315-320. ISBN 3-87017-270-3.
2. *Alumina Structural Hydroxyl as a Continuous Source of HF.* **Margaret Hyland, Edwin Patterson, Barry Welch.** [ed.] Alton T. Tabereaux. Auckland : s.n., 2004. TMS. pp. 361-365.
3. *The Behaviour of Moisture in Cryolite.* **Karen Sende Osen, Christian Rosenkilde, Asbjørn Solheim, Egil Skybakmoen.** San Fransisco : TMS, 2009. Light Metals. pp. 395-400.
4. **Sommerseth, Camilla.** *A Method for Comparing The HF Formation Potential of Aluminas eith Different Water Contents.* Trondheim : NTNU, 2010.
5. **Fellicia, Dian Mughni.** *The Rate of HF Formation During Addition of Aluminas in Cryolite Melts.* Material Science and Engineering, NTNU. Trondheim : s.n., 2012. pp. 3-11.
6. **Kvande, Halvor.** *Electrolyte Compositions for Aluminium Production.* Trondheim : s.n., February 27, 2012. p. 6.
7. **K. Grjotheim and H. Kvande.** *Introduction to ALuminium Electrolysis.* Dusseldorf : Aluminium-Verlag, 1993. pp. 2, 42. Vol. 2nd edition. ISBN 3-87017-233-9.
8. *Phase Composition and Its Impact on Bath Ratio Determination of Aluminum Electrolyte with Additives of KF and NaCl.* **Bingliang Gao, Dan Li, Xianwei Hu, Zhongning Shi, Zhaowen Wang.** Shenyang : IEEE, 2010, pp. 1-3. 97-1-4244-892.
9. **Kvande, Halvor.** *Alumina and its Properties.* Trondheim : s.n., April 25, 2012. pp. 1-36.
10. *Adsorption of Water Vapour on Activated Alumina I – Equilibrium Behaviour.* **R. Desai, M. Hussain and D.M. Ruthven.** 4, New Brunswick : The Canadian Journal of Chemical Engineering, August 1992, Vol. 70, pp. 699-706.
11. **Australia, Standards.** *Alumina Part 1: Determination of los of mass at 300°C and 1000°C.* s.l. : Standards Australia, 2000. pp. 1-15. ISBN 0733733255.
12. **Petterson, Edwin Campbell.** *Fluoride Emissions from Aluminium Electrolysis Cells.* New Zealand : University of Auckland, 2001. pp. 21-32.

13. *The Formation and Composition of the Fluoride Emissions from Aluminium Cells*. **K. Grjotheim, B. J. Welch, H. Kvande, and K. Motzfeldt**. s.l. : Canadian Metallurgical Quarterly, October-December 1972, Vol. 4, pp. 585-599.
14. *Predicting Moisture Content on Smelter Grade Alumina from Measurement of the Water Isotherm*. **M.M.Hyland, A.R.Gillespie and J.B.Metson**. Auckland : The Minerals, Metals & Materials Society, 1997. Light Metals. pp. 113-117.
15. *Mathematical Model of Fluoride Evolution from Hall-Heroult Cells*. **W.E. Haupin and H. Kvande**. Stabekk : The Minerals, Metals & Materials Society, 1993. Light Metals. pp. 257-263.
16. *Impact of Thermal Pretreatment on Alumina Dissolution Rate and HF Evolution*. **Neal Dando, Xiangwen Wang, Jack Sorensen, Weizong Xu**. Newburgh : TMS, 2011, pp. 541-546.
17. **As, Neo Monitors**. *User's Reference Version 1.4*. Lørenskog : Neo Monitors As.
18. <http://unix.eng.ua.edu>. [Online] [Cited: 06 03, 2012.]
<http://unix.eng.ua.edu/~che/class/che354/Che354Site/Library/Modules/Chapter1/CICSTR.pdf>.
19. CRCT (Center of Research in Computation in Thermochemistry). [Online] École Polytechnique de Montréal. [Cited: June 20, 2012.] <http://www.crct.polymtl.ca/equili.php>.
20. **Osen, Karen**. *Oppførsel av fukt i kryolittsmelter*. Trondheim : NTNU, 2005.
21. **Peter Entner**. Principles of the Hall-Héroult Process. *Software for Aluminium Smelting*. [Online] 2011. <http://peter-entner.com/E/Theory/PrincHH/PrincHH.aspx>.
22. **Tinto, Rio**. Specialty Aluminas. *Rio Tinto Alcan*. [Online] 2008. http://www.specialty-aluminas.riotintoalcan.com/gardanne/EVO_WebSpecialtyGlobal.nsf/vwUrl/MondeAlumine_FabricationAlumine_VI.
23. **Green, William H**. Continuous Stirred Tank Reactors (CSTRs). Boston : MIT, Spring 2007. pp. 1-3.

APPENDIX A DRAWING OF NICKEL CONTAINER



| Qty | Item | Part name | Material | Note |
|--|-------|--------------------------|----------|--|
| 1 | 9 | Lid | Brass | |
| 10 | 8 | Tube Ø8X15X20 | Alsint | |
| 5 | 7 | Radiation shield | Nickel | |
| 2 | 6 | Nut | Nickel | |
| 2 | 5 | Nickel rod | Nickel | |
| 2 | 4 | 1/4" Swagelok fitting | 316 | |
| 1 | 3 | Water cooling tube Ø1/2" | Copper | Tin soldered |
| 2 | 2 | Tube Ø10/12 | Brass | Silver soldered |
| 2 | 1 | Tube Ø1.5/17.5 | Brass | Silver soldered |
| Date: 20120221 Insp.: Design: Aksel Alstad Appr.: Proj.: Scale: 1:1 Size: A2 | | | | |
| Furnace lid | | | | NTNU Fakultet for naturvitenskap og teknologi Tekniske tjenester |
| Drawing no. NTV 1208 | | | | |
| Ref. | Calc. | | | |



| 1 | 12 | Inner container | Nickel | |
|-------------------|----------|------------------|-------------|--------------------------|
| 1 | 11 | Lid | Nickel | |
| 1 | 10 | Nickel Container | Nickel | Flange made of 316 steel |
| Qty | Item | Part name | Material | Note |
| Date | 20120411 | Design | Drawn | Scale |
| Insp. | Appr. | Proj | Proj | 1:1 |
| Nickel Containers | | | Size | A2 |
| Ref. | Calc. | | Drawing no. | |
| | | | NTV 1212 | |

NTNU
 Fakultet for naturvitenskap og teknologi
 Tekniske tjenester

APPENDIX B METHODS DEVELOPMENT

Methods development was conducted after found the result of melt experiment 1 below,

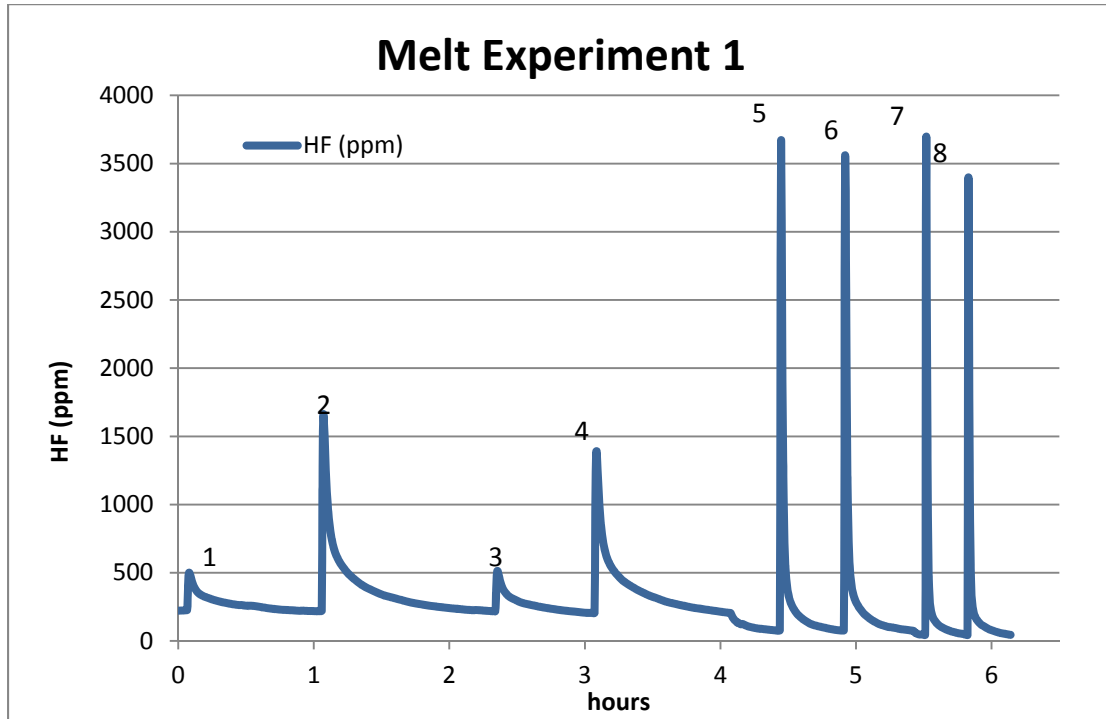


Figure 35. The plot of melt experiment 1

Table 17. The result of experimental data of melt experiment 1

| no | flow rate | HF(g/gAl ₂ O ₃) | comments | Al ₂ O ₃ (g) |
|----|-----------|--|--------------------|------------------------------------|
| 1 | 97 | 0.001942385 | calcined alumina A | 0.12 |
| 2 | 97 | 0.008217183 | alumina B | 0.12 |
| 3 | 97 | 0.001543507 | calcined alumina A | 0.12 |
| 4 | 97 | 0.007149464 | alumina B | 0.12 |
| 5 | 493 | 0.028888674 | alumina B | 0.09 |
| 6 | 493 | 0.02510041 | alumina B | 0.11 |
| 7 | 1108 | 0.035742148 | alumina B | 0.1 |
| 8 | 1108 | 0.032081868 | alumina B | 0.1 |

The trend of HF formation in the first melt experiment behaved differently from the previous autumn work. In this experiment, high flow of inert nitrogen gas generates highest amount of HF which is reverse from the previous work. To know the root cause of this problem there are several methods development were conduct.

1. The first thing to do was theoretically check whether the nickel container react with HF or not. According to CRCT⁽¹⁹⁾ when 1mol of HF and 1 mol of N were added in the software, the result is shows below.

Table 18. Activity of nickel and its compound

| | mol | ACTIVITY |
|-----------------|--------------|------------|
| Ni solid fuc(s) | 9.9975E-01 | 1.0000E+00 |
| Ni liquid(liq) | 0.0000E+00 | 6.5767E-01 |
| NiF2 solid(s) | 0.0000E+00 | 4.6720E-01 |
| Ni2H_solid(s) | T 0.0000E+00 | 1.7501E-05 |

From the table above, it can be concluded that Ni didn't react with HF.

2. Secondly after ensure that Ni didn't react with HF, testing of laser was conducted on 27-28 April 2012 as shows below,

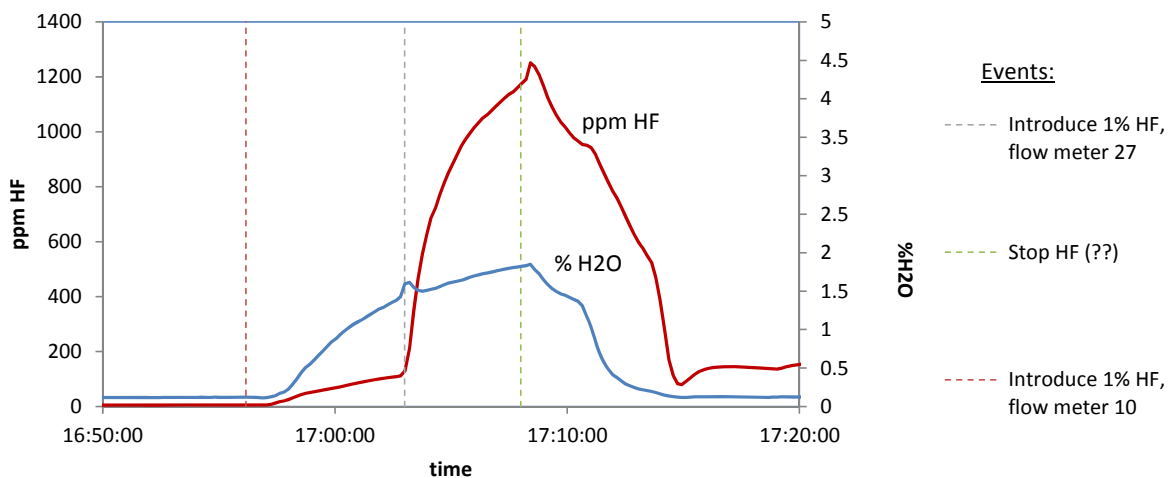


Figure 36. Testing of laser 27/4 before cleaning. Transmission 68%

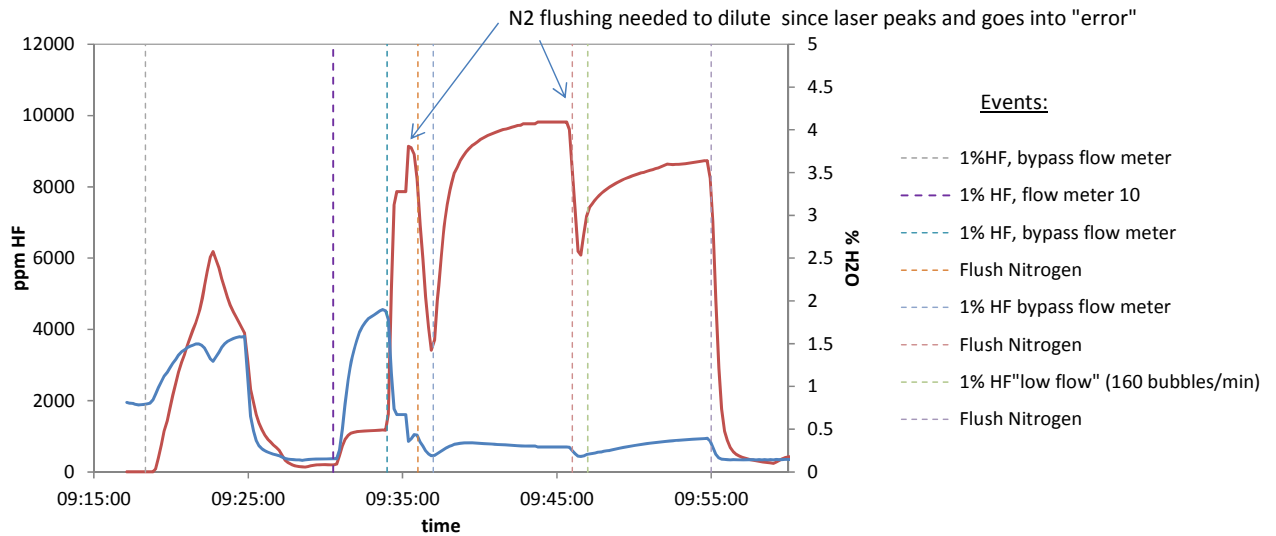


Figure 37. Testing laser after opening and cleaning. Transmission 99%

When the laser opened and cleaned, transmission went up from 68 to 99 % and the concentration approached 10000 ppm rapidly when 1%HF was introduced to the laser (Figure 40 at 9.30 AM and 9:34 AM)

There are three conclusion made according to this result,

- a. lots of dust in laser and too low transmission
 - b. The glass flow meter adsorbed/leaked HF (the gas bubbling after gas cleaning system did not indicate leakage)
 - c. There is nothing wrong with the laser since it can detect 10000ppm when 1% HF was introduced.
3. After check the laser, the set-up of the experiment was dismantled and it was found some white powder inside the furnace. To know the structure of the powder, XRD measurement was conducted. The structure of samples was investigated with X-ray diffraction using Cu-K- α radiation. The diffractograms were measured over an angular range of 20-60° (2 θ) in 0.010° steps and 1 second per step. The interpretation of the diffractograms was obtained by comparing the diffraction pattern with ICDD-PDF (International Centre for Diffraction Data-Powder Diffraction File) database. It was found that the main structure of the powder is AlF₃ and Na₅Al₃F₁₄. Since HF is sticky gas, all these powder might become the reason of the HF

trend. The action which was taken after know this finding was develop the routine to change and clean the gas outlet tube and also the hose from the furnace to the laser before every addition. (see Figure 41 to know the result of XRD)

2 (Coupled TwoTheta/Theta)

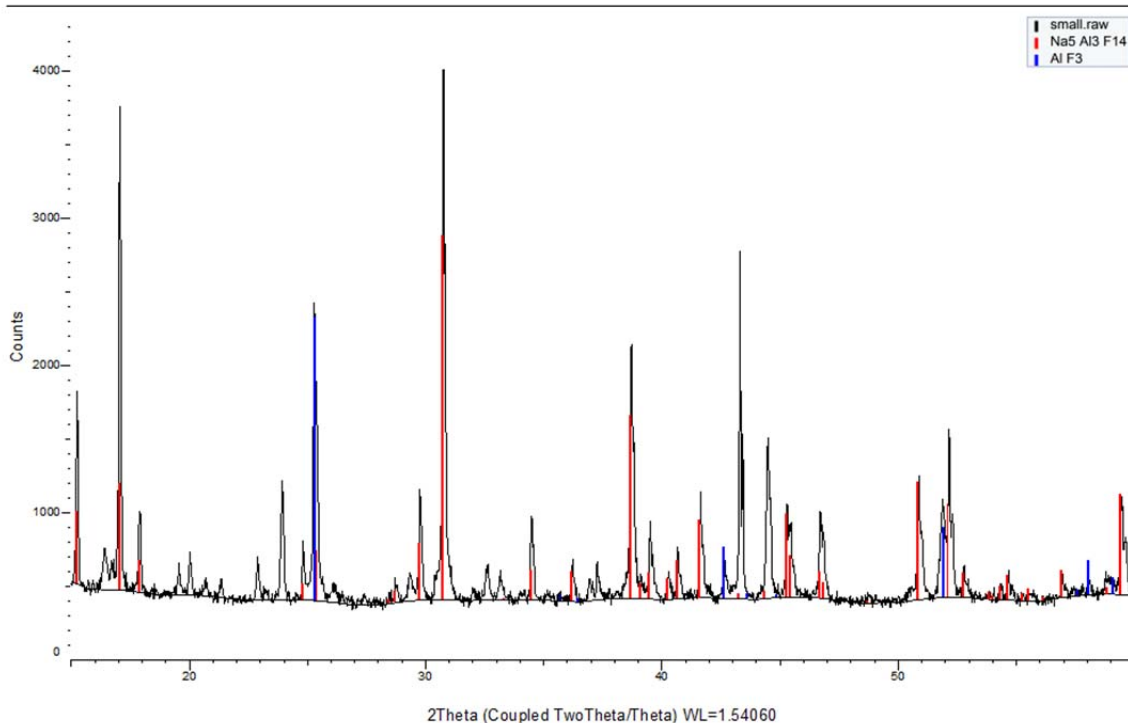


Figure 38. The structure of the powder inside the furnace after dismantled was performed

4. After ensure that the laser was okay and the furnace was cleaned, the routine method development for the argon with 1% HF experiment was performed. The challenge is to add known amounts of the gas since the flow meters didn't goes well with HF due to its very corrosive and sticky. Coped the problem, flow meter was put after the gas cleaning system. White deposit develops with time in the flow meters placed after the gas cleaning caused the 'ball' stuck after a while and routine cleaning was needed to remove the white deposit.
 - a. First method development of this experiment is using syringe as shown in the picture below.

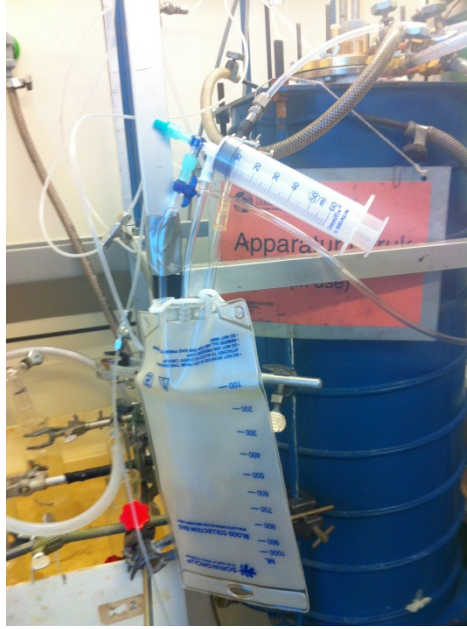


Figure 39. Method development of argon with 1% HF using syringe

The bag is used to collect the argon with 1% HF gas. The bag is connected to the syringe which sucked up 50ml argon with 1% HF gas from the bag for each addition of HF to the furnace. The method is seems reasonable to do until it was realized the big possibility of the syringe to detect the wrong gas (air can be sucked up in the syringe instead the argon with 1% HF gas) and when it happened the HF measurement by the laser was totally wrong.

- b. Since the time of injection of the argon with 1% HF should be more less the same for each addition, the three ways valve was introduce to the system. First the argon purged through te the three ways valves which opened to the gas cleaning system which equipped with rotameter to measure the flow rate of the argon with 1% HF. When the flow rate was already stable, three ways vale opened to the furnace and the time was counted for one minute.

APPENDIX C CALCULATION OF NaF and AlF₃

The following shows a calculation example to determine the quantities of NaF and AlF₃ needed to create a cryolitic melt with a cryolite ratio of 2.2 of 150 g.

An excess of AlF₃ of 12.7 wt% gives a cryolitic ratio of 2.2 on mol basis or 2.2 on molar ratio NaF/AlF₃

$$M_{AlF_3} = 83.98 \text{ g/mol}$$

$$M_{NaF} = 41.99 \text{ g/mol}$$

$$\frac{n_{NaF}}{n_{AlF_3}} = 2.2004 \quad (C.1)$$

Mol fraction

$$NaF = 0.6875$$

$$AlF_3 = 0.3125$$

$$M_{AlF_3} = 83.98 \cdot 0.3125 = 26.24 \text{ g/mol} \quad (C.2)$$

$$M_{NaF} = 41.99 \cdot 0.6875 = 28.87 \text{ g/mol} \quad (C.3)$$

In one mol the sum of the amounts of AlF₃ and NaF becomes:

$$28.87 + 26.24 = 55.11 \text{ g}$$

Weight percent of NaF and AlF₃ then becomes:

$$NaF: 0.5239$$

$$AlF_3: 0.4761$$

To create 150 g melt:

$$NaF: 78.59 \text{ g}$$

$$AlF_3: 71.42 \text{ g}$$

APPENDIX D RIEMANN SUMS

Equation below shows the calculation of the quantity of HF when using the riemann sum principle. All columns in a chosen time interval are then added together. To avoid negative value, the riemann sum calculation was terminated if the HF concentration measured reached the baseline given.

$$m_{HF} = \frac{\left((y(1)_{HF,ppm} - baseline_{ppm}) + (y(2)_{HF,ppm} - baseline_{ppm}) \right) \cdot v_{gas\ flow} \cdot \Delta t \cdot M_{HF}}{2 \cdot 10^6 \cdot V_m}$$

m_{HF} = the amount of HF in g

$V_{gas\ flow}$ = the volume flow of gas into the furnace (ml/s)

V_m = the volume of 1 mol ideal gas at 1 atm and 0°C (ml/mol)

Δt = time difference between each measurement on the x axis in seconds.

M_{HF} = molar mass of HF (g/mol).

Table 19 shows a summary of the parameters used. $y(1)$ and $y(2)$ represents two HF concentration values next to each other, taking the average value of the two (hence the division by two in the denominator).

Table 19. Parameters used when calculating the riemann sum of the HF formation

| Parameter | Quantity | Unit |
|--------------------|----------|--------|
| $V_{gas\ flow}$ | 0.45 | ml/s |
| 1 | 1.61 | ml/s |
| $V_{gas\ flow\ 2}$ | 4.23 | ml/s |
| $V_{gas\ flow\ 3}$ | 11.6 | ml/s |
| $V_{gas\ flow\ 4}$ | 17.21 | ml/s |
| $V_{gas\ flow\ 5}$ | 22.4 | ml/mol |
| V_m | 11.18 | s |
| Δt | 20 | g/mol |

APPENDIX E CALCULATION OF LOSS ON IGNITION

Equation E.1 shows how to calculate the LOI value from room temperature to 160°C. Equation E.2 shows how to calculate the LOI value from 160°C to 350°C. Equation E.3 shows how to calculate the undried basis LOI value from 350-1000°C and C.4 shows how to calculate the dried basis LOI value from 350-1000°C.

$$LOI(RT - 160^{\circ}\text{C}) = \frac{(m_2 - m_3) \cdot 100\%}{m_2 - m_1} \quad (\text{E.1})$$

$$LOI(160^{\circ}\text{C} - 350^{\circ}\text{C}) = \frac{(m_3 - m_4) \cdot 100\%}{m_2 - m_1} \quad (\text{E.2})$$

Undried basis

$$LOI(350^{\circ}\text{C} - 1000^{\circ}\text{C}) = \frac{(m_4 - m_5) \cdot 100\%}{m_2 - m_1} \quad (\text{E.3})$$

Dried basis

$$LOI(350^{\circ}\text{C} - 1000^{\circ}\text{C}) = \frac{(m_4 - m_5) \cdot 100\%}{m_4 - m_1} \quad (\text{E.4})$$

- m1 = mass of the empty crucible
- m2 = mass of the crucible and test sample
- m3 = mass of the crucible and dried sample (160°C)
- m4 = mass of the crucible and dried sample (350°C)
- m5 = mass of the crucible and ignited sample (1000°C)

APPENDIX F CALCULATION OF LOSS ON IGNITION IN FUNCTION OF TIME (160°C)

Equation F.1 up to F.10 shows how to calculate the LOI value in function of time at 160°C.

$$LOI\ 1\ (RT - 160^{\circ}C) = \frac{(m_2 - m_3) \cdot 100\%}{m_2 - m_1} \quad (F.1)$$

$$LOI\ 2\ (RT - 160^{\circ}C) = \frac{(m_2 - m_4) \cdot 100\%}{m_2 - m_1} \quad (F.2)$$

$$LOI\ 3\ (RT - 160^{\circ}C) = \frac{(m_2 - m_5) \cdot 100\%}{m_2 - m_1} \quad (F.3)$$

$$LOI\ 4\ (RT - 160^{\circ}C) = \frac{(m_2 - m_6) \cdot 100\%}{m_2 - m_1} \quad (F.4)$$

$$LOI\ 5\ (RT - 160^{\circ}C) = \frac{(m_2 - m_7) \cdot 100\%}{m_2 - m_1} \quad (F.5)$$

$$LOI\ 6\ (RT - 160^{\circ}C) = \frac{(m_2 - m_8) \cdot 100\%}{m_2 - m_1} \quad (F.6)$$

$$LOI\ 7\ (RT - 160^{\circ}C) = \frac{(m_2 - m_9) \cdot 100\%}{m_2 - m_1} \quad (F.7)$$

$$LOI\ 8\ (RT - 160^{\circ}C) = \frac{(m_2 - m_{10}) \cdot 100\%}{m_2 - m_1} \quad (F.8)$$

$$LOI\ 9\ (RT - 160^{\circ}C) = \frac{(m_2 - m_{11}) \cdot 100\%}{m_2 - m_1} \quad (F.9)$$

$$LOI\ 10\ (RT - 160^{\circ}C) = \frac{(m_2 - m_{12}) \cdot 100\%}{m_2 - m_1} \quad (F.10)$$

m1 = mass of the empty crucible

m2 = mass of the crucible and test sample

m3, 4, 5, 6, 7, 8, 9, 10, 11 & 12 = mass of the crucible and dried sample (160°C) in function of time

APPENDIX G GRAPHS OF THE EXPERIMENTS

Argon with 1% HF Experiment

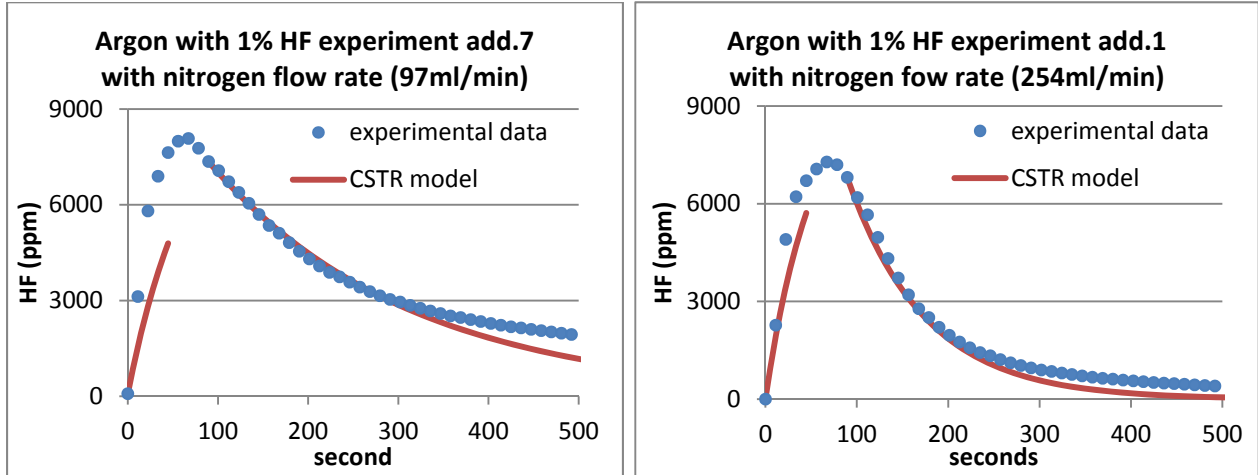


Figure 40. Argon with 1% HF experiment with nitrogen flow rate 97ml/min and 254ml/min

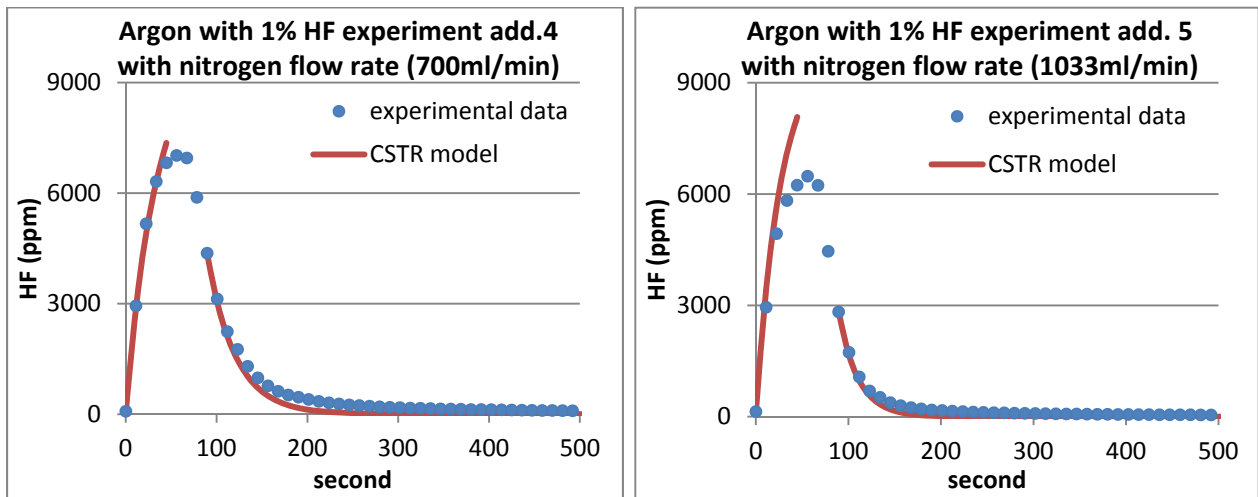


Figure 41. Argon with 1% HF experiment with nitrogen flow rate 700ml/min and 1033ml/min

Alumina Water Evolution Experiments

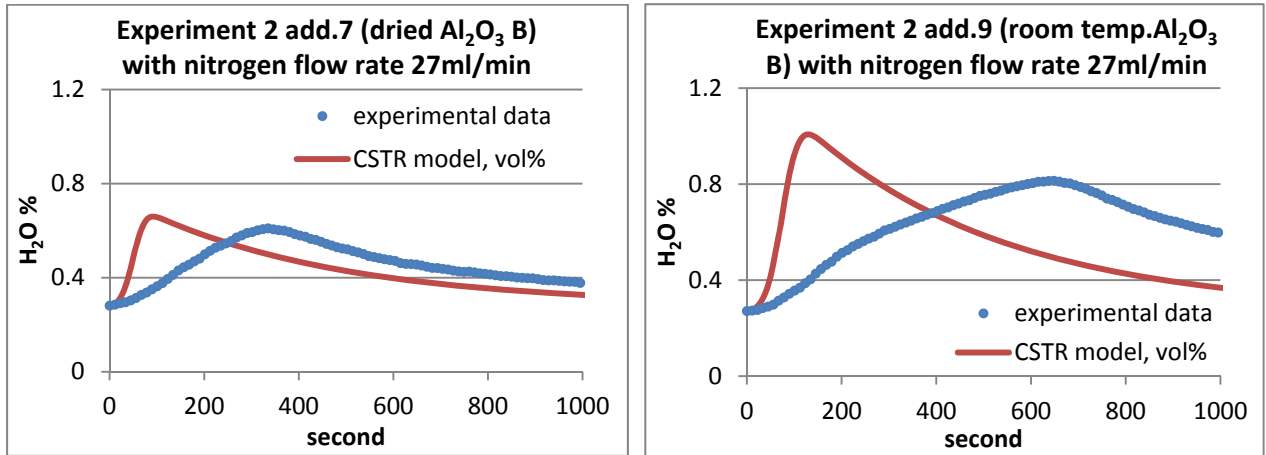


Figure 42. Alumina water evolution experiments dried Al₂O₃ B with nitrogen flow rate 27ml/min

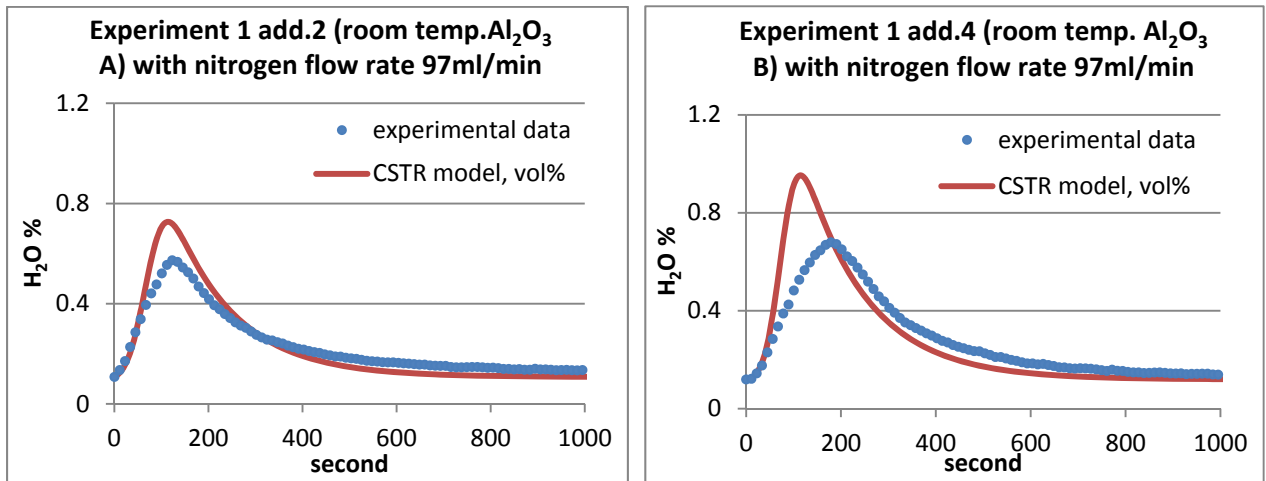


Figure 43. Alumina water evolution experiments room temperature Al₂O₃ A and B with nitrogen flow rate 97ml/min

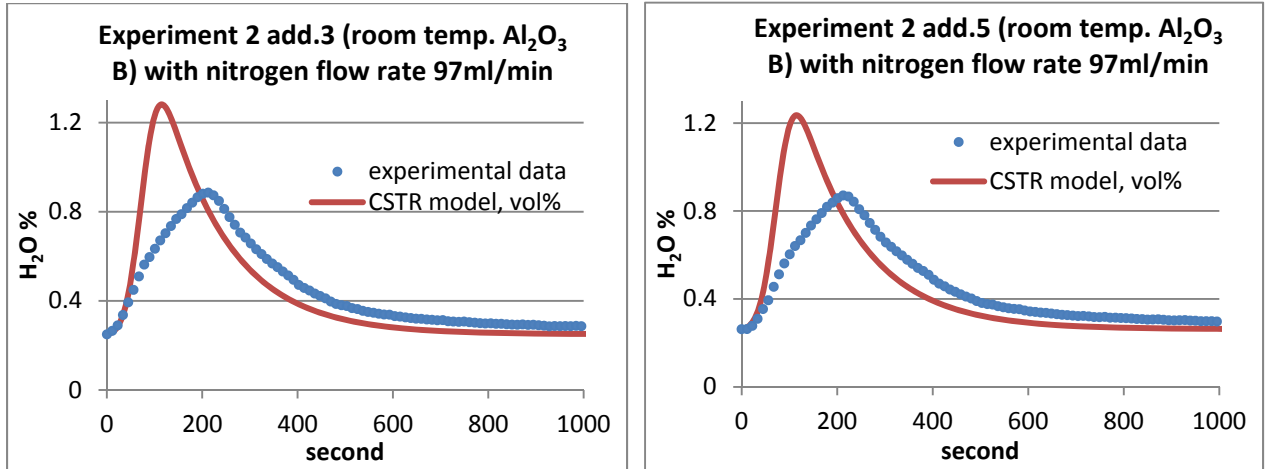


Figure 44. Alumina water evolution experiments room temperature Al₂O₃ B with nitrogen flow rate 97ml/min

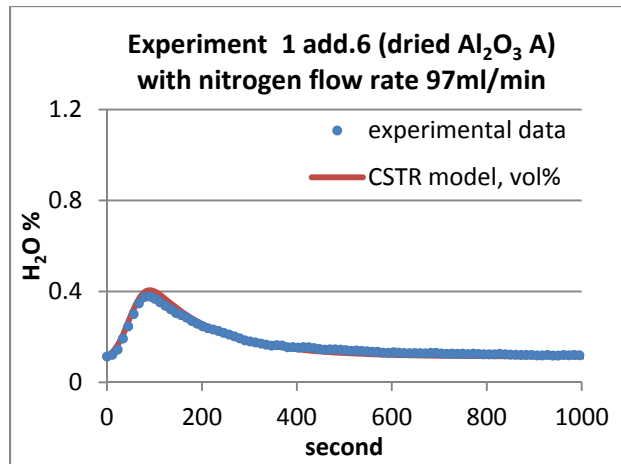


Figure 45. Alumina water evolution experiments dried Al₂O₃ A with nitrogen flow rate 97ml/min

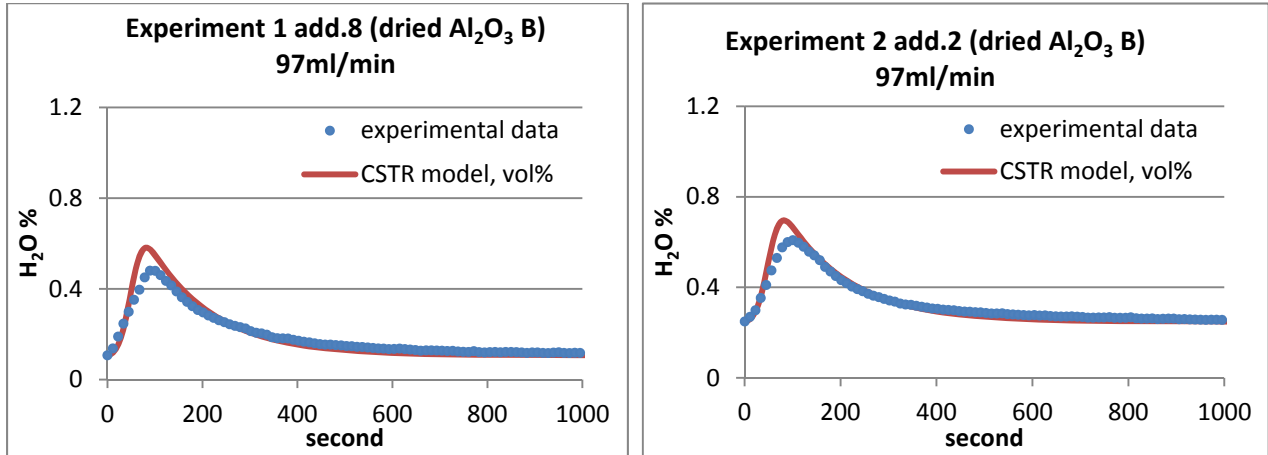


Figure 46. Alumina water evolution experiment dried Al₂O₃ B with nitrogen flow rate 97ml/min

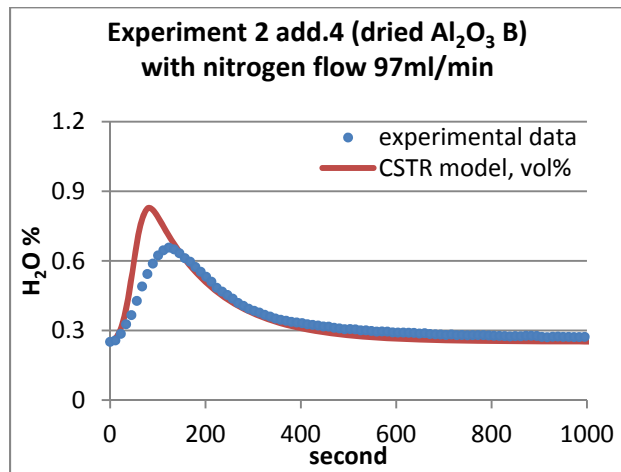


Figure 47. Alumina water evolution dried Al₂O₃ B experiment with nitrogen flow rate 97ml/min

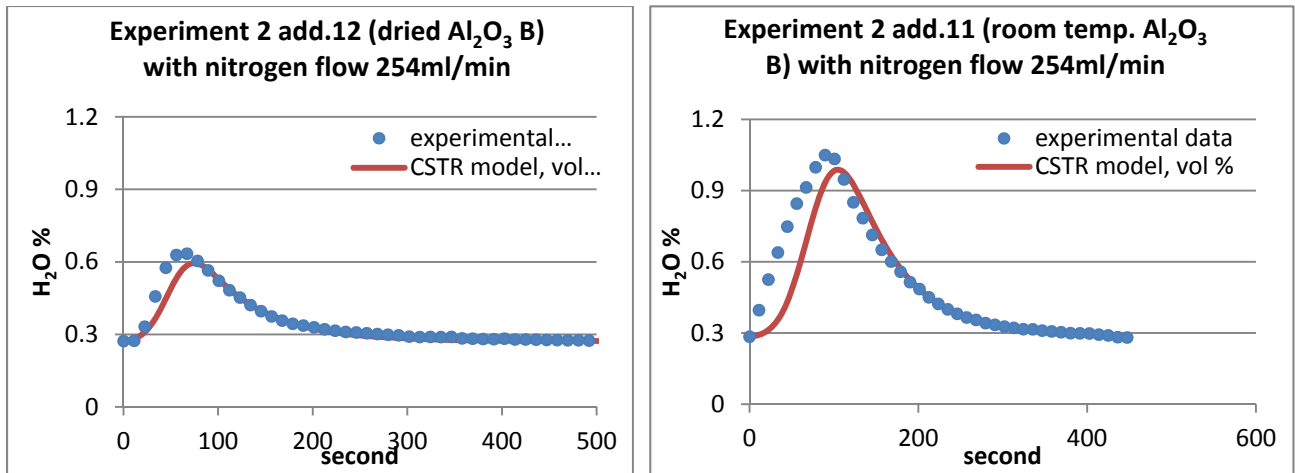


Figure 48. Alumina water evolution dried and room temperature Al₂O₃ B with nitrogen flow rate 254ml/min

MELT EXPERIMENTS

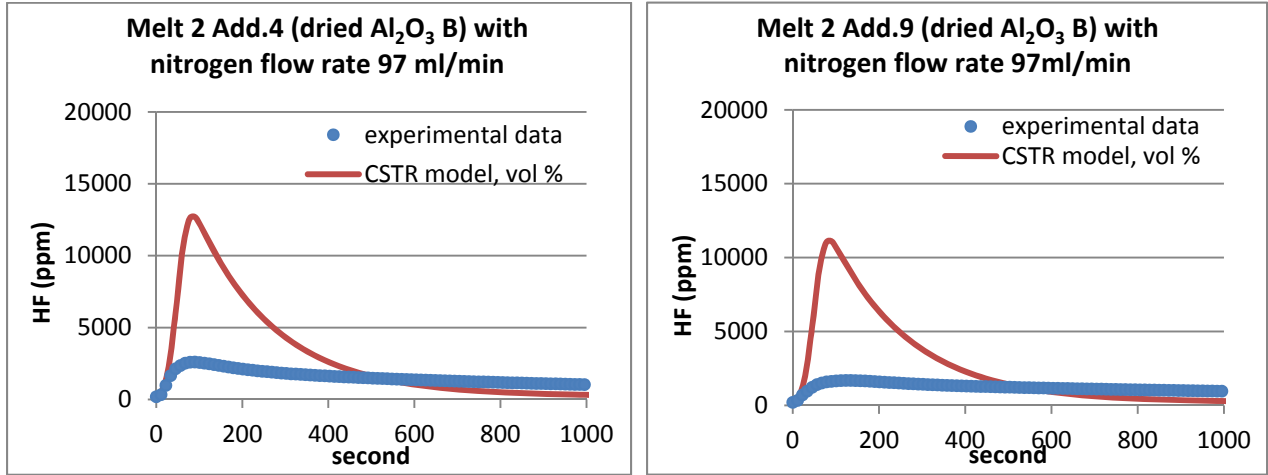


Figure 49. Melt experiment dried Al₂O₃ B with nitrogen flow rate 97ml/min

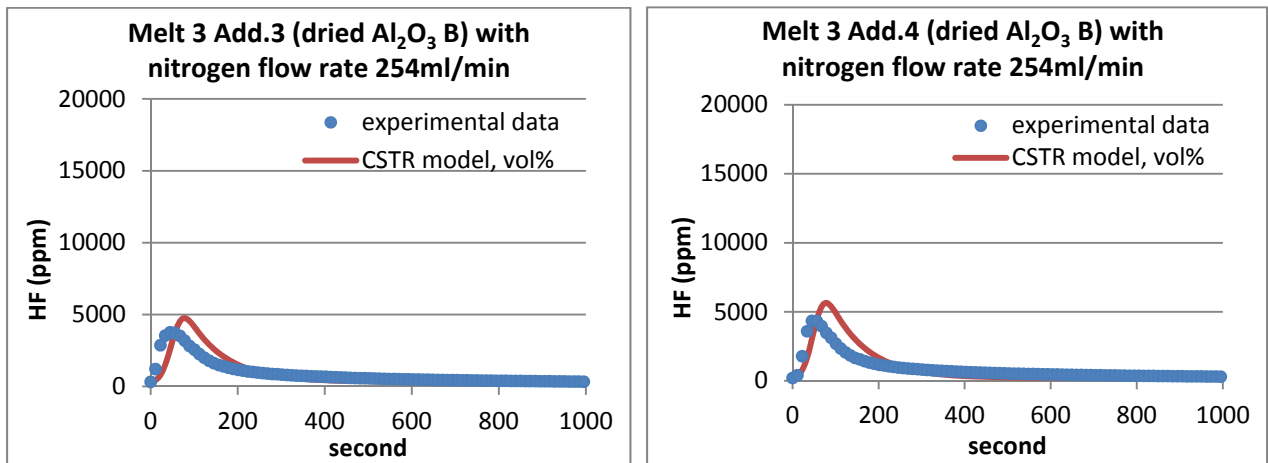


Figure 50. Melt experiment dried Al₂O₃ B with nitrogen flow rate 254ml/min

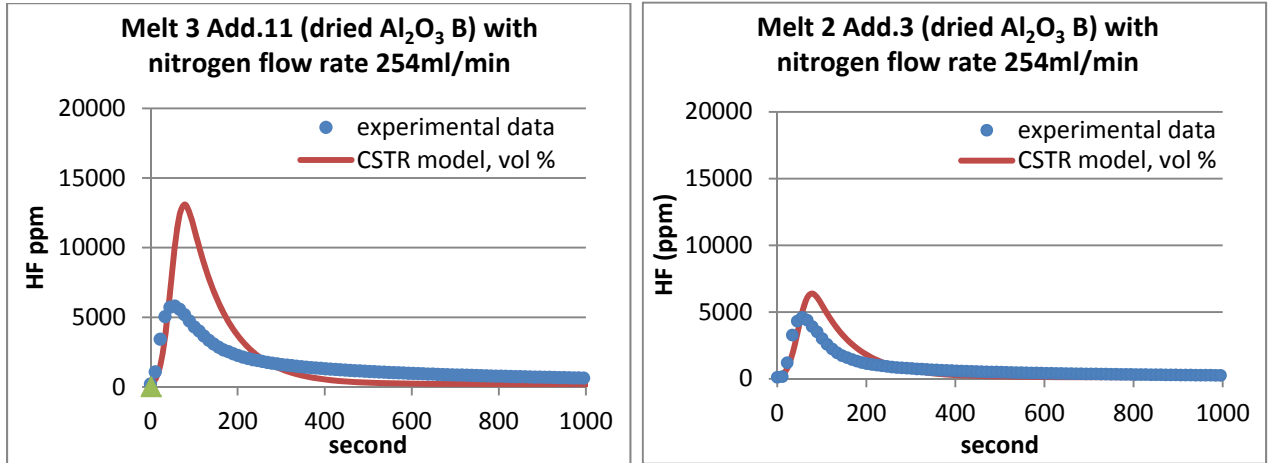


Figure 51. Melt experiments dried Al₂O₃ B with nitrogen flow rate 254ml/min

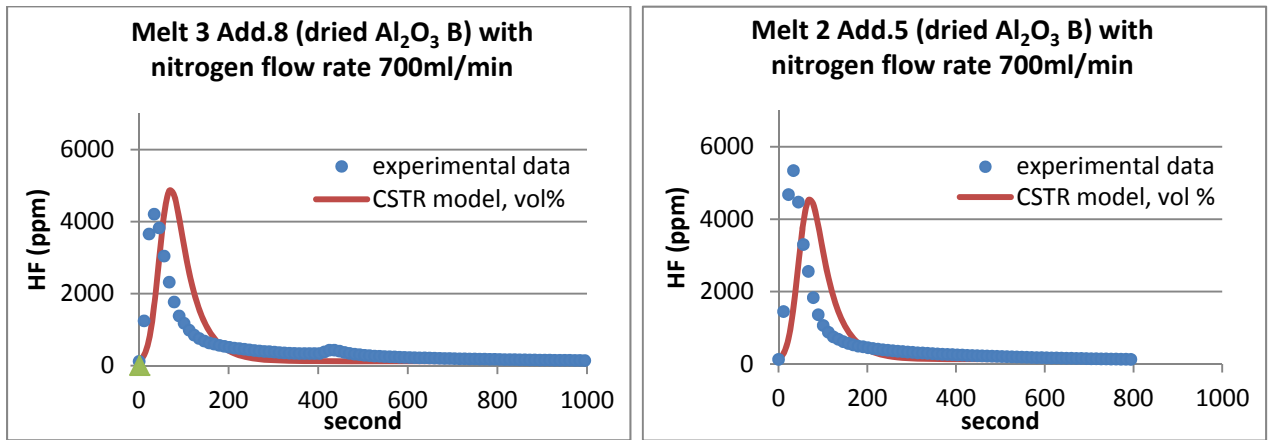


Figure 52. Melt experiments dried Al₂O₃ B with nitrogen flow rate 700ml/min

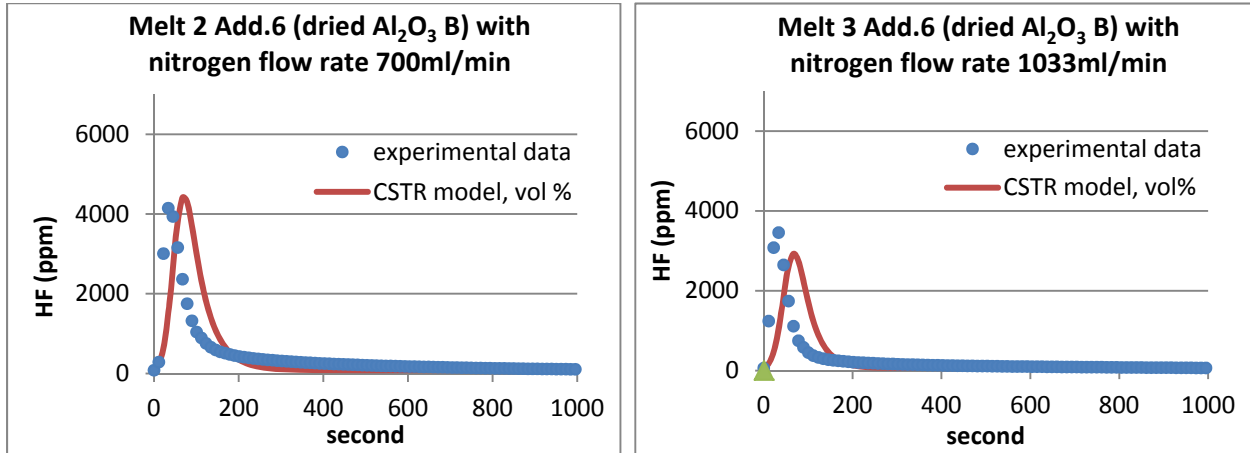


Figure 53. Melt experiment dried Al₂O₃ B with nitrogen flow rate 700ml/min

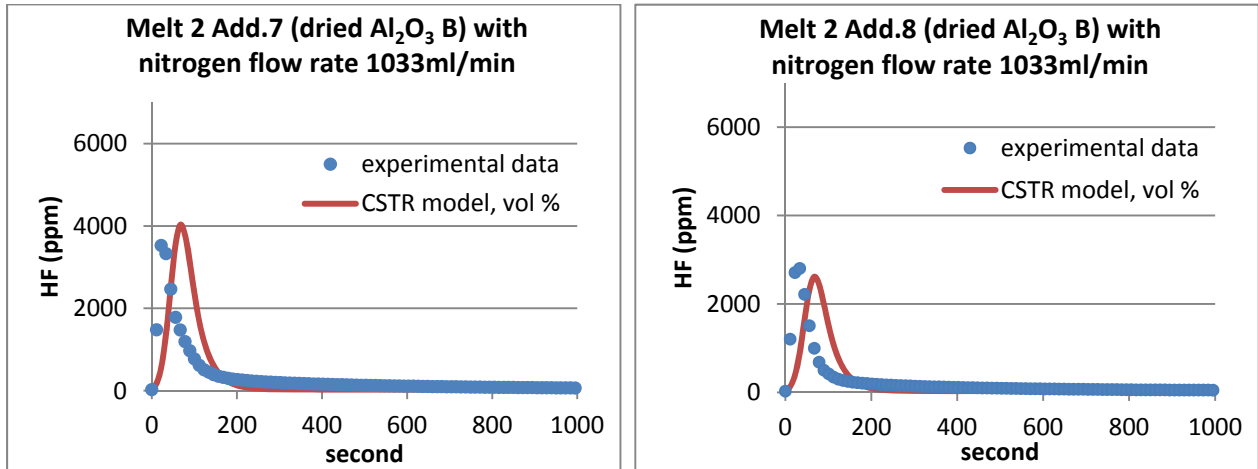


Figure 54. Melt experiment dried Al₂O₃ B with nitrogen flow rate 1033ml/min